International Journal of Photoenergy

Thermal Management and Efficiency Enhancement of Solar Systems 2021

Lead Guest Editor: Hafiz Muhammad Ali
Guest Editors: Josua Meyer and CC Wang

Thermal Management and Efficiency Enhancement of Solar Systems 2021

International Journal of Photoenergy

Thermal Management and Efficiency Enhancement of Solar Systems 2021

Lead Guest Editor: Hafiz Muhammad Ali
Guest Editors: Josua Meyer and CC Wang

Chief Editor

Academic Editors

Contents

Hindawi
International Journal of Photoenergy
Volume 2022, Article ID 9311686, 14 pages
https://doi.org/10.1155/2022/9311686

Research Article

Smart Integrated Decentralization Strategies of Solar Power System in Buildings

Syed Muhammad Kashif Shah,[1] Tanzeel Ur Rasheed,[1] and Hafiz Muhammad Ali[2,3]

[1]*Mechanical Engineering Department, University of Engineering and Technology, Taxila, Pakistan*
[2]*Mechanical Engineering Department, King Fahd University of Petroleum and Minerals, Dhahran 31261, Saudi Arabia*
[3]*Interdisciplinary Research Center for Renewable Energy and Power Systems (IRC-REPS), King Fahd University of Petroleum and Minerals, Dhahran 31261, Saudi Arabia*

Correspondence should be addressed to Hafiz Muhammad Ali; hafiz.ali@kfupm.edu.sa

Received 12 February 2022; Accepted 2 August 2022; Published 25 August 2022

Academic Editor: Ahmad Umar

This study signifies the need for a smart integrated decentralized solar energy system in Pakistan. Since the outlook of energy is highly dominated by its power sector, policy measures must be adopted to ensure its penetration in the system of any country. After the industrial, the housing sector is the major energy-consuming sector. The goal of this study is to assess energy generation through a smart integrated decentralized solar energy system in the power hub of a commercial area in Taxila, Pakistan. Model development involves a hypothetical model built on LabVIEW which allows the user interface a way to intermingle with the source code. It permits the user to the transformation of the values sent to the source code and sees the information that the source code calculates. The proposed system is a collaborative sharing integrated decentralized solar system that credits sunlight-based energy framework proprietors for the power they add to different buildings due to the collaborative sharing mechanism at Rs.10 per kWh. This low-cost electricity is available at your doorstep that you can share according to the collaborative sharing basis that will not range any certain variable. Results from the literature describe that 30% of the cost associated with the commercial price of electricity amounts to distribution cost. This system of the utilization of energy would be applied at a local level to achieve the maximum power generation from solar panels through blockchain use of solar systems, especially in regions that have no entrance to traditional power with little odds of getting associated in the next 5-10 years.

1. Introduction

The utilization of diverse types of energy is added to the exponential improvement of human personal satisfaction during the most recent two centuries. During this cultural development, petroleum products have driven all energy-based advancements. Since the coal-period appearance, the world's interest in power kept on heightening and has kept on doing as such till date. Truth be told, measurements confirm that during the following couple of decades, the social and mechanical advancement of China will prompt a huge development in China's power request; more noteworthy than the absolute current interest in the United States of America and Japan took together [1]. Besides, the dispersion of new power-based advancements, for example, electrical vehicles, will build the power request in industrialized locales, for example, Europe and the United States, also which will prompt a general multiplication of power requests on the planet [2]. The expansion in power utilization is a vital issue that instigates to assume and design the amount and in this manner the sort of energy assets to use inside what is to come. Truth be told, the utilization of regular energy assets is over and over addressed due to its various hurtful ramifications on the general public and condition [3]. The dependable and prudent availability of these assets has turned into a reason for worry for some nations around the globe. Truth be told, nonrenewable energy sources are found uniquely in limited locales on the

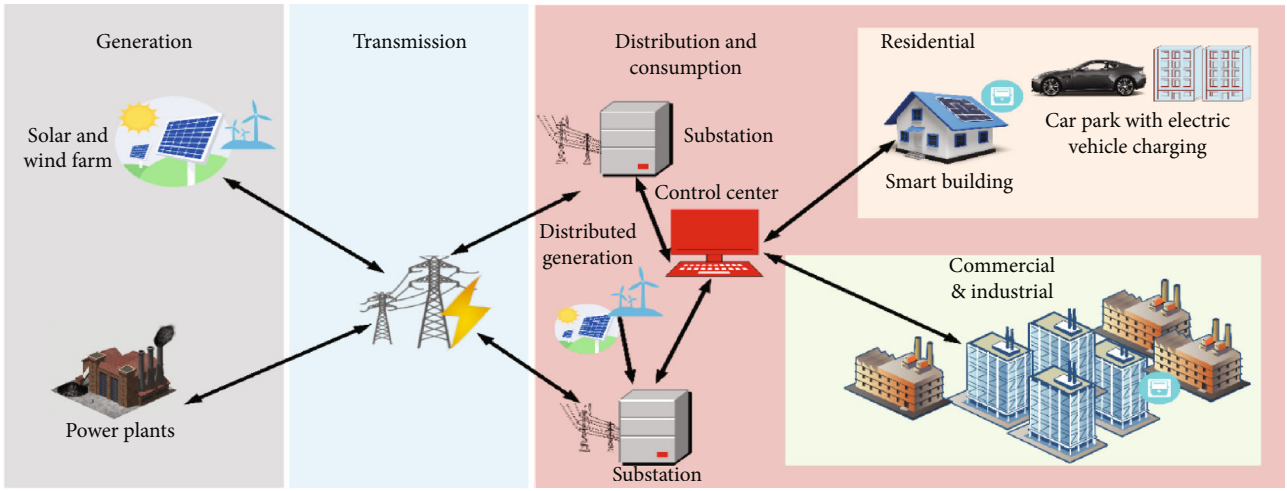

Figure 1: Model structure [7].

earth and are exposed to political understandings and relations. Their accessibility and value regularly reflect political strains between significant topographical districts and represent an enormous hazard for both created and creating nations the same. Also, in the course of the most recent decades, extraction of customary energizes has turned out to be progressively harder and frequently prompted immense discussion between governments, tree huggers, extraction organizations, and well-being specialists [4].

Talks on hold water contamination and man-initiated tremors because of shale gas extraction are a flow model. Besides, the examinations of the outcomes of climatic change are creating tremendous open and political mindfulness and instigating in these entertainers the need to take activities in this viewpoint. Prohibition of ecological variables can never again be managed while taking political and monetary choices. Henceforth, many created nations have chosen to fix an atmosphere objective to restrain the earth from warming more than 2°C [5]. In 2016, the carbon dioxide outflows from the power division in the USA alone had added up to around 1 million and 800 thousand metric tons, which records for about 35% of the complete emanations in the USA [6]. Furthermore, statistics suggest that a huge part of these emissions originate from coal-based technologies.

Hence, this study identifies the major challenges in the adoption of renewable energy systems in Pakistan through a decentralized solar system.

1.1. Research Motivation. The overall energy deficiency has upset the budgetary viewpoints, society, progression of the nations, and circumstances through ozone-exhausting substances (GHGs) and by grabbing carbon credits. The creating enthusiasm for power over the world is being future and recorded to be exponential. Nonattendance of advantage with out-of-date framework system, ecological variation, and increasing fuel costs has come about inefficient and dynamically flimsy electrical structure. Accordingly, the overall concern has raised certain fundamental centers whereupon the energy change for a green and sustainable future is certain and came about in Figure 1.

1.2. Energy Efficiencies. The new system for energy unergy utilization should get political help [8]. The test ahead will require inventive power structure planning including both new types of progress and better approaches for dealing with the system to guarantee an understanding between contrasts in energy requesting and supply [9]. The key pieces of this new power structure arrangement are little scale cross segments, awe-inspiring grids, and a convincing gigantic scale super framework, which could expect a stand-out movement in patching up the general energy situation with elements like systems, principle, and productivity of market with costs, good conditions, and organizations which in like way regulates the power and energy advance with the decay of carbon impressions and foot pulling the GHG discharges [10].

1.3. Problem Statement. The economic activities of a country are highly driven by its power sector. Despite having a generation capacity greater than demand, the country's power system is incapable to meet the electricity demand due to transmission losses and management lacks. These days' renewable energy technologies have been cost-effective in many parts of the world.

A society can be made more cost-effective by using decentralized solar power systems. This study investigates the merits of collaborative sharing of decentralized solar power systems connected as small networks. The underline research finds the pathway to reduce the technological gaps for small networks of a solar power system. The literature suggests that decentralized solar power systems reveal more cost-effective solutions to society. In case of transformation towards renewable energy centralized solar power systems, we must face some disadvantages—massive land used, big transmission loss, and high maintenance cost in comparison to decentralized solar power systems.

1.4. Research Questions. How to integrate the decentralized solar power system into small networks?

What are the drawbacks of a decentralized solar power system?

How can the technological gaps be overcome to develop a small network of solar PV systems for collaborative sharing?

How societies can be made more cost-effective by implementing the strategies of solar PV networks?

The main aims and objectives of this project are as follows:

(i) Develop an integrated simulation model of decentralized solar PV system for small networks

(ii) Develop a better technical model for collaborating sharing mechanism

(iii) Develop a better finical model for small networks

The remainder of this paper is organized as follows: Section 2 provides a survey of the literature on current research work on this topic. The suggested architecture and approach are described in Section 3. Section 4 presents experimental data as well as a comparison of classification techniques. Finally, Section 5 discusses the paper's conclusion.

2. Literature Review

Pakistan, especially considering the rural areas that are in a state of neglect concerning an electrification perspective, has been in an energy-related crisis for over the last two decades. Research shows that rural electrification is possible through the implementation of a decentralized system of electrical generation using PV, wind, or even a hybrid of PVs, and diesel-powered generational alternatives. However, no research or attention has been paid to the system and has not been implemented.

To deal with the drawbacks, the implementation of a system of decentralized generation has been proposed based on the generation of solar energy previously implemented in several countries. The system works over the process of generation of electricity on a relatively smaller scale, however, designed to power a specific locale without connections to an electrical grid [11].

The distributed and decentralized generation scheme has proven to overcome the shortcomings of the centralized generation and distribution model with special regard to rural electrification; however, it comes with slight drawback as given in [12]. [13] conducted a study concerning rural electrification and proposed the implementation of decentralized, off-the-grid solutions towards that end and described it as being beneficial in contrast to the government/public preference towards centralized electrification due to a bad track record. The study is conducted to test the feasibility of decentralized, renewable electrical generation systems, resulting from which it can be concluded that they do not fit into any of the available models concerning electrical generation; however, they have demonstrated their feasibility, and their local ownership ensures sustainability. [14] implemented a comparison of other countries using distributed generation (DG) as an electrical generational method for its feasibility, especially focused on rural areas in Indonesia. According to the study, "The elementary impression is to change "self-governing rural power creators". The goal is not just the creation of power, but also to aid in the financial growth of townships." It was analyzed that DG does prove to have some problems such as the high costs of implementation; however, solutions towards that end exist, and it is concluded that DG does prove to be an ample solution for rural areas subject to geographical disadvantages [15], enumerated benefits of off-grid, renewable energy solutions especially concerning rural, and geographically challenged areas. This study is aimed at rural areas where connections from the central grid are extensively unfavorable due to factors such as high costs and line losses (up to 30%). From the results of the study, for target areas, power services provided through low-cost solar PVs should be accompanied by diesel and microhydro systems to form a hybrid system for areas that have a higher demand for power.

The study also validates the use of neural networks for the allocation of energy in the country. [16] conducted an analysis of the efficiency of emergent systems for the generation of electricity using renewable, decentralized, solar methods showing their efficiency and increasing demand. The study dictates an implementation of a system based on main power system evolution based on a model by CIGRE using open database data. While taking the European and COP21 standards as a reference, the study concludes that decentralization also comes with regulatory frameworks. To support obstacles towards the shifting of duty and roles towards the development of the system [17], the examination exhorts a unique estimating philosophy that offers a market-based intention to drive decentralized energy to improve monetary advantage through the investigation of a value-responsive model for the appropriated wellsprings of energy. A versatile 3-level system is structured that incorporates adjusting of small-scale networks, booking of the aggregator, just as exchange advancement that advances the spot costs for the members. From the aftereffects of the examination, it very well may be seen that the plan can distinguish a successful win system to understand the improvement of small-scale matrices and appropriate [18]. This examination is gone for a survey of the boundaries that private division organizations face in cooperation I decentralized jolt extends just as measures taken against these obstructions. From the consequences of the investigation, it is resolved that a more noteworthy comprehension of the elements that impact rustic interest for energy and how they react to evaluating plans would improve potential. Focused on the provision of a cost-effective solution for the electrification of Kenya, the study focuses on the comparison of grid extensions with standalone photovoltaic systems using microdata from common households. It can be seen from the results that a decentralized system of PVs can make an important impact over an area electrical status (more efficient than grid extensions). 17% of the total population will have access to cost-effective electricity through off-grid PV systems by 2020. The examination is led to propose a sun-based power age figure to help the evaluation of the operational save for ongoing planning, with respect to the decentralized, sun-based controlled microgrids. An execution of control is seen regarding a DC microgrid that is inserted into

an elevated structure of the urban territory that creates a 375 V current on gauge. The consequences of the examination direct that a DC microgrid is increasingly reasonable towards the age in the accompanying case.

2.1. Generation over Centralized Power Plants. The plan of action of the electric business stayed unaltered for over a century, utilizing incorporated power stations to create all the power and conveying it to singular clients with transmission and dissemination arrangements. Notwithstanding little scale age frameworks, for example, sun-powered photovoltaic exhibits presently permit age at the purpose of utilization, and this is carrying exceptional changes to the power part. With private and business universes, power purchasers can likewise move toward becoming makers. Any age achieved nearby is subtracted from the power bill, and surplus kilowatt-hours can be sent out in return for a feed-in tax.

Another financial [19] preferred position of disseminated age is decreasing the weight on the transmission foundation. Think about that the power system has possession costs: activity, upkeep, and capital consumption in a new foundation. Power networks are expensive for countries. Electrical cables are the best energy transmission strategy in the world, regarding both speed and effectiveness. Nevertheless, systems are not immaculate, and some energy is dispersed as warmth during transmission and dissemination. These misfortunes speak to age that has an expense however is never offered to end clients and influences organizations to repay by adding system charges to power duties.

Power systems are costly because their ability must be sufficient for the most appeal expected in the entire year. Sadly, these power service organizations put resources to a limit that is just utilized occasionally.

The most popular, for the most part, happens just during the most smoking, long stretches of summer when cooling frameworks are working at full yield [20–22]. The development of new power stations can be postponed, and arranged limit redesigns can likewise be deferred. Therefore, with decreased interest in the new foundation [22], transmission and circulation charges in power bills are balanced out. System misfortunes are likewise decreased, since a noteworthy bit of the power devoured is presently being created for utilization. Expecting a power framework could depend 100% on conveyed age; the system would, in any case, be significant, yet its jobs would change. Provide auxiliary administrations to keep the power supply steady, for example, voltage and recurrence guidelines [23]. Energy exchange between organizing clients: owners of appropriated age with a surplus limit can offer their yield to different clients. Solar power can adjust to any property while having the absolute most reduced age costs on the planet. If photovoltaic innovation is joined with energy stockpiling, alongside other age frameworks that can be depended on around evening time or on shady days, dispersed age is feasible as the essential wellspring of power [24].

3. Methodology

The major energy consumer in the residential sector consumes up to 40% of the world's energy. All the developed and developing countries use sustainable methods to meet the required energy in the residential sector [26]. Pakistan is suffering from major energy crises due to electricity theft, transmission, distribution losses, and lack of sustainable resources also lacks technology and planning. Given such circumstances, it was necessary to develop and introduce a new innovative electricity generation system and methodology to reduce the electricity crisis in Pakistan (Figure 2).

3.1. Policy Review. Research shows that rural electrification is possible through the implementation of a decentralized system of electrical generation using PV, wind, or even a hybrid of PVs and diesel-powered generational alternatives. However, no research or attention has been paid to the system and has not been implemented. Centralized system of electicity generation is preferred mode by government [22].

3.2. Identify Problems. To deal with the drawbacks, the implementation of a system of decentralized generation has been proposed based on the generation of solar energy [26].

3.3. Technological Review. Solar power plants with substations are needed, and the transmission lines should be kept running over long separations to get that perfect sun-based power into the lattice and the customer [27].

3.4. Socioeconomic Review. Sun-based energy does not depend on mining crude materials, it does not bring about the obliteration of woods and eco-frameworks that happens with numerous nonrenewable energy source activities. So, this system is a more compatible and reasonable form of green energy as compared to other energy sources.

3.4.1. Analysis of Proposed Scheme Model. As per the field model study and their energy consumption requirements, the proposed model of sustainable green energy shows a tremendous output of saving energy. They have recorded energy consumption analysis of WAPDA and solar energy. Solar energy gives highlights, brilliant offers, loads of preference, and future viewpoints [28].

3.4.2. Data Collection. The experimental data collection is from the installed four solar panels on the experimental basis to study the generation and consumption at the other end [29].

3.4.3. International Sources. Power systems are costly on the grounds because of their losses, installation, and insufficient at some point to reach diverse areas.

3.4.4. Implementation of Scheme Model. The capacity of this framework is not unique concerning bought together sunlight-based energy framework. So, every one of the components can be utilized by willing at all. A framework is interconnected to the dispersion arrangement that provisions power to a restricted gathering of clients. This model is preferable for the business sector and residential sectors as well.

3.4.5. Financial Model. After this experimental research now, we can compare our results data to previous existing models

Figure 2: Experimental procedure [25].

like WAPDA on a monthly or yearly basis to justify the whole gap between power and economic consumption and give a better finical model to the investors and consumers.

3.4.6. Results. This solar system is focusing on those areas which have no access to conventional energy lines and minimal possibility of getting associated with the framework near future. Also, this system-utilized energy is to be applied at the local level to achieve maximum power generation from solar panels through blockchain use of the solar system.

3.5. Solar System. Monocrystalline PV solar panel consumes sunlight as a source of energy to produce power. A monocrystalline photovoltaic (PV) module is a blend of photovoltaic sun-based cells accessible in various voltages and wattages. It is established of a variety of photovoltaic system that produces and supplies sun-based power in business and nearby areas. It has modules that involve wafer-based crystal-like silicon compartments or wobbly film cells [30, 31] (Figure 3).

The cells are associated electrically in arrangement to each other to an ideal voltage and after that in parallel to expand ampere. The voltage and amperage of the module are increased to make the wattage of the module (Figure 4).

A PV connection box (ensure connections and give well-being hindrances) is connected to the back of the solar panel, and it is its produce interface. PV modules use an MC4 connector's sort to encourage simple weatherproof connections with the framework. Module connections are made in arrangement to accomplish an ideal produce voltage or in parallel to give an ideal current ability (amperes) of solar panel. The directing wires that take the current off the modules are estimated by the limit. Sidestep diodes are utilized remotely for halfway module sharing to boost the yield. Sun-powered boards additionally utilize metal casings comprising racking segments, sections, reflector shapes, and troughs to bolster the board structure more readily.

Figure 3: Solar panels [31].

3.5.1. Decentralized System. The decentralized solar power system is likewise an energy arrangement with less or no voltage misfortunes. It alludes to littler energy frameworks that produce energy on location or close to the site. The shopper regularly claims the framework and straightforwardly gets the money-related advantages of the framework. This framework can be more unreservedly worked in any geographic area.

3.5.2. Working. In this system, I will propose a research model to begin the research methodology on the chosen topic. This model will further be integrated to perform the research. I collected the data from four house buildings which we selected earlier to run the proposed system. The solar systems have been implanted in these four house

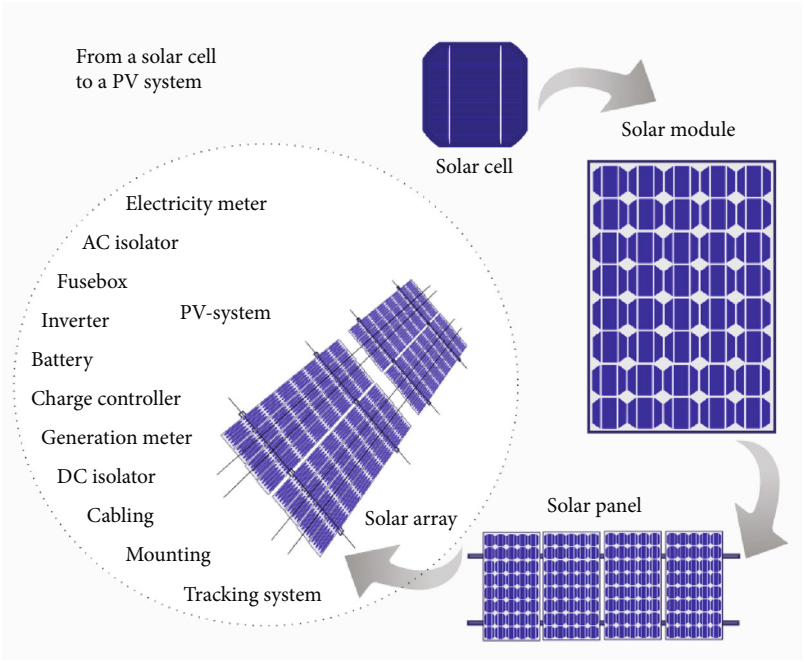

Figure 4: PV system model [31].

buildings after the data collection. This gathered data was recorded and monitored in the next process. Then, I analyzed the recorded data. Furthermore, I inspected the behavior of almost 1-year data. Based on the behavior of the inspected data, I examined the performance of my system according to the Global Horizontal Irradiance (GHI). Using the SAM model and LabVIEW generated the hypothetical model for the project and scanned the resulting outcome from the data. So, in this entire description regarding the collection of data, recording, monitoring, and analysis of data, I have explained all the major processing regarding my project of decentralized solar energy system; every one of the components can be utilized by the willing [32] of the buyer. It relies upon the heaps whether it will control for both day and night or likewise in capricious circumstances. The present innovation has progressed to the point that numerous devices and gadgets have been imagined that can keep running by sun-powered legitimately. On the off chance that a buyer possesses those advances, he/she needs not bother with additional energy to run them for quite a while. Subsequently, the loads can be wiped out, and energy can be spared.

Examples:

(i) Decentralized. Solar-based energy

(ii) Decentralized. Solar-based road lighting network

(iii) Decentralized. Solar-based energy traffic control

(iv) Devoted solar charging pac

3.6. Experimental Setup. The capacity of this framework is not unique to brought together sunlight-based energy framework. Every one of the components can be utilized by a willing buyer. It relies on the condition that it will control for both day and night additionally [33]. A smaller than usually coordinated framework alludes to a lot of power age and energy stockpiling. Frameworks are interconnected to the dispersion arrangement that provisions power to a restricted gathering of clients. Smaller than expected coordinated frameworks are bigger than miniaturized scale. The kinds of burdens that are served on a smaller scale are typically private or are extremely little businesses while a scaled-down incorporated framework can serve huge businesses and little industrial burden [34].

Under this experimental setup, we have four buildings that have monocrystalline solar panels of 250 W power. These buildings have smart integrated decentralized solar energy systems. They are integrated and working on a collaborative sharing mechanism of load sharing and balancing with the help of a controller [35]. This system has a tripped alarm that will begin when there will be a trip in power. Generation capacity is shown on the right side of the figure during different hours of the day [36]. There is also a simulation stop button to stop the simulation. The power capacity of the building and total load according to a requirement are shown with overall Global Horizontal Irradiance.

3.6.1. PV System Designing.

$$\begin{aligned} &\text{Ø Power consumption (who/day)} \\ &\quad = \Sigma\,(\text{watt of appliances} * \text{hours used}). \end{aligned} \tag{1}$$

PV panel capacity (Wp) = (total power consumption ∗ 1.5 /power generation factor)

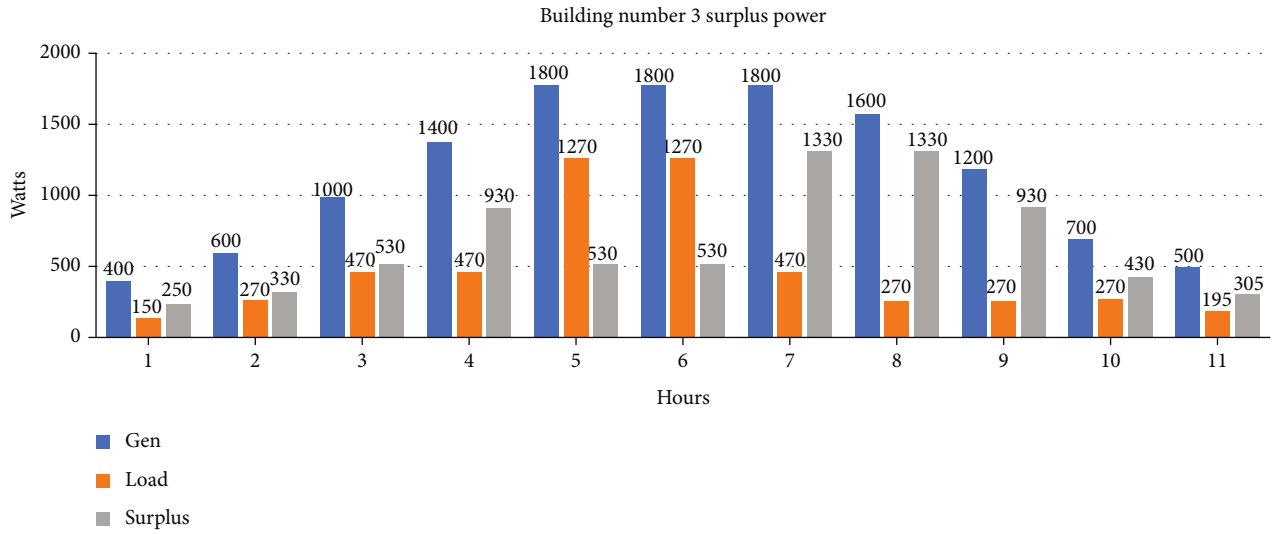

Figure 5: Building's behavior capacity.

Table 1: Collaborating on sharing electricity bills.

Collaborating on sharing electricity billings monthly basis								
Sr.#	Buildings	Electricity generation (kWh)	Electricity consumed (kWh)	Required electricity (kWh)	Surplus electricity (kWh)	Shared electricity (kWh)	Remaining surplus electricity (kWh)	Total bill unit s*10 = RS PKR
1	B1	266	138		128		16	
2	B2	245	357	112		B1 shared 112 units with B2		1,120
3	B3	354	454	100		B4 shared 100 units with B3		1000
4	B4	225	100		125		25	

(i) Here, 1.5 = energy loss in the system

(ii) Power generation factor (PGF) is used in calculating PV panel size, and it varies from location to location depending upon the climate condition of the site

No.of PV panels needed = (watt – peak/panel rating)
Total watt of appliances = Σ watt of appliances

(iii) Inverter size should be larger than 25-30% of the total watt of appliances

Battery capacity (Ah) = total watt – hour per day $*$ days of autonomy

(iv) Battery loss$*$DOD$*$nominal battery voltage

Charge controller rating = total short- circuit current of PV array $*$ 1.3

(v) Solar panels adjust on an aluminum frame; there are 3 frames on the rooftop with an angle inclination (182 degree south or zero degree north). Each frame consists of two 250-watt solar panels

3.7. Capacity. The capacity of the building is 1500 watts for buildings 1, 2, and 4 whereas building no. 2 is 2000 watts.

Depending on the power of the building, we have different no. of panels for each building as follows:

No. of panels for 1500 W buildings = 1500/250 = 6 panels

No. of panels for 2000 W buildings = 2000/250 = 8 panels.

Thus, buildings 1, 2, and 4 have six monocrystalline solar panels whereas building 4 has 8 panels.

4. Result and Discussion

The process is done based on a collaborative sharing system of individuals where each of them would share the electricity load. This collaborative sharing model is highly recommendable to dig maximum benefits out of solar energy. The leading prospect of this project is the collaborative sharing of the energy where the surplus light of each house would be traveled to the houses with less light comparatively. This could be rated as the foremost emerging business model as well.

4.1. Decentralized Integrated System. This system has worked on the principle of a collaborative sharing mechanism as the buildings are integrated. Due to integration, there will be no wastage of electricity. These buildings share the extra amount of electricity that will be recorded by our

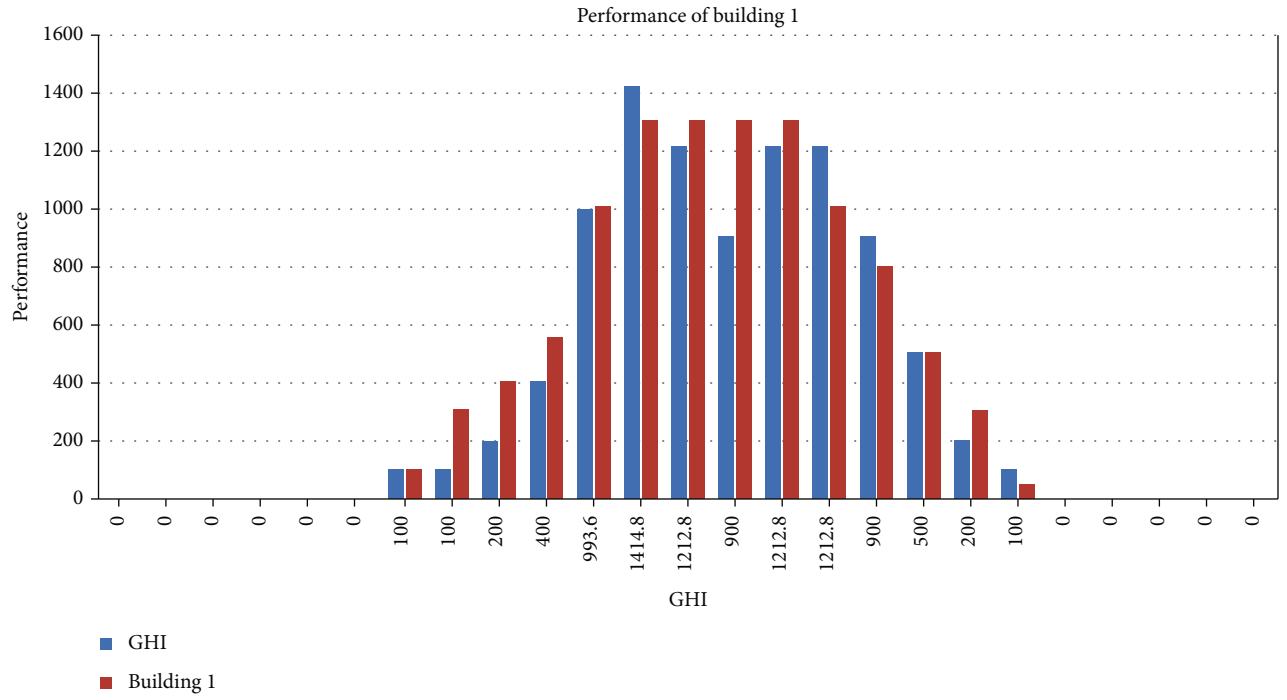

Figure 6: Performance of building 1 GHI.

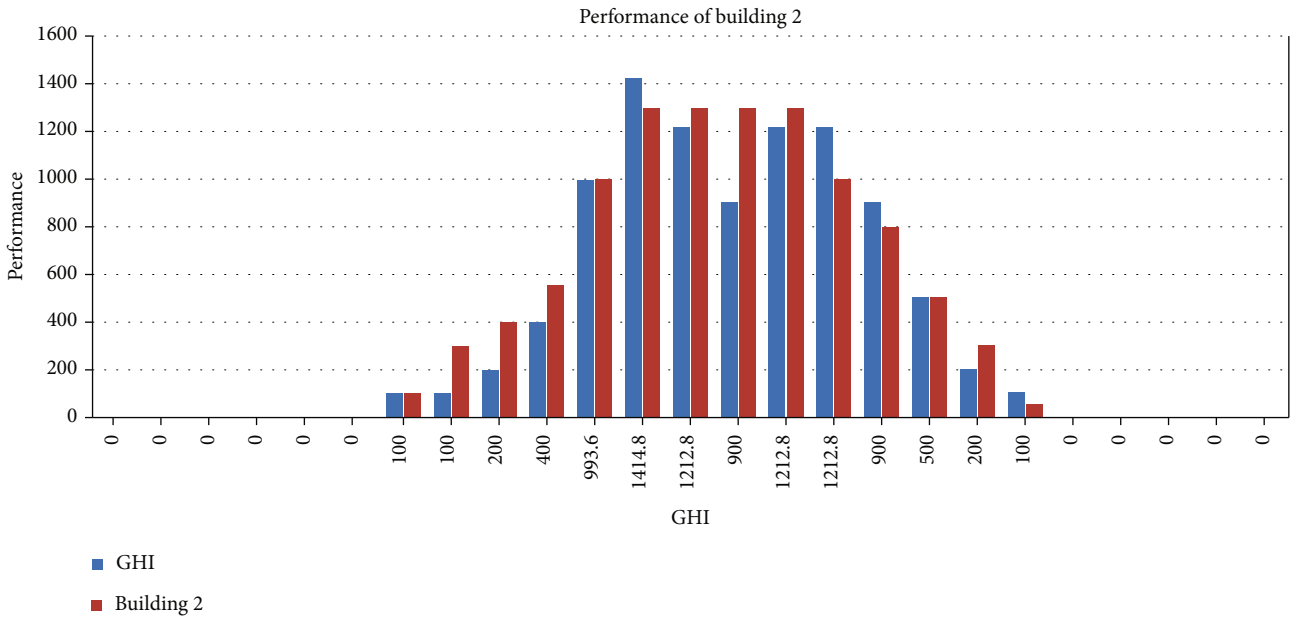

Figure 7: Performance of building 2 GHI.

decentralized solar energy system. In this way, there is maximum usage of solar electricity.

4.1.1. Good Business Model. Due to maximum usage of energy and cost minimization, this system is a good individual and industrial business model. Similarly, it has maximum efficiency and a minimum lifetime of 25 years when the load is 80%.

4.1.2. Surplus Power Generation and Utilization. Our system has efficiently recorded the power generation and utilization by all the buildings. Similarly, any building has surplus power that will also show in our record. The following figure shows the complete data including power generation, utilization, and surplus power. There are energy meters attached to each home in the entire building and an energy meter overall for a building. These

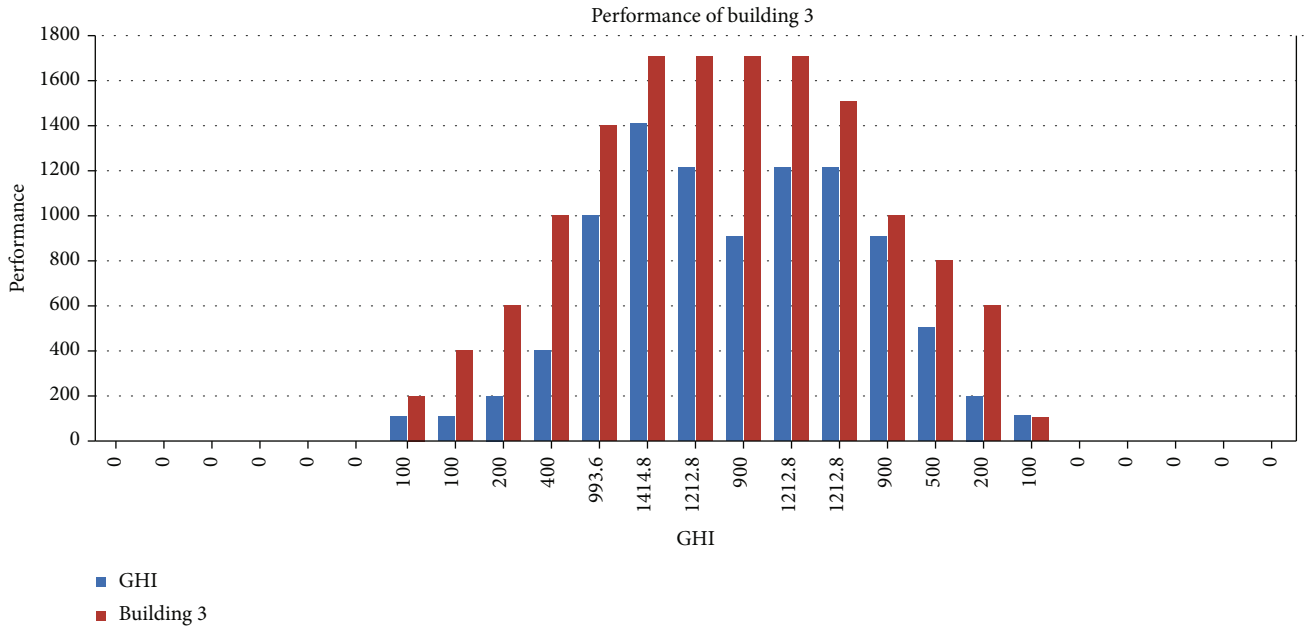

Figure 8: Performance of building 3 w.r.t GHI.

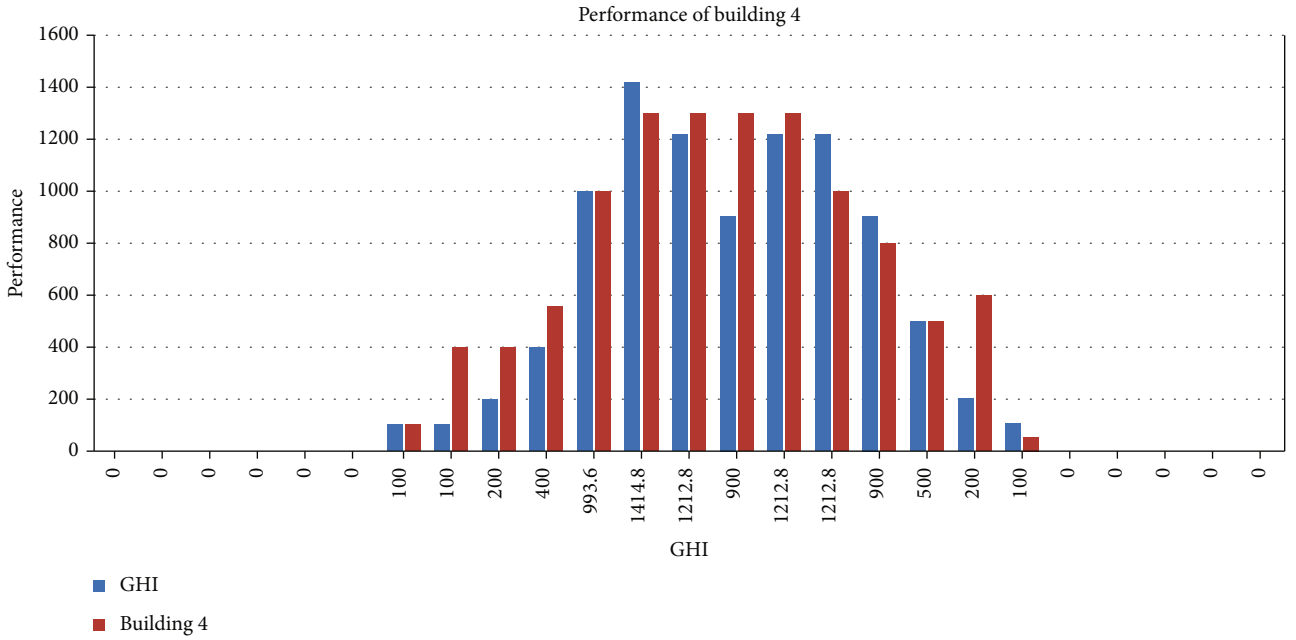

Figure 9: Performance of building 4 w.r.t GHI.

meters calculate records of energy used, and an overall meter calculates the energy produces utilized and surplus power. Similarly, there is also a recording unit shared by a building with another building. Due to the integrated system, the surplus power is shared between all the buildings depending upon their requirements and is recorded by our system. Smart integrated decentralization is a business model; it is a billing mechanism that credits solar energy system owners for the electricity they add to the other buildings due to a collaborative sharing mechanism. For example, on the off chance that a private client has a PV framework on their rooftop, it might create more power than the home uses during sunlight hours.

How much does a smart integrated decentralized solar energy system saves consumers?

To help clients understand how much they will save from this system, we are providing a simple formula to calculate your savings.

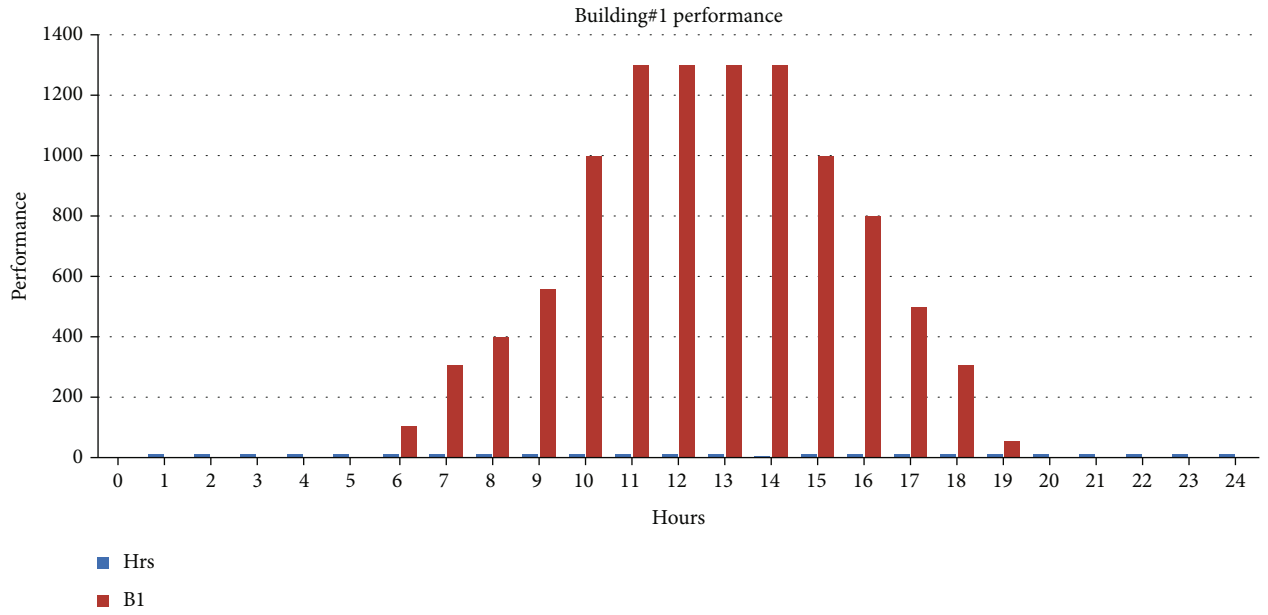

Figure 10: Performance of building 1 on hourly basis.

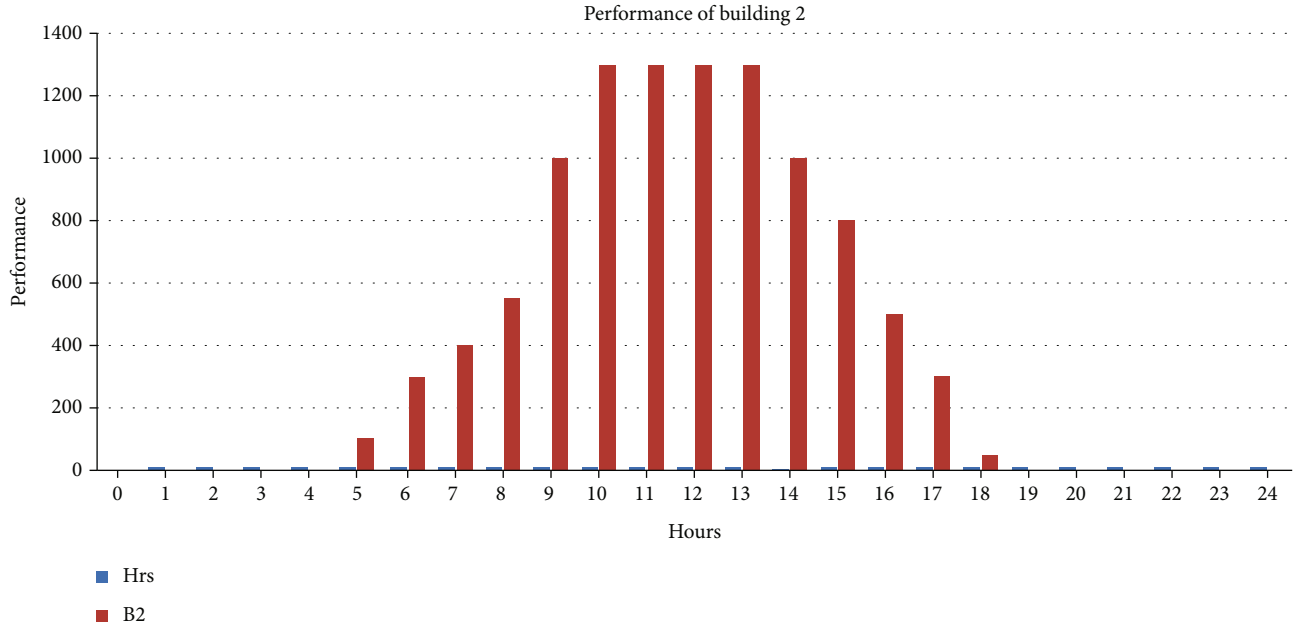

Figure 11: Performance of building 2 on hourly basis.

$$\text{Saving formula : solar panels installed (watts)} \times (\text{surplus power per day(units)}) \times \text{electricity unit rate (Rs.)}. \quad (2)$$

Installing 1000-watt (250 watt × 4 pcs) solar panels (A1 brand) by applying the power factor of $(1.5 * 1000) = 1500$ watts (250 watt × 6 pcs) will generate consumers an average of 4,000 watts per day; this equals savings of 4 electricity WAPDA units per day as shown in Figure 5.

Similarly, installing 2000-watt solar panels will generate consumers (A1 brand) by applying the power an average of 7425 watts per day; this equals to savings of 7.4 electricity WAPDA units per day on average. However, solar power generation is likely to increase during summers when we receive a sample amount of sunshine.

4.2. Collaborative Sharing Financial Model. The recent electricity bill of Islamabad Electric Supply Company (IESCO) WAPDA is calculated. The calculated weight of consumed

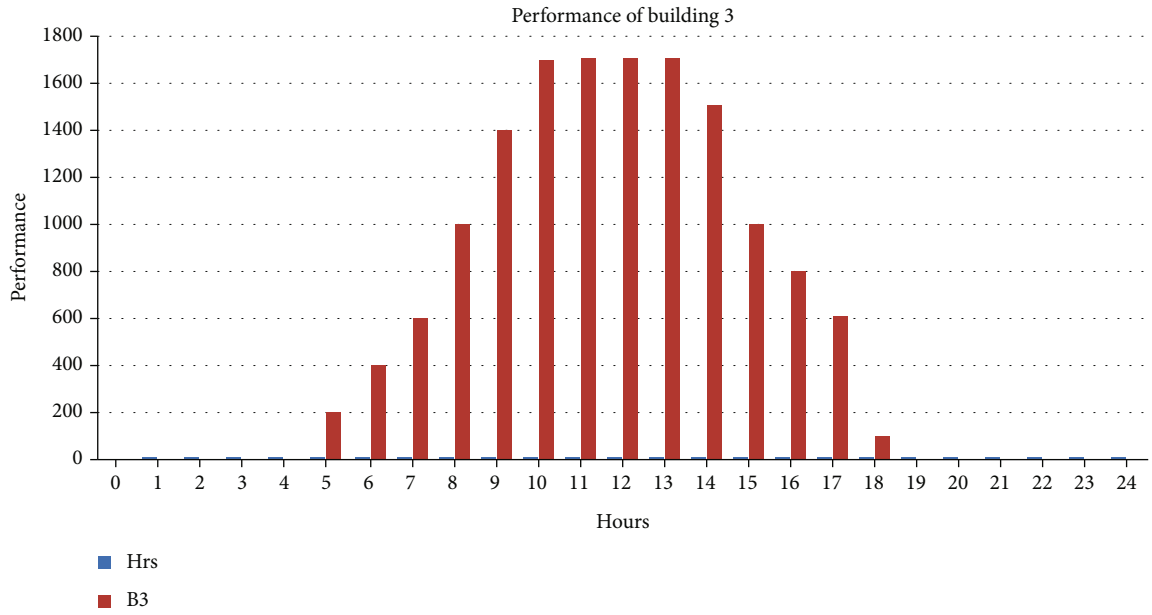

Figure 12: Performance of building 3 on hourly basis.

units is as follows: they consumed three hundred units that were rated at Rs.10.20 per unit, and seventy-one units were calculated at Rs.17.60 per unit. According to these calculations, the total sum was Rs.4309.6. These readings are excluding the taxes yet. It means that the WAPDA bill has quite different ratings every month. And if we include the taxes in these readings, we get the total amount of Rs.5707. This entire calculation is considered to aware the consumer that the WAPDA bill deviates every month. Per unit, the rate is increased as well. If we divide the total amount of Rs.5707 by the total unit consumed 371, we can get a per unit cost that is Rs.15.23. If we compare the WAPDA rate with my introduced decentralized solar energy system, the WAPDA rate is much higher. I have fixed the rate at Rs.10 per unit in my newly launched business model. There will be no additional charges, duty charges, or hidden taxes. So, the electricity I am selling at the fixed rate of Rs.10 per unit is ridiculously cheap in the market. This low-cost electricity is available at your doorstep that you can share according to the collaborative sharing basis that will not range any certain variable.

This financial model included the comparison of WAPDA electricity bills which were chosen from the IESCO market with my proposed cost per unit. These calculations are to make sure that proposed system is much better than WAPDA system.

4.2.1. Collaborating on Sharing Electricity Billings Monthly Basic. Table 1 explains the process through which the consumers will utilize the electricity on a collaborative sharing basis. Building one is generating 266 kWh electricity, consuming 138 kWh with the surplus electricity of 128 kWh. If we look at the remaining surplus electricity, its reading is 16 kWh. Coming towards the second building, it is generating 245 kWh power; its electricity consumption is 357 kWh, and the required electricity is 112 kWh. As building two has less power generation in comparison to building 1, the electricity load of building 2 is greater than its generation, so required 112 kWh. Building one will share 112 units with building 2. The total bill will be paid by building two at the end of the month which is calculated at Rs.1120 according to the fixed per unit rate of Rs.10. Building three is generating 354 kWh, its electricity consumption is 454 kWh, and the required electricity is 100 kWh which is not enough for building 3 so it will fulfill its need from building 4 by sharing 100 kWh, whereas building four generates 225 kWh units and its consumption is 100 kWh with the surplus light of 125 kWh. A remaining surplus would be 25 kWh, and the total bill will be paid by building three which is calculated to be Rs.1000.

4.3. TMY File and Irradiance. Taking the exact data of Taxila and attached a TMY file with it and checked the irradiance of Taxila. According to that irradiance, we have installed the setup, and our performance is based upon that. I have compared the Global Horizontal Irradiance (GHI) to find out the actual performance of buildings. That comparison is shown in the graphs.

4.3.1. Performance of Building 1 w.r.t GHI. Providing the load on the system of building 1 and due to irradiance, the performance of the building is as follows: here, on the x -axis, we have irradiance (GHI), and on the y-axis, we have a performance of the building concerning the GHI.

This graph explains the performance of Figure 6 concerning irradiance.

4.3.2. Performance of Building 2 w.r.t GHI. This graph explains the performance of building 2 concerning irradiance (Figure 7).

4.3.3. Performance of Building 3 w.r.t GHI. Similarly, like other buildings, by providing the load on the system of building 3 and due to irradiance, the performance of the

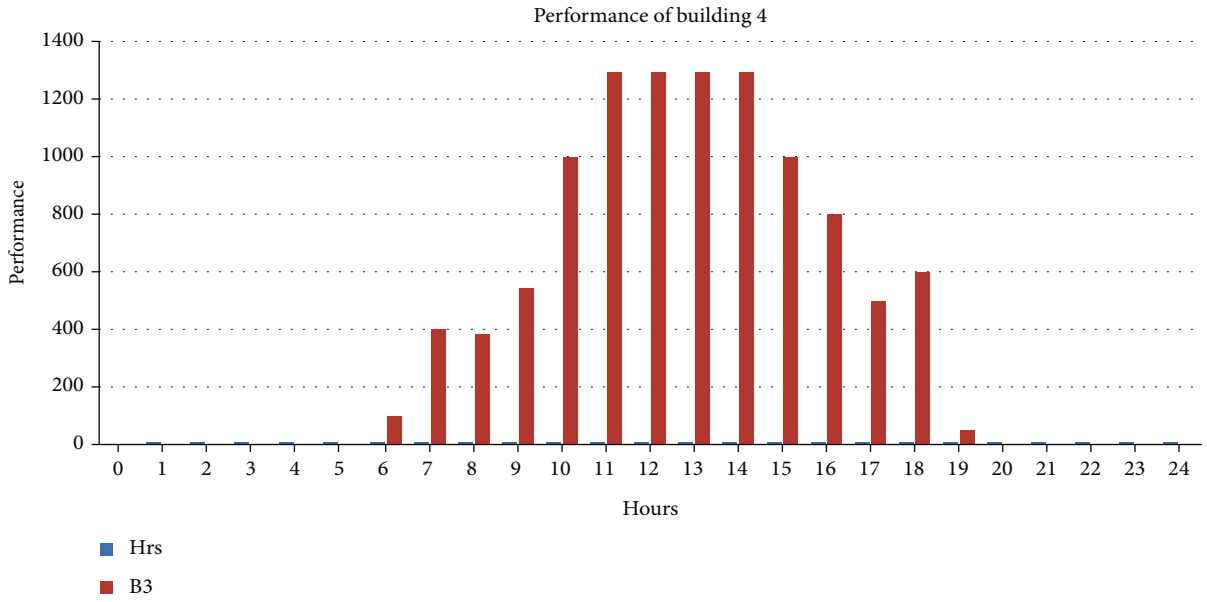

Figure 13: Performance of building 4 on hourly basis.

building is as follows: here, on the x-axis, we have irradiance (GHI), and on the y-axis, we have a performance of building concerning the GHI.

This graph explains the performance of building (Figure 8) concerning irradiance.

4.3.4. Performance of Building 4 w.r.t GHI. This graph explains the performance of building 9 concerning irradiance (Figure 9).

4.4. Building Performance on Hourly Basis. During the measurement of the performance of buildings, I also have calculated their performance on an hourly basis for a day. It is a one-day generation of solar panels according to the impact of irradiance of the TMY file. The following graphs explain the performance of the building on an hourly basis of a day.

4.4.1. Performance of Building 1 on an Hourly Basis. This graph explains the B1 performance of a day on an hourly basis (Figure 10).

4.4.2. Performance of Building 2 on an Hourly Basis. This graph explains the B2 performance of a day on an hourly basis (Figure 11).

4.4.3. Performance of Building 3 on an Hourly Basis. This graph explains the B3 performance of a day on an hourly basis (Figure 12).

4.4.4. Performance of Building 4 on an Hourly Basis. This graph explains the B4 performance of a day on an hourly basis (Figure 13).

Societies can be made more cost-effective by using this smart integrated decentralized solar energy system; people will get the benefit of using cheap electricity at their doorstep. By implementing the strategies of solar energy systems in small networks, the society will get a chance to buy the cheapest electricity in the town at the fixed rate of Rs.10 per unit (kWh) which will inspire a better idea of electricity consumption at a lower rate.

5. Conclusion

I started comparing among the unit consumers monthly and yearly for 2018 and 2019. After this field, study data also calculated the unit's prices of WAPDA with a comparison of our system. The Arduino Mega 2560 microcontroller has been used in this project. This microcontroller is used for this system for data monitoring and data recording and working efficiently for surplus light and shared with other buildings. The leading prospect of this project is the collaborative sharing of the energy where the surplus light of each house would be traveled to the houses with less light comparatively. This could be rated as the foremost emerging business model as well.

The generation of kWh from this decentralized integrated solar energy system and the working process of the system are listed below:

(i) The basic reason and working process is to read out the power generated and then deliver this information to the controller

(ii) All that process will resume after judging, monitoring, and specifying the data

(iii) Some relay switches deal with the function of monitoring the data inflow and outflow on the meter

(iv) After that, the energy will be traveled to the house where there would be a need for extra units through these relay switches

Integrated decentralized solar energy system will offer cheaper and fixed electricity rates than regular market rates offered by WAPDA to the layperson which will create a massive change in the electricity bills. The power will be generated and utilized by all the buildings. Similarly, if any building has surplus power that will also be shown in our record, it will be shared with the required house that will have less electricity generation. Due to maximum usage of energy and cost minimization, this system is a good industrial business model.

Data Availability

Data will be made available on reasonable request.

Conflicts of Interest

The authors declare that they have no conflicts of interest.

References

[1] B. Lertanantawong, A. Krishna Prasad, T. C. Bun, K. Vestergaard, and W. Srebrenica, "Multiplexed DNA detection with DNA tweezers in a one-pot reaction," *Materials Science for Energy Technologies*, vol. 2, no. 3, pp. 503–508, 2019.

[2] A. Kumar, N. Varshney, S. Poddar, K. Felipa, and S. Kumar, "Optimizing a detection method for estimating polyunsaturated fatty acid in human milk based on colorimetric sensors," *Materials Science for Energy Technologies*, vol. 2, no. 3, pp. 624–628, 2019.

[3] P. Raised, A. Suhail, and P. Singh, "Photocatalytic water decontamination using graphene and ZnO coupled photocatalysts: a review," *Materials Science for Energy Technologies*, vol. 2, no. 3, pp. 509–525, 2019.

[4] M. M. Chaitra and J. G. Manjunath, "Poly (l-Proline) modified carbon paste electrode as the voltammetric sensor for the detection of estriol and its simultaneous determination with folic and ascorbic acid," *Materials Science for Energy Technologies*, vol. 2, no. 3, pp. 365–371, 2019.

[5] V. Arora, R. Kumar, R. Kumar, and S. Yadav, "Separation and sequestration of CO_2 in geological formations," *Materials Science for Energy Technologies*, vol. 2, no. 3, pp. 647–656, 2019.

[6] V. Bores and R. Srivastava, "Process parameter optimization for lateral flow immunosensing," *Materials Science for Energy Technologies*, vol. 2, no. 3, pp. 434–441, 2019.

[7] K. L. Palin, "Atmospheric electrification in the solar system," *Surd Geophysics*, vol. 27, no. 1, pp. 63–108, 2006.

[8] S. Devasthanam, G. Bhaskar, and C. Must Ansar, "Utilization and recycling of end of life plastics for sustainable and clean industrial processes including the iron and steel industry," *Materials Science for Energy Technologies*, vol. 2, no. 3, pp. 634–646, 2019.

[9] A. B. Kulkarni and S. N. Mathcad, "Variation in structural and mechanical properties of Cd-doped Co-Zn ferrites," *Materials Science for Energy Technologies*, vol. 2, no. 3, pp. 455–462, 2019.

[10] K. N. Nwangwu, P. Metabola, and E. Donta, "An overview of solar power (PV systems) integration into electricity grids," *Materials Science for Energy Technologies*, vol. 2, no. 3, pp. 629–633, 2019.

[11] S. Dey and G. C. Dhal, "Catalytic conversion of carbon monoxide into carbon dioxide over spinel catalysts: an overview," *Materials Science for Energy Technologies*, vol. 2, no. 3, pp. 575–588, 2019.

[12] S. K. Sahu, A. K. Bohra, P. G. Abichandani et al., "Design and development of DC to DC voltage booster to integrate with PbTe/TAGS-85 based thermoelectric power generators," *Materials Science for Energy Technologies*, vol. 2, no. 3, pp. 429–433, 2019.

[13] D. C. Sharma, "Article in press: transforming rural lives through decentralized green power," *Futures*, vol. 39, pp. 583–596, 2007.

[14] Z. Yuridia, "Opportunities and challenges of renewable energy and distributed generation promotion for rural electrification in Indonesia," *Green Energy and Technology*, pp. 102–107, 2010.

[15] C. S. Factors, *Rural electrify cation*, pp. 28–31, 2001.

[16] M. Luisa, D. Silvestre, S. Fauzia, E. R. San Severino, and G. Zizzi, "How decarbonization, digitalization and decentralization are changing key power infrastructures," *Renewable and Sustainable Energy Reviews*, vol. 93, pp. 483–498, 2018.

[17] Y. Liu, K. Zou, X. A. Liu, J. Liu, and J. M. Kennedy, "Dynamic pricing for decentralized energy trading in micro-grids," *Applied Energy*, vol. 228, no. May, pp. 689–699, 2018.

[18] M. J. Naga, *Challenges facing deputy head teachers in managing students in secondary schools in Kangema district*, Murang'a County, 2013.

[19] G. B. Kufa, *Challenges of implementation of strategic plans in public secondary schools in Limuru district*, Kiambu county, 2014.

[20] J. Leakey, *Evaluating Computer-Assisted Language Learning: An Integrated Approach to Effectiveness Research in CALL*, Peter Lang, Oxford; New York, 2011.

[21] D. P. M. Maithya, "Evaluation of implementation of the revised Kiswahili curriculum: a case of a teachers' college in Kenya," *Journal of Education and Practice*, p. 6, 2013.

[22] G. A. Karimi, *Factors affecting the use of information and communication technology in teaching and learning in secondary schools in Kangema- Murang'a county*.

[23] M. J. Jangir and M. James, *Loan repayment and sustainability of government funded micro-credit initiatives in Murang'a county*, vol. 5, no. 10, 2014Kenya, 2014.

[24] M. W. Sawka, S. T. Niche, and P. G. Kagoro, *Influence of school language policy on pupils' achievement in English language composition in public primary schools in Trans-Nozi West Sub-County*, Kenya, 2019.

[25] M. Hasan Nia, A. Abbas Nejd, A. M. Goaders, M. Alizadeh, and P. Saadian, "Cogeneration solar system using thermoelectric module and Fresnel lens," *Energy Conversion and Management*, vol. 84, pp. 305–310, 2014.

[26] K. Gillingham, A. Keyes, and K. Palmer, "Advances in evaluating energy efficiency policies and programs," *Anu. Rev. Retour. Econ.*, vol. 10, no. 1, pp. 511–532, 2018.

[27] M. O. I. Musa, T. E. H. El-Gorshin, and J. M. H. Amirkhani, "Bounds on GreenTouch GreenMeter network energy efficiency," *Journal of Lightwave Technology*, vol. 36, no. 23, pp. 5395–5405, 2018.

[28] H. Tatiana, L. M. Karpenko, F. V. Olesya, S. I. Yu, and D. Svetlana, "Innovative methods of performance evaluation of energy efficiency projects," vol. 17, no. 2, p. 12, 2018.

[29] E. Shove, "What is wrong with energy efficiency?," *Research & Information*, vol. 46, no. 7, pp. 779–789, 2018.

[30] L. Haise, M. Ellsberg, and M. Gott Moeller, "A global overview of gender-based violence," *International Journal of Gynaecology and Obstetrics*, vol. 78, pp. S5–S14, 2002.

[31] C. T. Russell, T. L. Zhang, M. Delve, W. Magness, R. J. Strangeways, and H. Y. Wei, "Lightning on Venus inferred from whistler-mode waves in the ionosphere," *Nature*, vol. 450, no. 7170, pp. 661-662, 2007.

[32] I. G. Lozoya, A. S. Martínez, N. G. Sánchez et al., "Experiences end relation con la violence de genaro de la población que consulta end Atencio Primaria," *Revista Clínica de Medicina de Familia*, vol. 3, no. 2, 2010.

[33] G. Terry, Ed., *Gender-Based Violence*, Oxfam, Oxford, 2007.

[34] N. F. Russo and A. Pimlott, "Gender-based violence: concepts, methods, and findings," *Annals of the New York Academy of Sciences*, vol. 1087, no. 1, pp. 178–205, 2006.

[35] J. L. Jacobson, "Transforming family planning programmes: towards a framework for advancing the reproductive rights agenda," *Reproductive Health Matters*, vol. 8, no. 15, pp. 21–32, 2000.

[36] D. Olaseni and T. G. Adegoke, "Personal, situational and socio-cultural factors as correlates of intimates partner abuse in Nigeria," *Journal of Social Sciences*, vol. 16, no. 1, pp. 57–62, 2008.

Hindawi
International Journal of Photoenergy
Volume 2022, Article ID 7715214, 14 pages
https://doi.org/10.1155/2022/7715214

Research Article

Experimental Investigation and Comparison of the Net Energy Yield Using Control-Based Solar Tracking Systems

Ibrahim Sufian Osman, Ibrahim Khalil Almadani, Nasir Ghazi Hariri, and Taher Saleh Maatallah

Department of Mechanical and Energy Engineering, College of Engineering, Imam Abdulrahman Bin Faisal University, P. O. Box 1982, Dammam 31441, Saudi Arabia

Correspondence should be addressed to Ibrahim Sufian Osman; ibrahim-sufian@hotmail.com

Received 28 March 2022; Accepted 6 June 2022; Published 18 June 2022

Academic Editor: Hafiz Muhammad Ali

As the world trend is going towards renewable energy, solar photovoltaic (PV) energy shines the most due to the low generation cost especially by using the latest PV cell technologies and materials, although the conventional silicon cell has an efficiency in the range of 15-16%. A PV tracking system (PVTS) could be a considerable method to increase electrical PV efficiency. In this study, the performance enhancement of the daily output power and energy has been experimentally investigated using single- and dual-axis tracking mechanisms for flat-plate conventional PV panels under the insolation conditions of the Eastern province of Saudi Arabia (SA). In the current study, the active PVTS has been designed and implemented with PID controllers and controlled in real-time with an embedded system. The fixed-tilt (FTPV), single-axis solar tracking system (SAST), and dual-axis solar tracking system (DAST) were tested simultaneously under clear-sky conditions. The PV electrical energy balance has revealed that the energy consumed by the electrical controllers of the SAST and DAST is 3.4% and 3.9%, respectively. In addition, the energy losses due to the actuators of the SAST and DAST are 7.8% and 13.0%, respectively, where they contributed mainly to the energy losses. However, the PV energy production by the DAST was high enough to compensate for the higher actuating mechanism losing rate compared to the SAST and performed incremental net energy output of around 8.64%. On other hand, the DAST and SAST were more efficient than the FTPV recording higher net energy increase by 28.98% and 18.73%, respectively.

1. Introduction

As the human population grew alongside technology, the energy demand increased rapidly day after another, which led to the industrial revolution at the end of the 19th century, causing a vast consumption of fossil fuel. Although it is a dependable energy source, it has many drawbacks such as greenhouse gas emissions, transportation adversity, and exhaustibility [1–3]. Due to these flaws, in the last decade, renewable energy sources like wind, solar, and geothermal became relevant as they are infinite and most importantly eco-friendly [1–4].

Solar energy is the most used and promising renewable energy source since solar energy technologies have shown considerable improvements in performance and reduction in cost in the past few years [5, 6]. In addition, the annual energy potential received from the sun is approximately 8000 times more than the average energy usage of the whole world [7]. There are three main solar systems: photovoltaic (PV) system, solar thermal system, and hybrid system [8], where a photovoltaic system produces electrical energy, a solar thermal system produces thermal energy, and a hybrid system produces both electric and thermal energy [9]. Recently, energy generated from PV systems became dominant in the market considering that it is noise-free, highly efficient, and inexpensive in production and maintenance costs [3, 10, 11].

Overall, the efficiency of a PV system is affected by many factors, including environmental conditions, such as the PV cell temperature, the amount of solar irradiance, and soiling effect [12–15]. One approach to enhance the overall efficiency of a PV system is by increasing the amount of solar

irradiance that the system receives [12, 14]. The amount of solar irradiance depends significantly on the angle between the sun rays and the normal of the module (incidence angle), so as long as the panel is fixed, it can only receive the maximum amount of irradiance when the sun is perpendicular to the module's surface. Thus, a PVTS tends to improve the PV system efficiency via detecting the direction of the sun rays and adjusting the orientation of the PV module to minimize the incidence angle [16–18].

Solar tracking systems (STS) have three main categories: solar trackers based on driving technique, solar trackers based on movement degree of freedom, and solar trackers based on control method [9]. The first category is solar trackers based on driving techniques with two main types of driving techniques: passive STS and active STS [5, 19, 20]. The second category is solar trackers based on the degree of freedom of the motion, which in general are divided into two subcategories, single-axis solar tracking systems (SAST) and dual-axis solar tracking systems (DAST) [21, 22]. The third category is solar trackers based on the control method, and they have three primal types of control scheme, open-loop, closed-loop, and hybrid (combined) control systems [9, 23, 24]. Various control algorithms can be implemented in solar tracking (ST) techniques, for example, simple on-off, PID, fuzzy, and LQR controllers [25–28]. [29] states that the on-off, fuzzy, and PID controllers are the most used controllers with a utilization percentage of 57.02%, 10.53%, and 6.14% of STS, respectively, while 26.31% of STS are other types of control algorithms. Although all these controllers are used to optimize the PV system power consumption, there are still some concerns regarding the ST technology, such as shading effect, performance under different weather conditions or different regions, initial cost, and maintenance cost.

da Rocha Queiroz, J. et al. [22] assembled a DAST based on Arduino integrated development environment in process language. The DAST has shown a 67.28% total gain and 63.22% net gain while on a cloudy day the total gain was 37.84% and the net gain was equal to 28.99%. In the case of a rainy day, 11.71% total gain is recorded and 19.47% loss. That shows the effect of different weather conditions on the DAST PV system, even though the DAST shows a performance improvement when appropriately applied.

Du, X. et al. [30] highlighted that DAST technology fabrication cost is almost 40% of the total cost of the whole PV system. Furthermore, DAST with an active driving technique consumes more energy than SAST to alter its position regarding the sun since it usually consists of two motors that might consume more power than gained, causing the net efficiency to drop. The cost of the DAST may lead to a greater economic-friendly alternative, and that is the SAST.

Ngo, X. C. et al. [31] studied the efficiency of the SAST in Vietnam (Quang Tri Province) while considering the tracking system energy consumption on different weather conditions. The performance on a sunny day showed an increase of 33.3% in energy generation and an efficiency increase of about 30.3%. While on a cloudy day, a huge efficiency drop accrues compared to a sunny day, where the net increase in efficiency is measured to be 3.2%. The worst-case scenario is when it is rainy; although there is a power generation difference of 6.7%, the net efficiency drops to about -2% since the power consumed via the tracking is more than the energy gained by the solar system itself.

Ruelas, J. et al. [32] made a low-cost PV SAST by using the efficiency as a function of time technique (EFO) at Mexico (Cd. Obregón). The prototype was designed with specific parameters to maintain the cost of production and maintenance low, while its working principle is based on three-point motion control with azimuth angles of 30°, 90°, and 120°. It was found that the system achieved an increase in the collection efficiency of about 24% and a price of 27% lower than the traditional commercial trackers. It is noticeable that the STS has different outcomes depending on the weather conditions of where it is installed, which needs to be further studied.

Eldin, S. A. S. et al. [16] studied the effects of extreme exposure to solar irradiance and how it affects the PVTS temperature and performance. The results of the study showed a 39% gain in electrical energy in a cold environment (Berlin, Germany). On the other hand, results of the same PV STS in the hot environment (Aswan, Egypt) showed an electrical energy gain that does not exceed 8%. The study concludes that the energy consumption from the tracking system was considerable, where the tracking system would not be as useful in hot weather areas as it is in cold weather areas.

In the literature, few studies were conducted in the Arab Gulf countries regarding the feasibility of STS, and most of them are simulation-based ones. In effect, [33] studied the effect of different STS configurations and adjustment periods on the power production in the western region of Saudi Arabia (in Makkah city, SA). The simulation study found that the DAST and SAST produced 34% and 20% power more than the FTPV, respectively. Similarly, [34] investigated the effect of STS on multiple performance indicators in 32 sites in SA. The simulation-based results concluded that DAST is an infeasible choice for the region from an economical point of view, since the difference in energy production between SAST and DAST is only 3-4.5%, and SAST produces 28-33% energy more than the FTPV. Another simulation work was elaborated by [35] in Kuwait, and it was found that using SAST and DAST, the annual energy yield could be increased by 24.7% and 29%, respectively. Furthermore, [36] experimentally carried out a study in order to optimize and investigate the performance of SAST in Bahrain using a micro-controller-based system. The optimized STS has shown that the energy yield might be increased up to 40% compared to FTPV using the proposed STS. [37] compared the experimental average power production of the FTPV and STS systems against their simulation results using the local weather conditions of the United Arab Emirates (UAE). The obtained results showed that there is an increase in the output power of the PV modules of 17.28% compared to FTPV by using an azimuthal STS. The simulation results showed a good agreement with the experimental ones, and the mean relative error was about 2.7%. Moreover, another work was conducted in UAE [38] to evaluate the rate of output power increment that can be achieved by

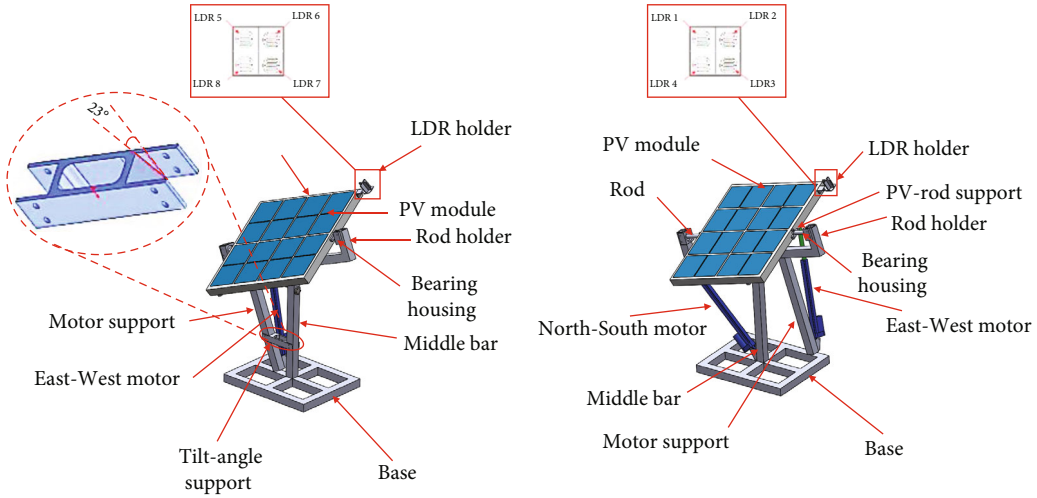

Figure 1: (a) SAST and (b) DAST CAD models.

Table 1: The electrical setup for the experiment.

Component	Model	Specification	Qty
Current sensor	ASC712	Input: 5 V Frequency: 80 kHz Sensitivity: 185 mV/A Error: 1.5%	6
Motor driver	L298N	Input: 12 V Operating current: 0-36 mA Peak current: 2 A	2
Secure digital (SD)	SDHC	Input: 5 V Operating current: 0.2-200 mA	2
Real-time clock (RTC)	DS3231	Input: 5 V Frequency: 100 kHz	1
Power resistor	JIANXIN-09-13-318-02	Power rating: 100 W Resistance value: 8 Ω Tolerance: 5%	3
On/off switch	—	Rating: 3A/6A 250 V Electrical life: 10^3 cycles	1
LDR	—	Input: 5 V	6
Arduino Mega	ATmega2560	Input: 12 V Frequency: 16 MHz	1
Linear motor	—	Input: 12 V Max. speed: 20 mm/s	3
PV module	—	Pmax = 54.2 W Imax = 3.28 W Vmax = 16.54 W Efficiency = 14.24 W	3
Battery	—	Capacity: 100 Ah	1

integrating the STS to a PV panel and Fresnel linear concentrating system. The simulation results revealed that tracking the sun-azimuth can increase the electrical output power by 14.8% and 15.3% compared to the FTPV panel and linear PV concentrator, respectively. Finally, [39] designed a cheap, high-accuracy, and closed-loop DAST using a sun position algorithm with the aim of studying the feasibility of the system in Qatar. The results demonstrated that using such a system may lead to an increase in the PV power generation by 13.9% with respect to the FTPV.

In all the studies mentioned above, researchers have carried on the gain in instantaneous and integrated power yields over a typical measurement time frame that was made by solar tracking mechanisms with respect to FTPV.

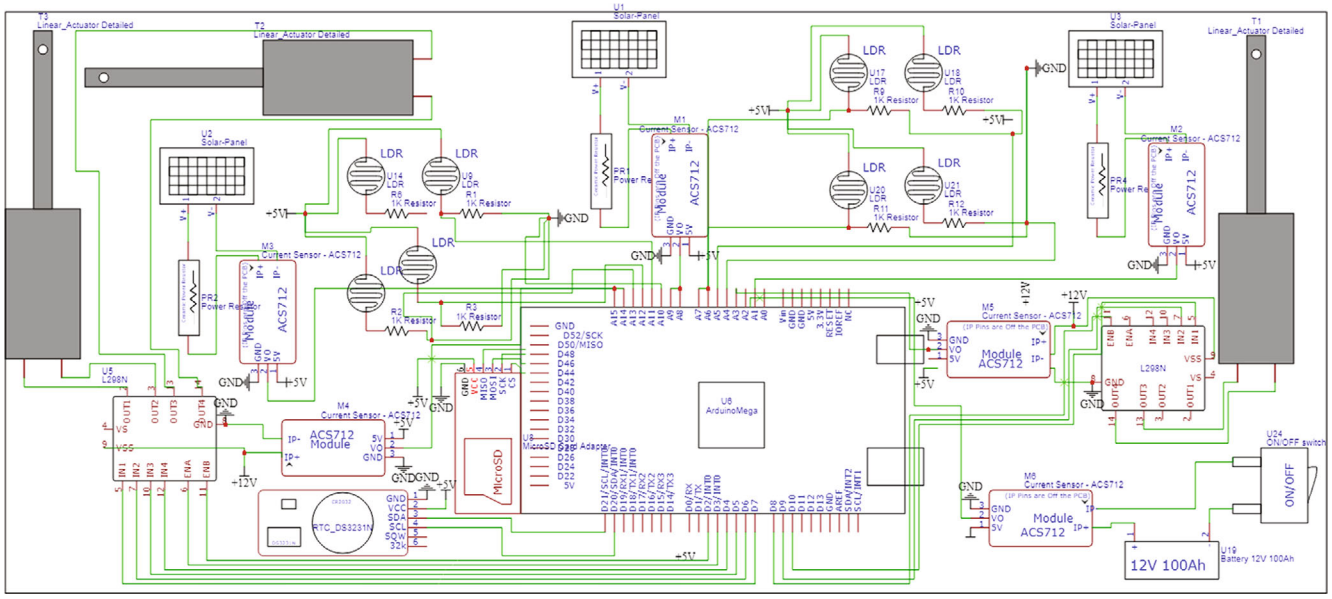

Figure 2: The electrical schematic diagram for the FTPV, SAST, and DAST.

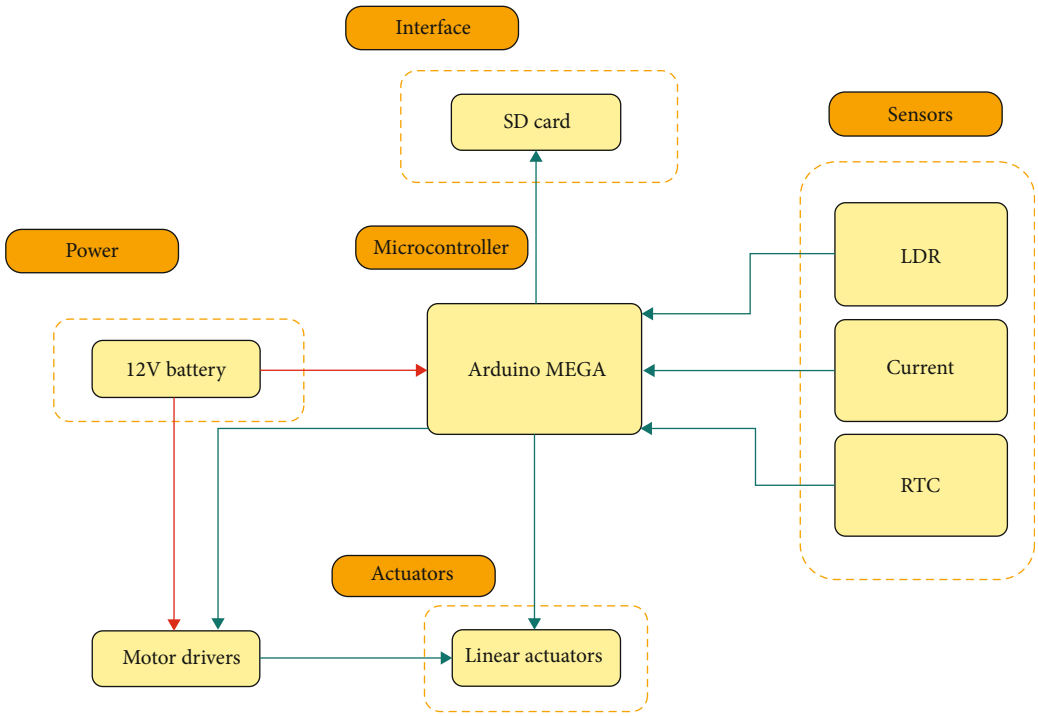

Figure 3: Electrical block diagram for SAST and DAST.

However, the contribution of the actuators and particularly the controllers in the energy consumption and therefore the net output power of the tracked flat-plate PV panels have never been analyzed and discussed in detail. Furthermore, the improvement rates in power and energy of the tracking systems have neither been numerically nor experimentally investigated under the local weather conditions. This is because no previous research studies have experimentally analyzed the net electrical energy of a self-consumption fixed or tracked PV panel under the Saudi environmental conditions and more particularly of Dammam city (26°26′03″ N, 50°06′11″ E).

2. Materials and Methods

2.1. Mechanical Design. The mechanical design of SAST and DAST is firstly made using a computer-aided design (CAD) software and underwent many enhancements and improvements to the mechanical structure of the trackers (as seen in Figure 1). The design had to be flexible enough to give

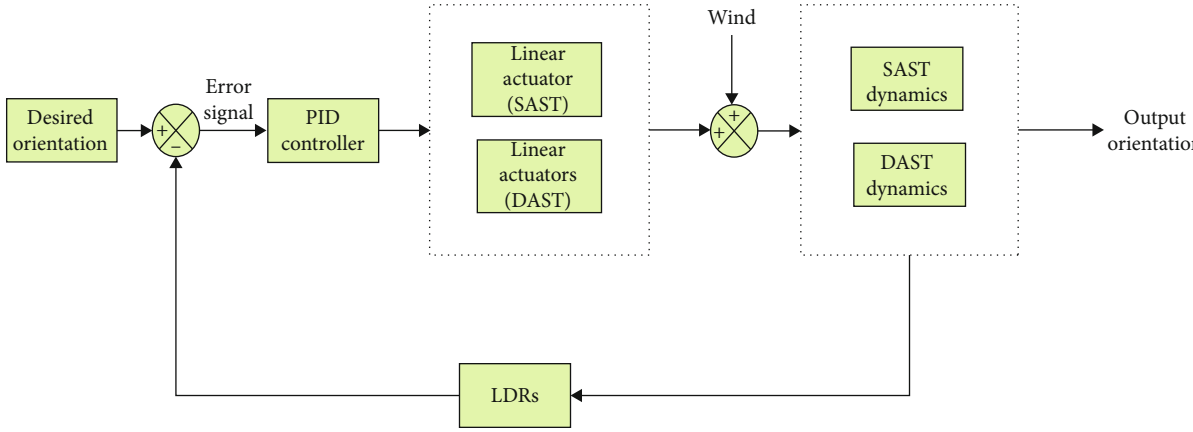

Figure 4: Block diagram of the close-loop feedback system.

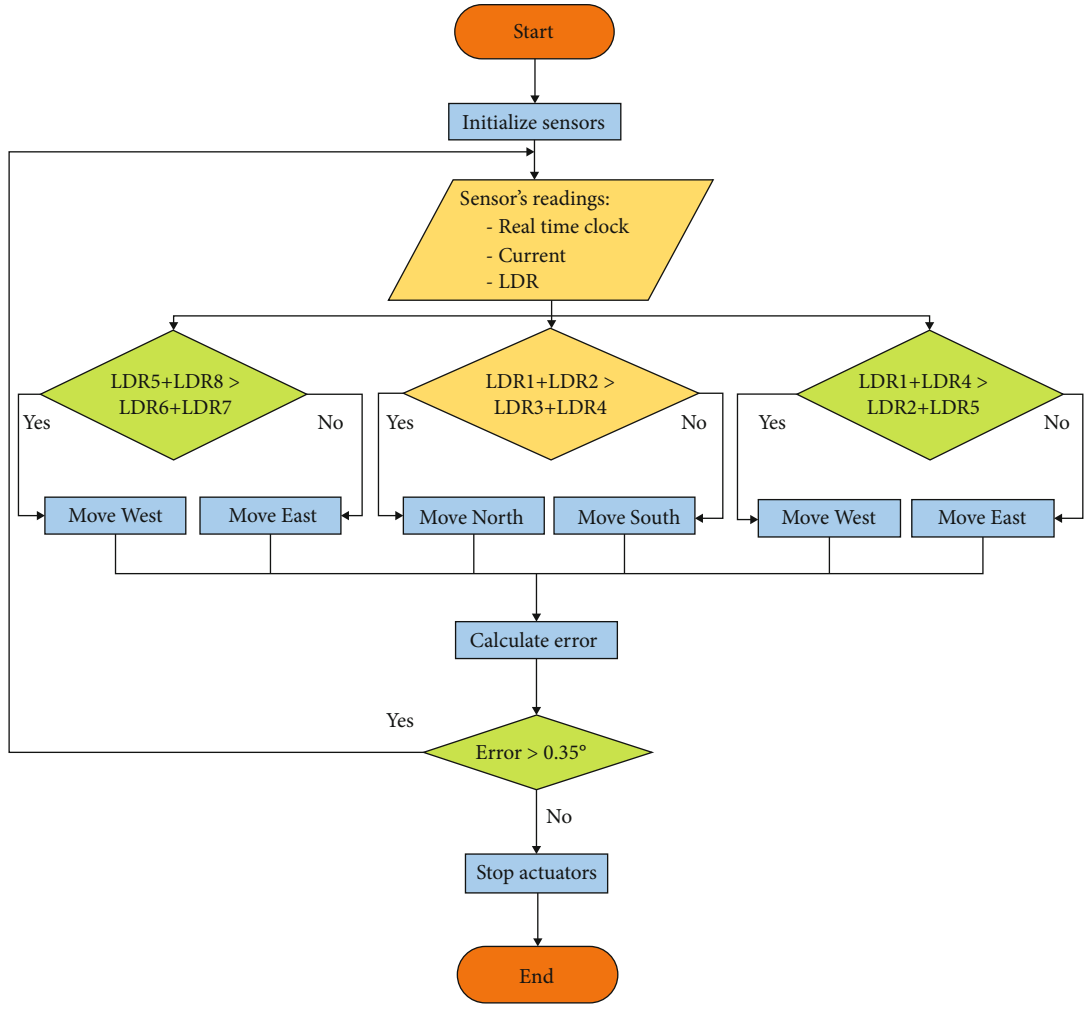

Figure 5: SAST and DAST working principle's flow chart.

effective degrees of freedom; in addition, it has to be stable under windy weather conditions or any other external disturbances. The actual models have been fabricated and manufactured in the mechanical workshop at Imam Abdulrahman Bin Faisal University (IAU).

2.2. Electrical Setup. To make the mechanical model of SAST and DAST functional, linear actuators have been integrated to give movement for the 50 W PV modules. The linear actuators receive signals via the motor drivers from an embedded controller (Arduino Mega) based on the light

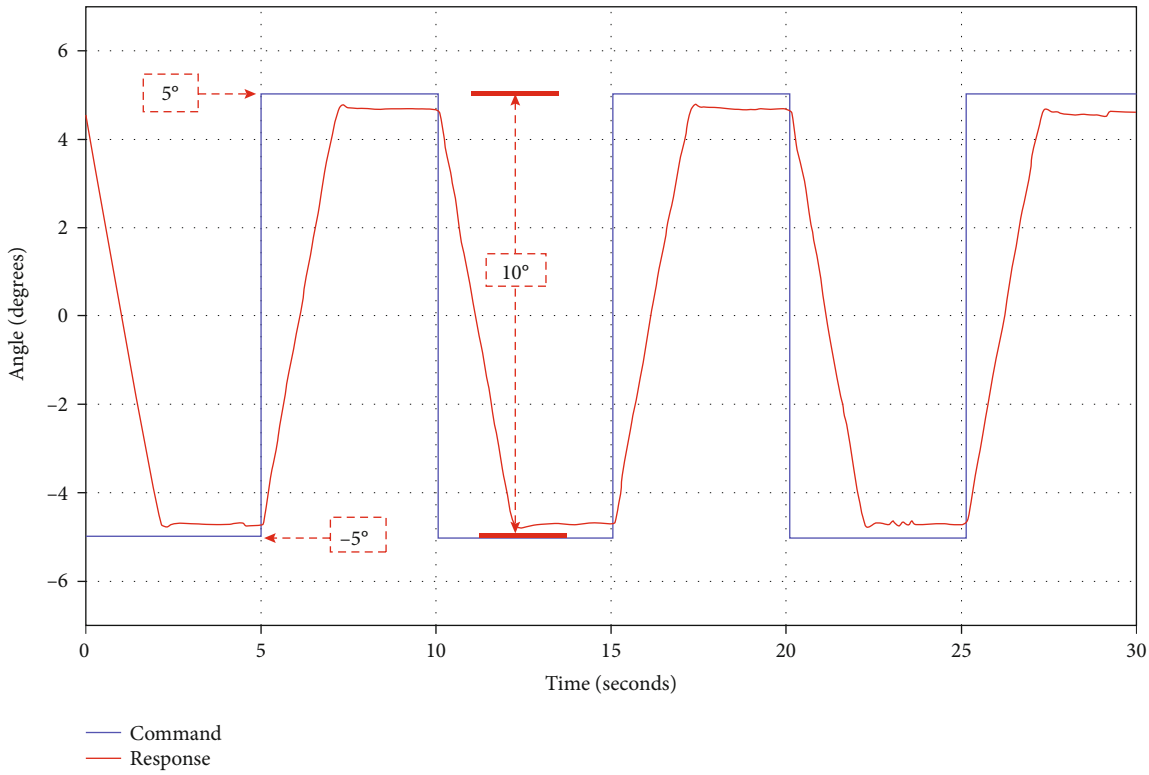

Figure 6: System's PID response.

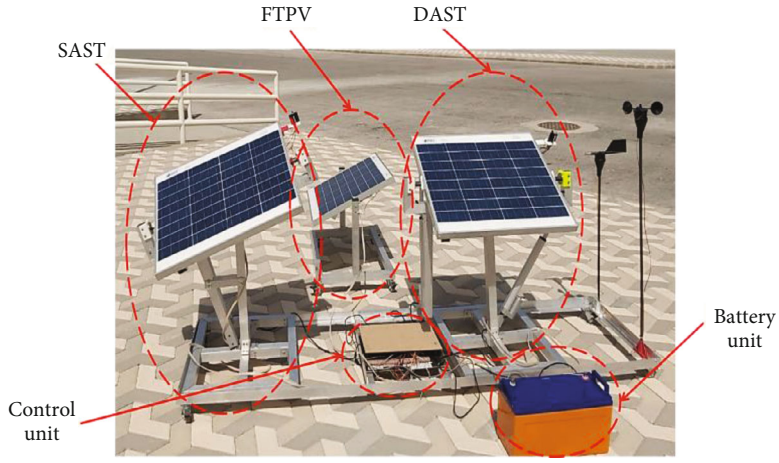

Figure 7: Experimental setup for FTPV, SAST, and DAST.

dependent resistor (LDR) readings. In addition to the electrical setup of SAST and DAST, an electrical set up for the measurement and acquisition of the sensors' signals has been constructed to achieve the goal of this experimental study as seen in Table 1 and Figures 2 and 3. The current measurements generated via each PV module have been recorded using a current sensor. At the same time, the currents consumed by each motor and the electrical control system have been measured using current sensors also. Furthermore, real-time-clock (RTC) has been used to give the time and date of the collected experimental data.

2.3. Control Schema. The controller used to manipulate the closed-loop system is a proportional integral derivative (PID) controller tuned experimentally to achieve an accurate, smooth, and power-friendly response based on equation (1). The STS under investigation has no input; instead, LDRs act as the sensors that provide the feedback signal to the PID controller upon which error calculations are made, following equation (2), equation (3), and equation (4), and orientation adjustments are decided (based on the highest intensity direction). After that, the microcontroller sends a signal to the actuators (linear motors) accordingly

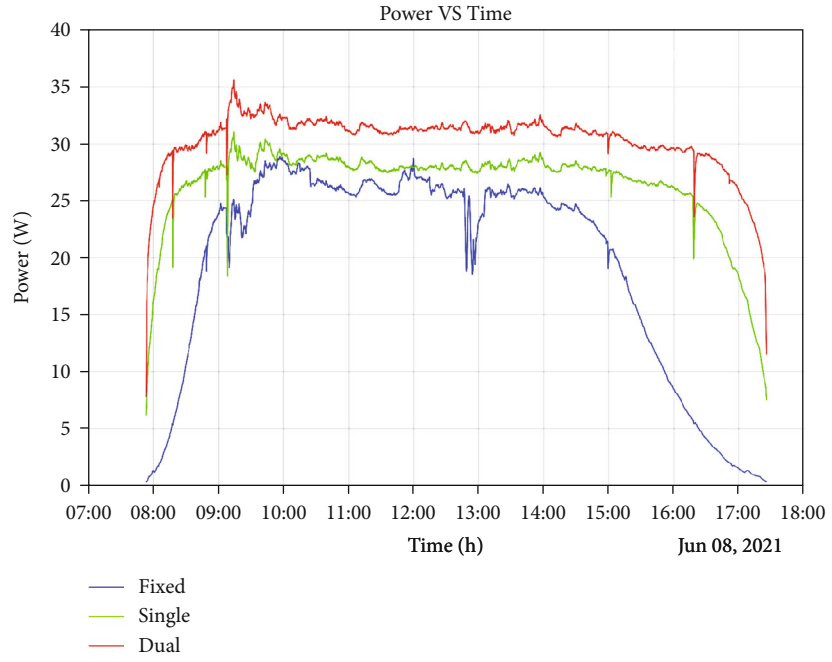

Figure 8: FTPV, SAST, and DAST power generation.

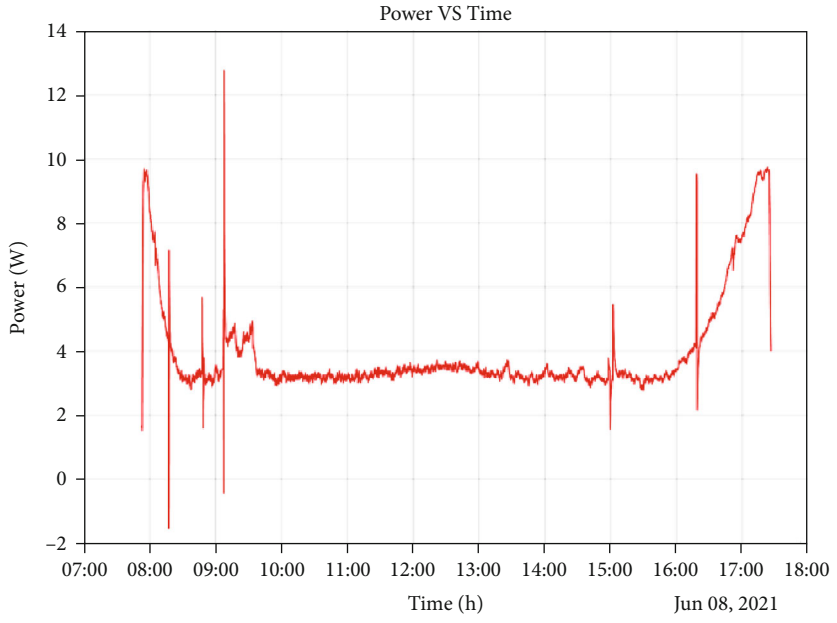

Figure 9: The difference in power generation between DAST and SAST.

(Figures 4 and 5).

$$\text{PID} = \left(K_p * E\right) + \left(K_i * iE\right) + \left(K_d * dE\right), \quad (1)$$

$$E = \text{CMD} - \text{feedback}, \quad (2)$$

$$iE = E * dt + iE\_\text{Prev}, \quad (3)$$

$$dE = \frac{E - E\_\text{Prev}}{dt}, \quad (4)$$

where K_p is the proportional component, E is the error, K_i is the integral component, E_i is the integral error, K_d is the derivative component, E_d is the derivative error, CMD is the command, and Prev is the previous.

2.4. Tracking System Resolution. An indoor experiment was implemented to determine the accuracy of the experiment's tracking systems. In this test, angles were given to the system as a command, and then, the actual tilt angles of the PV module were measured using an accelerometer sensor. After that, the actual angle measured was compared to the command given to the systems. Results of the resolution test

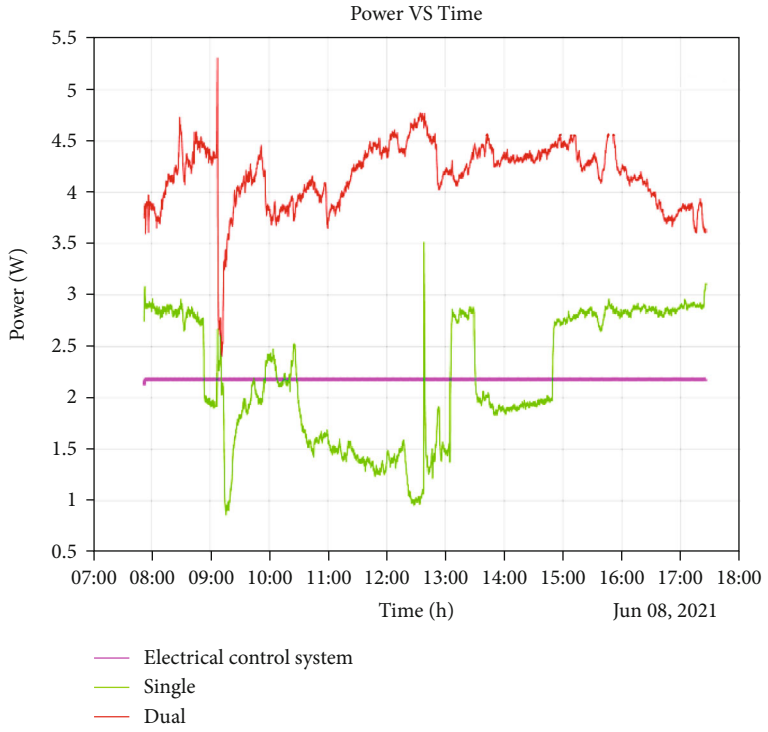

Figure 10: FTPV, SAST, and DAST power consumption.

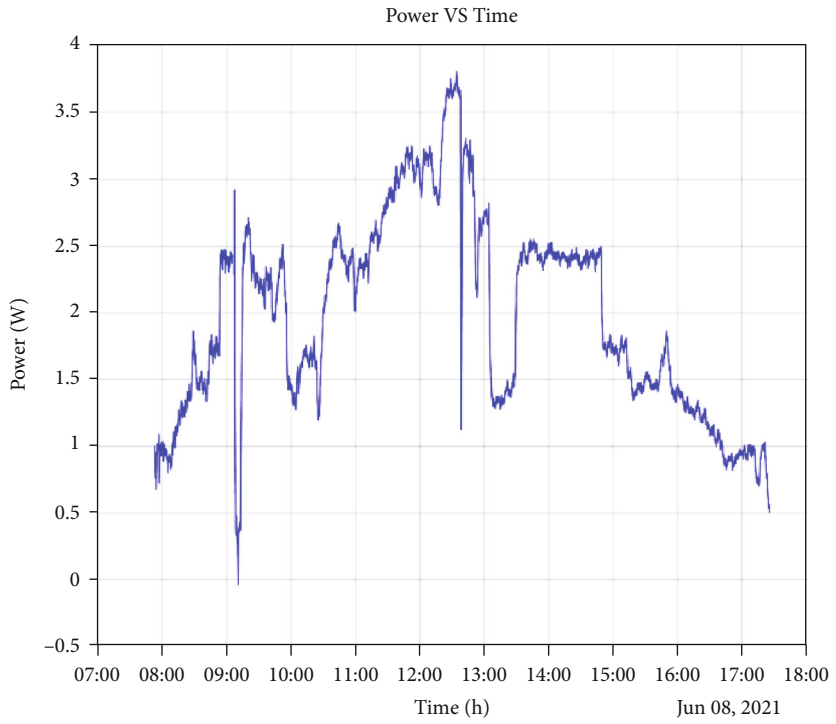

Figure 11: The difference in power consumption between DAST and SAST.

showed a high accuracy achieved by the developed tracking mechanism of about 0.35° as seen in Figure 6.

2.5. Experimental Procedure. The experiment presented in this study was conducted at IAU, in the city of Dammam, SA (26.4° latitude). The data is collected on June 8, 2021, on a sunny, clear day. To set up the experimental platforms for testing, the FTPV, single, and dual STS were placed and examined simultaneously to increase the reliability of the comparison as seen in Figure 7. The FTPV and SAST were

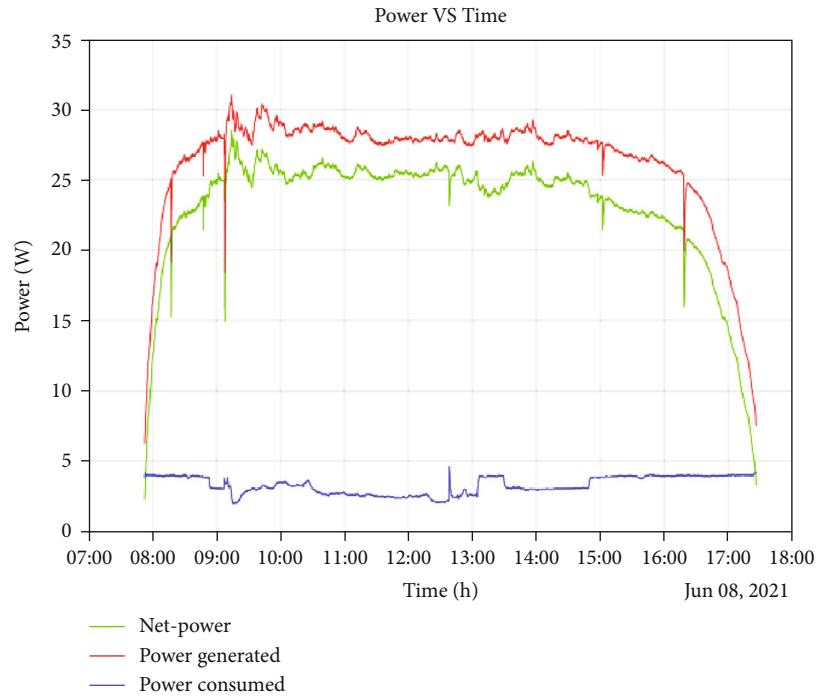

(a)

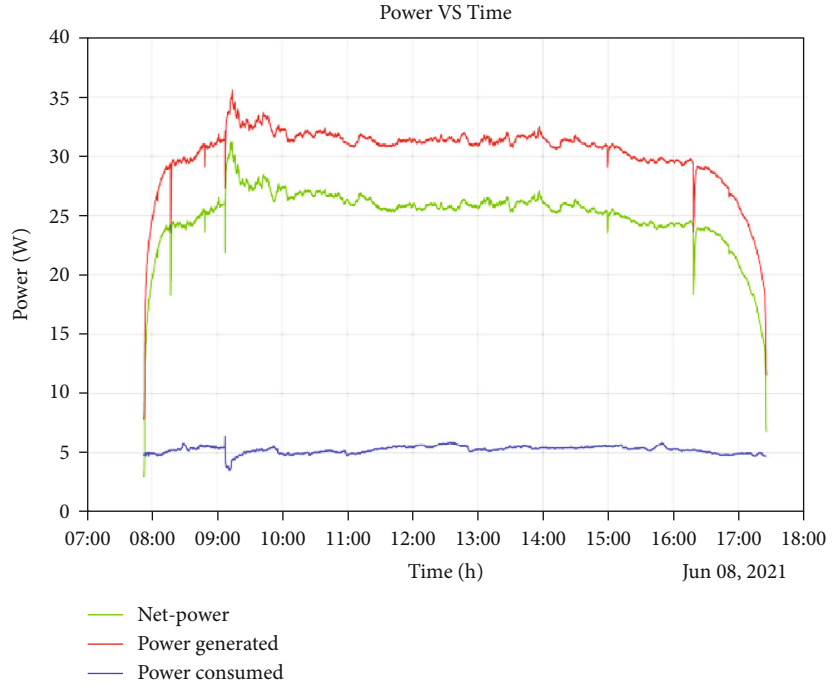

(b)

Figure 12: Continued.

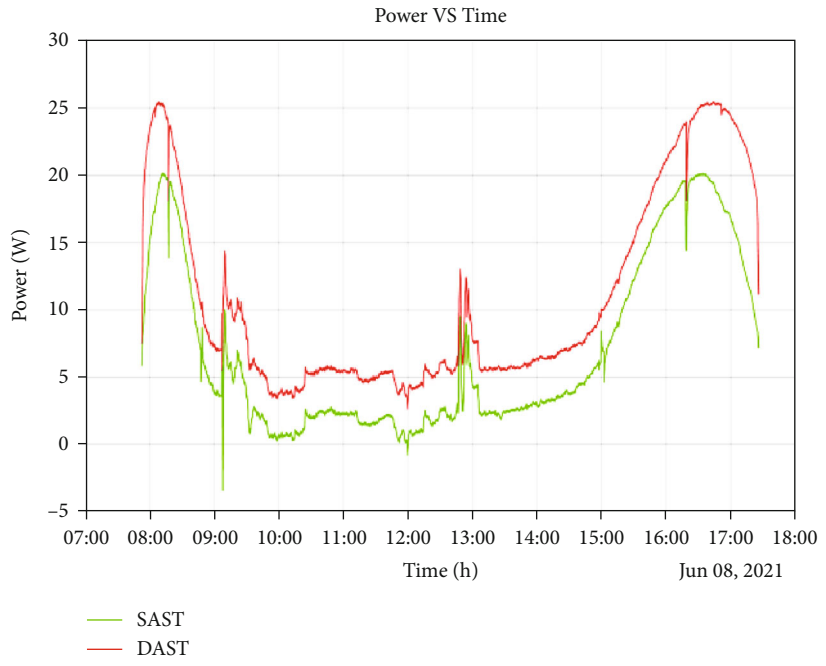

(c)

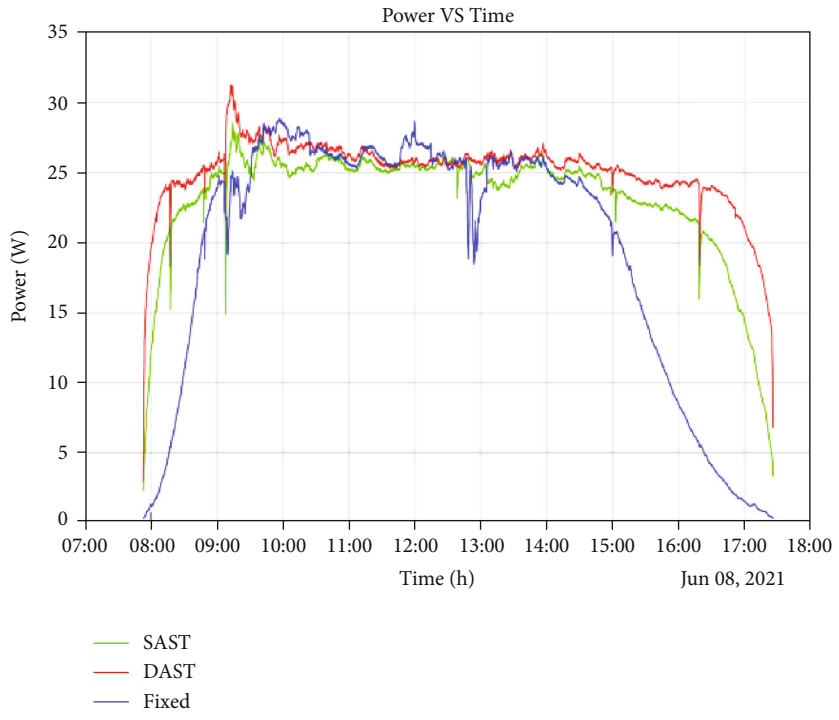

(d)

Figure 12: (a) Power generation, consumption, and the net power of SAST. (b) Power generation, consumption, and net power of DAST. (c) Increase in power (power improvement) of SAST and DAST. (d) Net power of SAST, DAST, and FTPV.

Table 2: Energy generated, consumed, and net energy via each system.

Energy generated (kJ)	
FTPV	398.6
SAST	536.3
DAST	615.4
Energy consumed (kJ)	
Electrical control system	42.3
SAST_actuator	42
DAST_actuators	80.2
Net energy (kJ)	
FTPV	398.6
SAST	473.2
DAST	514.1

initially oriented toward the optimal yearly tilt angle (OYTA) which is about 23°, since the latitude is between 25° and 50° and according to equation (5) [40]. In addition, as SA is located in the northern hemisphere, both FTPV and SAST were placed to face the south.

$$\text{OYTA} = (\text{latitude} * 0.76) + 3.1. \quad (5)$$

3. Results and Discussion

3.1. Power. The power production and consumption of FTPV, SAST, and DAST have been calculated throughout the day. The measurements for the power production of PV modules were recorded by utilizing the current measurements through power resistors acting as dummy-load (this strategy enables to measure the power without any voltage sensor), while the measurements of the power consumption through the actuators and the controllers were acquired via utilizing the current measurements with the known input voltage.

3.1.1. Power Production. The results of the power production showed expected outcomes since DAST showed the highest power production throughout the day. On the other hand, the FTPV showed the lowest power production, and the SAST power production was somewhere in between Figure 8. Furthermore, the power generation of SAST and DAST was almost the same at the beginning and the end of the experiment, while a significant difference occurred between these times. Also, the graph shows that the huge difference between FTPV and the PVTS is at the early and late hours of the day.

Figure 9 shows the difference in power generation between DAST and SAST. Remarkably, the highest difference in power generation occurs after the starting point by a few minutes as same as before the ending point by a few minutes. However, the average difference in power is about 3.9 W; although that seems low, the accumulation of this power with time leads to a high energy difference.

3.1.2. Power Consumption. In regard to power consumption, most papers claim that most of the power wasted is due to the actuators (motors) not the electrical system and that is what is studied in this section. The data collected from the experiment proved that the dominant power waste is due to the actuators (Figure 10) which is the same as what previous studies suggested.

The difference in power consumption between DAST and SAST, which is shown in Figure 11, proves that the difference in power consumption is not high (between 1 W and 3.5 W), although this slight difference leads to high energy consumption at the end of the day. Additionally, it is noticeable that the difference in power consumption starts to increase from the beginning and then starts to decrease after 12 : 30 approximately. And in terms of average value, the average difference of power consumption was about 2 W.

3.1.3. Net Power. To calculate the net power of SAST and DAST, the power produced by each system has been subtracted from the consumption of the motors and the electrical control system. Both SAST and DAST show positive net power as expected in Figures 12(a) and 12(b), which led to the understanding that both of these systems are beneficial. The increase in power (power improvement) of SAST and DAST was maximum at the beginning and the end of the test since the FTPV produced the lowest power in these times; however, it was minimum in the noon (Figure 12 (c)). In addition, the comparison between the net power of SAST, DAST, and FTPV shows similar results, since the net power of both SAST and DAST was maximum in comparison to FTPV at the beginning and end of the day (Figure 12(d)), while the net power was almost the same for all systems from 9 AM to 2 : 30 PM.

3.2. Energy. The energy can be calculated via taking the integration of any power VS time curve, and that was the approach to calculate the energy in this paper. Energy generated, consumed, and net energy of all systems are listed in Table 2. The energy generated from the FTPV was about 399 kJ, while SAST and DAST generate 34.6% and 54.4% more energy, respectively. On the other hand, the energy consumed via SAST is about 7.8% of its total generated energy, while DAST is about 13.0% of its total generated energy. Furthermore, the energy consumed from the SAST and the whole electrical control system was almost similar to each other, and the energy consumption for the DAST is almost equal to the sum of the energy consumed by both SAST and the control system, while the energy consumed via the electrical control system of SAST is about 3.9% of its total energy production, and the electrical control system of DAST consumed about 3.4% of its total energy production.

Most importantly, the increase in the net energy (INE) of SAST and DAST compared to FTPV has been calculated using equation (6). As a result, DAST achieves 28.98% INE while the SAST achieves 18.72% INE.

$$\text{INE} = (E_{\text{TS}} - (E_C + E_F)) * \frac{100}{E_F}, \quad (6)$$

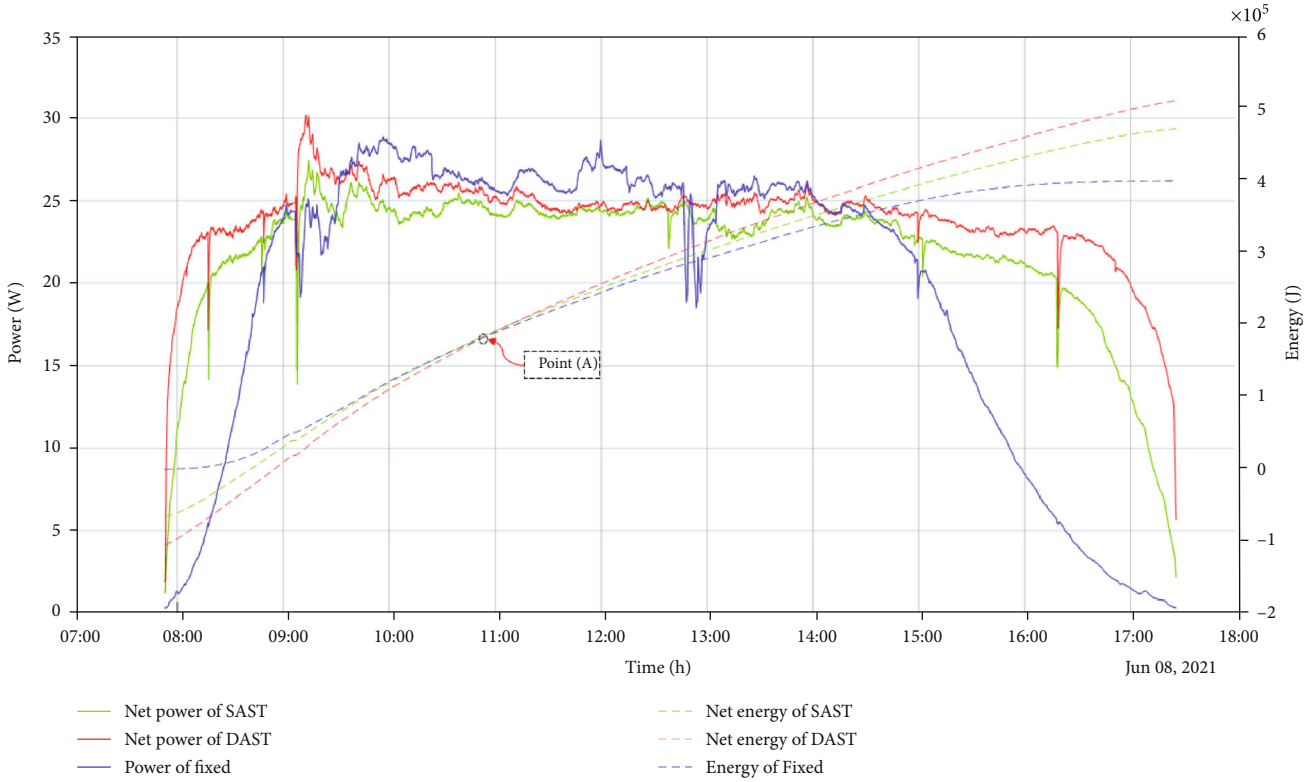

Figure 13: Net power and energy of SAST, DAST, and FTPV.

where INE is the increase in net energy of SAST or DAST, E_{TS} is the energy generated by SAST or DAST, E_F is the energy generated by FTPV, and E_C is the total energy consumed by SAST or DAST. Figure 13 shows the net power and energy of SAST, DAST, and FTPV. This graph is capable to show the power and the accumulation of energy throughout the day. A critical point in the energy curve is point (A) since the graph demonstrates that the net energy of each system from the highest to the lowest was as flows: FTPV, SAST, and DAST. In contrast after point (A), the graph shows the opposite order of net energy production.

The energy difference demonstrated at the beginning of the day between the FTPV, SAST, and DAST is due to the actuation mechanism compared to the production of the modules. After a few hours, the accumulation of energy for all three systems meets at point (A) (Figure 13) starting from which the DAST starts to have the most energy accumulation since it has the highest net power production. Also, the DAST has the highest power consumption since it has two actuators to adjust its orientation. Therefore, the energy curve of the DAST starts at the bottom and ends at the top. Additionally, point (A) clarifies that if DAST and SAST were exposed to the sun for an insufficient time (e.g., from 8 AM to 11 AM), both systems would be useless and cause negative INP.

4. Conclusion and Future Work

To sum up, in this study, the assembly and mechanization of single-axis and dual-axis microcontrolled PV tracking systems are demonstrated in order to determine the most efficient PV system for the region. Additionally, a unique investigation for the net energy generated and consumed by each system is carried out in the study.

The PVTS is actuated using linear motors and controlled via PID controllers in order to reorient 50 W PV modules to the direction of the sunlight. The algorithms of the PVTS were able to trace the sunlight with a resolution of 0.35°. The sheer amount of energy produced via the PVTS has recorded massive increases in comparison to the FTPV with an increase in energy production of 34.5% and 54.4% for SAST and DAST, respectively. However, after considering the power consumption of different components in the PVTS (the actuators and the electrical control setup), the net increase in energy is recorded to be about 18.72% and 28.98% for SAST and DAST, respectively, which demonstrates that DAST, SAST, and FTPV are the most efficient systems for the region, respectively. It is concluded that most of the energy consumption is due to the actuation mechanism, since SAST consumed about 7.8% of its total energy production, while DADT consumed 13.06% of its total energy production. The energy consumed by the electrical control system was 3.4% and 3.9% of the total energy production from SAST and DAST, respectively.

Although the result shows that DAST and SAST are compatible with the region in terms of increase in net energy, a financial analysis must be one to determine if the increase in energy production would cover the cost of manufacturing and maintenance, especially for DAST. Moreover, in order to further optimize the mechanical of the PVTS, a study of the wind profile should be made to investigate the effect of the wind force on the energy

consumption of the actuators. Furthermore, an investigation of various STS control algorithms on the consumption of the actuators should be carried out.

Abbreviations

PV: Solar photovoltaic
PVTS: Solar photovoltaic tracking system
FTPV: Fixed-tilt photovoltaic system
SAST: Single-axis solar tracking system
DAST: Dual-axis solar tracking system
STS: Solar tracking systems
CAD: Computer-aided design
LDR: Light dependent resistors
RTC: Real-time clock
Qty: Quantity
K_p: Proportional component
E: Error
K_i: Integral component
E_i: Integral error
K_d: Derivative component
E_d: Derivative error
CMD: Command
Prev: Previous.

Data Availability

The data used to support the findings of this study are included within the article, and references are described in the text of the article.

Conflicts of Interest

The authors declare that they have no known competing financial interests or personal relationships that could have appeared to influence the work reported in this paper.

Acknowledgments

The authors are grateful to the Deanship of Scientific Research (DSR) at Imam Abdulrahman bin Faisal University, Kingdom of Saudi Arabia, for their continuous guidance and support.

References

[1] S. Mubaarak, D. Zhang, Y. Chen et al., "Techno-economic analysis of grid-connected PV and fuel cell hybrid system using different PV tracking techniques," *Applied Sciences*, vol. 10, no. 23, p. 8515, 2020.

[2] M. S. Shaari, Z. Abdul Karim, and N. Zainol Abidin, "The effects of energy consumption and national output on CO2 emissions: new evidence from OIC countries using a panel ARDL analysis," *Sustainability*, vol. 12, no. 8, p. 3312, 2020.

[3] F. J. Gómez-Uceda, J. Ramirez-Faz, M. Varo-Martinez, and L. M. Fernández-Ahumada, "New omnidirectional sensor based on open-source software and hardware for tracking and backtracking of dual-axis solar trackers in photovoltaic plants," *Sensors*, vol. 21, no. 3, p. 726, 2021.

[4] M. I. Hussain and J.-T. Kim, "Performance evaluation of photovoltaic/thermal (PV/T) system using different design configurations," *Sustainability*, vol. 12, no. 22, p. 9520, 2020.

[5] F. M. Mustafa, "Dual-axis solar tracking over fixed solar systems," *International Journal of Advances in Engineering and Technology*, vol. 9, no. 5, p. 563, 2016.

[6] C. Alexandru, "Optimization of the bi-axial tracking system for a photovoltaic platform," *Energies*, vol. 14, no. 3, p. 535, 2021.

[7] H. Zsiborács, A. Bai, J. Popp et al., "Change of real and simulated energy production of certain photovoltaic technologies in relation to orientation," *Sustainability*, vol. 10, no. 5, p. 1394, 2018.

[8] J. Siecker, K. Kusakana, and B. P. Numbi, "A review of solar photovoltaic systems cooling technologies," *Renewable & Sustainable Energy Reviews*, vol. 79, pp. 192–203, 2017.

[9] S. Seme, B. Štumberger, M. Hadžiselimović, and K. Sredenšek, "Solar photovoltaic tracking systems for electricity generation: a review," *Energies*, vol. 13, no. 16, p. 4224, 2020.

[10] S. Das, S. Chakraborty, P. K. Sadhu, and O. S. Sastry, "Design and experimental execution of a microcontroller (μC)-based smart dual- axis automatic solar tracking system," *Energy Science & Engineering*, vol. 3, no. 6, pp. 558–564, 2015.

[11] R. J. Mustafa, M. R. Gomaa, M. Al-Dhaifallah, and H. Rezk, "Environmental impacts on the performance of solar photovoltaic systems," *Sustainability*, vol. 12, no. 2, p. 608, 2020.

[12] A. Masih and I. Odinaev, "Performance Comparison of Dual Axis Solar Tracker with Static Solar System in Ural Region of Russia," in *2019 Ural Symposium on Biomedical Engineering, Radioelectronics and Information Technology (USBEREIT)*, pp. 375–378, Yekaterinburg, Russia, 2019.

[13] A. E. Hammoumi, S. Motahhir, A. E. Ghzizal, A. Chalh, and A. Derouich, "A simple and low-cost active dual-axis solar tracker," *Energy Science & Engineering*, vol. 6, no. 5, pp. 607–620, 2018.

[14] W. Nsengiyumva, S. G. Chen, L. Hu, and X. Chen, "Recent advancements and challenges in solar tracking systems (STS): a review," *Renewable & Sustainable Energy Reviews*, vol. 81, pp. 250–279, 2018.

[15] F. Grubišić-Čabo, S. Nižetić, I. Marinić Kragić, and D. Čoko, "Further progress in the research of fin-based passive cooling technique for the free-standing silicon photovoltaic panels," *International Journal of Energy Research*, vol. 43, no. 8, pp. 3475–3495, 2019.

[16] S. A. S. Eldin, M. S. Abd-Elhady, and H. A. Kandil, "Feasibility of solar tracking systems for PV panels in hot and cold regions," *Renewable Energy*, vol. 85, pp. 228–233, 2016.

[17] S. Racharla and K. Rajan, "Solar tracking system - a review," *International Journal of Sustainable Engineering*, vol. 10, no. 2, pp. 72–81, 2017.

[18] M. N. A. M. Said, S. A. Jumaat, and C. R. A. Jawa, "Dual axis solar tracker with IoT monitoring system using arduino," *International Journal of Power Electronics and Drive Systems*, vol. 11, no. 1, p. 451, 2020.

[19] A. Z. Hafez, A. M. Yousef, and N. M. Harag, "Solar tracking systems: technologies and trackers drive types - a review," *Renewable & Sustainable Energy Reviews*, vol. 91, pp. 754–782, 2018.

[20] S. Gutierrez, P. M. Rodrigo, J. Alvarez, A. Acero, and A. Montoya, "Development and testing of a single-axis photovoltaic sun tracker through the Internet of Things," *Energies*, vol. 13, no. 10, p. 2547, 2020.

[21] N. Al-Rousan, N. A. M. Isa, and M. K. M. Desa, "Advances in solar photovoltaic tracking systems: a review," *Renewable & Sustainable Energy Reviews*, vol. 82, pp. 2548–2569, 2018.

[22] J. da Rocha Queiroz, A. da Silva Souza, M. K. Gussoli, J. C. D. de Oliveira, and C. M. G. Andrade, "Construction and automation of a microcontrolled solar tracker," *Processes*, vol. 8, no. 1309, 2020.

[23] A. J. Farhan, "Fabrication and development low cost dual axis solar tracking system," *Materials Science and Engineering*, vol. 757, no. 1, article 012042, 2020.

[24] R. F. Fuentes-Morales, A. Diaz-Ponce, M. I. Peña-Cruz et al., "Control algorithms applied to active solar tracking systems: a review," *Solar Energy*, vol. 212, pp. 203–219, 2020.

[25] D. Mazumdar, D. Sinha, S. Panja, and D. K. Dhak, "Design of LQR controller for solar tracking system," in *2015 IEEE International Conference on Electrical, Computer and Communication Technologies (ICECCT)*, pp. 1–5, Coimbatore, India, 2015.

[26] T. Laseinde and D. Ramere, "Low-cost automatic multi-axis solar tracking system for performance improvement in vertical support solar panels using Arduino board," *International Journal of Low Carbon Technologies*, vol. 14, no. 1, pp. 76–82, 2019.

[27] Q. Li and M. E. Baran, "A novel frequency support control method for PV plants using tracking LQR," *IEEE Transactions on Sustainable Energy*, vol. 11, no. 4, pp. 2263–2273, 2020.

[28] A. Rawat, S. K. Jha, and B. Kumar, "Position controlling of sun tracking system using optimization technique," *Energy Reports*, vol. 6, pp. 304–309, 2020.

[29] N. Arab, B. Kedjar, A. Javadi, and K. Al-Haddad, "A multifunctional single-phase grid-integrated residential solar PV systems based on LQR control," *IEEE Transactions on Industry Applications*, vol. 55, no. 2, pp. 2099–2109, 2019.

[30] X. Du, Y. Li, P. Wang, Z. Ma, D. Li, and C. Wu, "Design and optimization of solar tracker with U-PRU-PUS parallel mechanism," *Mechanism and Machine Theory*, vol. 155, article 104107, 2021.

[31] X. C. Ngo, T. H. Nguyen, N. Y. Do et al., "Grid-connected photovoltaic systems with single-axis sun tracker: case study for Central Vietnam," *Energies*, vol. 13, no. 6, p. 1457, 2020.

[32] J. Ruelas, F. Muñoz, B. Lucero, and J. Palomares, "PV tracking design methodology based on an orientation efficiency chart," *Applied Sciences*, vol. 9, no. 5, p. 894, 2019.

[33] H. Z. Al Garni, A. Awasthi, and M. A. M. Ramli, "Optimal design and analysis of grid-connected photovoltaic under different tracking systems using HOMER," *Energy Conversion and Management*, vol. 155, pp. 42–57, 2018.

[34] A. F. Almarshoud, "Performance of solar resources in Saudi Arabia," *Renewable and Sustainable Energy Reviews*, vol. 66, pp. 694–701, 2016.

[35] A. Alrashidi, *Investigating the Feasibility of Solar Photovoltaic Systems in Kuwait, [Ph.D]*, Loughborough University, 2017.

[36] M. Ghassoul, "Single axis automatic tracking system based on PILOT scheme to control the solar panel to optimize solar energy extraction," *Energy Reports*, vol. 4, pp. 520–527, 2018.

[37] F. F. Ahmad, M. Abdelsalam, A. K. Hamid, C. Ghenai, W. Obaid, and M. Bettayeb, "Experimental Validation of PVSYST Simulation for Fix Oriented and Azimuth Tracking Solar PV System," in *International Conference on Modelling, Simulation and Intelligent Computing*, N. Goel, S. Hasan, and V. Kalaichelvi, Eds., vol. 659 of Lecture Notes in Electrical Engineering, pp. 227–235, Springer, Singapore, 2020.

[38] N. Al Safarini, O. Akash, M. Mohsen, and Z. Iqbal, "Performance evaluation of solar tracking systems for power generation based on simulation analysis: solar island concept," in *2017 International Conference on Electrical and Computing Technologies and Applications (ICECTA)*, pp. 1–4, Ras Al Khaimah, United Arab Emirates, 2017.

[39] M. E. H. Chowdhury, A. Khandakar, B. Hossain, and R. Abouhasera, "A low-cost closed-loop solar tracking system based on the sun position algorithm," *Journal of Sensors*, vol. 2019, Article ID 3681031, 11 pages, 2019.

[40] D. Torres and J. Crichigno, "Influence of reflectivity and cloud cover on the optimal tiltangle of solar panels," *Resources (Basel)*, vol. 4, no. 4, pp. 736–750, 2015.

Hindawi
International Journal of Photoenergy
Volume 2022, Article ID 9882195, 6 pages
https://doi.org/10.1155/2022/9882195

Research Article

Investigation of the Effect of Physical Factors on Exergy Efficiency of a Photovoltaic Thermal (PV/T) with Air Cooling

Reza Alayi,[1] **Farnaz Jahanbin**,[2] **Hikmet Ş. Aybar**,[3,4] **Mohsen Sharifpur**,[5,6] **and Nima Khalilpoor**[7]

[1]*Department of Mechanics, Germi Branch, Islamic Azad University, Germi, Iran*
[2]*Department of Chemistry, Mashhad Branch, Islamic Azad University, Mashhad, Iran*
[3]*Department of Mechanical Engineering, Eastern Mediterranean University, G. Magosa, TRNC via Mersin 10, Turkey*
[4]*Faculty of Electrical and Electronics Engineering, Ton Duc Thang University, Ho Chi Minh City, Vietnam*
[5]*Clean Energy Research Group, Department of Mechanical and Aeronautical Engineering, University of Pretoria, Hatfield, Pretoria, South Africa*
[6]*Department of Medical Research, China Medical University Hospital, China Medical University, Taichung 404, Taiwan*
[7]*Department of Energy Engineering, Graduate School of the Environment and Energy, Science and Research Branch, Islamic Azad University, Tehran, Iran*

Correspondence should be addressed to Reza Alayi; reza.alayi@yahoo.com, Mohsen Sharifpur; mohsen.sharifpur@up.ac.za, and Nima Khalilpoor; nimakhalilpoor@gmail.com

Received 13 November 2021; Revised 23 March 2022; Accepted 15 April 2022; Published 5 May 2022

Academic Editor: Alberto Álvarez-Gallegos

Thermal photovoltaic systems are used to harness solar energy to generate electricity and thermal at the same time. In this technology, electrical efficiency is very low compared to thermal efficiency; as the cell surface temperature rises, the electrical efficiency decreases, so one of the ways to achieve high efficiency is exergy analysis. Exergy analysis of a process or system shows how much of the ability to perform the work or input exergy has been consumed by that process or system. In this research, an ordinary thermal photovoltaic panel with air cooling has been examined for exergy. To do this, it has identified the effective performance variables from a mechanical point of view, which are inlet air temperature, inlet air flow, and length (number of modules that are connected in series). The effect of changing each of the variables based on Saveh weather conditions has been simulated using MATLAB software. The results show that the exergy efficiency of the panel decreases with the inlet air temperature increasing. It was also observed that the optimal airflow is 0012 (kg/s) and will have the highest efficiency per 8.8 m length.

1. Introduction

Energy is a basic need for continued economic development, human welfare, and comfort. World energy consumption has increased from 10 Gtoelyr crude oil to 14 Gtoelyr by 2020 and is projected to multiply in the near future. Will fossil energy sources meet the world's energy needs for survival, growth, and development in the next century [1–3]? Rising air pollution, including carbon dioxide, has left the world with irreversible and threatening changes, with consequences such as global warming, climate change, rising sea levels, and escalating international conflicts [4–6]. On the other hand, due to the destruction of fossil resources and the prediction of rising prices, policymakers and researchers should think about controlling the environment and renewable sources because these resources are compatible with nature and there is no end to them. Other features of these resources, their dispersion, expansion around the world, the need for less technology, and renewable energy have become more attractive, especially for developing countries [7–10].

Therefore, renewable energy sources have been given a special role in international programs and policies, including UN programs, for sustainable global development. But

adopting renewables, with the current system of world energy consumption, it is still associated with problems that have been addressed by a significant amount of world scientific research in recent decades [11, 12]. Wolf introduced the basic concepts of PVT collectors in 1970 [13]. Zhang et al. used a computer simulation of the amount of solar radiation absorbed and the amount of infrared emission in thermal photovoltaic transducers working with weather-working fluid to be less than the type working with water-carrying fluid [14]. Researches examined the exergy performance of a greenhouse-connected photovoltaic module and provided an exergy efficiency of 4% for the system [15, 16]. The exergy and energetic analysis of a thermal photovoltaic cell without a glass cover was conducted. The use of a glass cover is suitable for the photothermic process. If the use of cover is not suitable for the photovoltaic process and due to various applications, it is not possible to determine exactly which one is more economical to use [17, 18]. The electrical and thermal efficiency of a PVT collector with air-operated fluid was determined. They supplied the required power to the fan directly from the photovoltaic panel and showed that there is the highest efficiency for the two collectors in the case of using two fans [19, 20]. Researches evaluated and optimized the performance of a photovoltaic array from the perspective of exergy. They show that the best state occurs when the temperature of the photovoltaic modulus is close to the ambient temperature [21–23]. Finally, different exergies of each component of PVT/water are calculated and a relationship is obtained based on loss of exergy [24–26].

The purpose of this study is to investigate the photovoltaic-thermal system with air cooling, in which exergy analysis has been performed to achieve high efficiency. In this regard, factors such as inlet air temperature-inlet flow and system length are problem variables. The impact of each of these factors has been evaluated for a sample area.

2. Materials and Methods

2.1. Fundamentals of Exergy Analysis. Exergy is the maximum useful work that results from a certain amount of available energy or flow of materials. In exergy analysis, the main purpose is to determine the location and amount of production of irreversibility during different processes of the thermodynamic cycle and the factors affecting the production of this irreversibility. In this way, in addition to evaluating the efficiency of different components of the thermodynamic cycle, ways to increase the efficiency of the cycle are also identified. Exergy analysis tries to obtain the most work produced in the cycle by simultaneously applying the first and second laws of thermodynamics and using the environment as a reference state.

2.2. Principles of Exergy Analysis of Thermal Photovoltaic Panels with Air Cooling. This study is aimed at analyzing the exergy of a photovoltaic-thermal collector with air cooling. Exergy analysis is a new and alternative method to older methods. This method is based on the concept of exergy. Exergy is defined with a bit of negligence as the ability to do work or the quality of different types of energy in a given environment. Exergy analysis of a process shows how much input or exergy functionality has been consumed by that process or system or, in other words, wasted. Contrary to current performance criteria, the concept of irreversibility is based on both laws of thermodynamics. The relation used for exergy analysis is obtained by combining the steady-state energy equation (first law) with the entropy production rate (second law).

However, the second law is not explicitly used in the analysis of exergy. But as stated, using the above method to evaluate the system implicitly requires applying the results of the second rule. The study of different forms of irreversibility gives a better understanding of it compared to the mere study of relevance and formulas related to the second law. Figure 1 shows the energy balance of the focal area of a thermal photovoltaic system.

The high efficiency of a system is not always a sufficient condition for its feasibility and cost-effectiveness. Factors such as initial costs, maintenance costs, and fuel consumption can affect whether or not a project is viable. In general, PVT collectors can be evaluated in two main ways: (a) exergy analysis and (b) energy analysis. Figure 2 shows the outline of a PVT.

Exergy balance for the collector of the following form is suggested:

$$\sum E_{X\text{out}} = \sum E_{X\text{thermal}} + \sum E_{X\text{electrical}}. \quad (1)$$

Table 1 shows the functional characteristics of the modeling photovoltaic cell.

2.3. Exergy Balance in General for PVT. As can be seen from the above relation, the input exergy caused by solar radiation minus the thermal exergy and electrical exergy will be equal to the exergy loss. Also, the exergy balance for the above collector is in the following form:

$$\begin{bmatrix}\text{rate of solar}\\ \text{energy availabel}\\ \text{on solar cell}\end{bmatrix} = \begin{bmatrix}\text{rate of heat loss from}\\ \text{top surface of solar cell}\\ \text{to ambient}\end{bmatrix} + \begin{bmatrix}\text{rate of heat transfer}\\ \text{from solar cell to}\\ \text{flowing fluid, i.e.,air}\end{bmatrix} + \begin{bmatrix}\text{rate of}\\ \text{electrical energy}\\ \text{produced}\end{bmatrix}$$

The above relationship is the basis for future relationships that will be expanded below. In general, we have presented two basic equations above. These two equations are the basis of energy analysis and exergy analysis of PVT collectors. Finally, with their help, more practical equations can be achieved. In this research, we have tried to perform the analysis based on design and performance parameters and the goal is to find the optimal points in the performance and design parameters so that the exergy efficiency is maximized. From the balance of exergy presented above, the cell

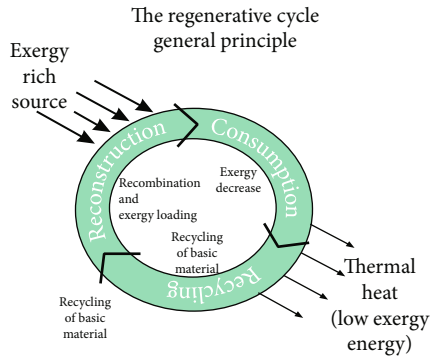

Figure 1: Exergy analysis.

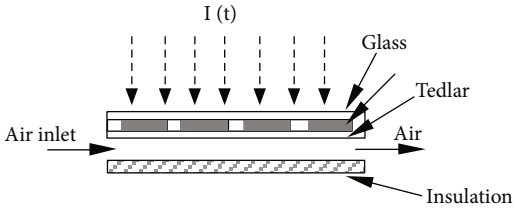

Figure 2: Overview of a PVT air cooler.

Table 1: Photovoltaic module specifications.

Parameter	Quantity
Maximum power	150 V
Maximum voltage	34.5 V
Maximum flow	4.35 A
Short circuit current	4.75 A
Open circuit voltage	43.5 V
Flow temperature coefficient	(0.065 ± 0.015) %/°C
Voltage temperature coefficient	-(160 ± 20) mV/°C
The effect of temperature on power	-(0.5 ± 0.05) %/°C
Nominal temperature of cell function	47 ± 2°C

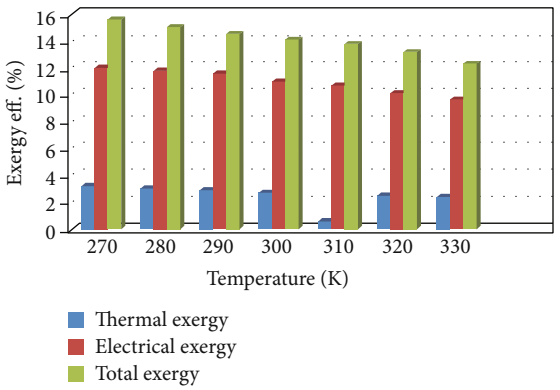

Figure 3: Effect of inlet air temperature change on exergy efficiency.

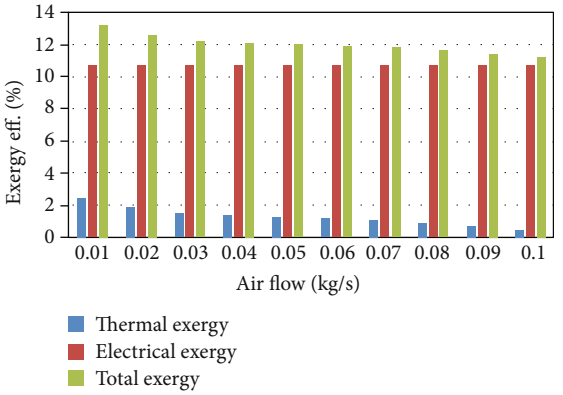

Figure 4: The effect of air flow change on exergy efficiency.

temperature will be obtained as follows [27, 28]:

$$T_c = \frac{((\alpha_{\text{eff}}.I(t)) + (Utca.Ta) + (Tbs.UT))}{Utca + UT}. \quad (2)$$

In the above relation α_{eff} is equal to

$$\alpha_{\text{eff}} = \tau_g(\alpha c.\beta + \alpha T.(1-\beta) - \eta.\beta). \quad (3)$$

The relationship between temperature and electrical efficiency is expressed as follows:

$$\eta = \eta_0[1 - \beta_0(T_C - T_a)]. \quad (4)$$

For the surface behind Tedlar,

$$U_T(T_C - T_{bs})bdx = h_T(T_{bs} - T_f)bdx, \quad (5)$$

$$\begin{bmatrix}\text{the rate of heat}\\ \text{transfer from cell to}\\ \text{back surface of Tedlar}\end{bmatrix} = \begin{bmatrix}\text{the rate of heat transfer}\\ \text{from back suface of Tedlar}\\ \text{to flowing fluid}\end{bmatrix}$$

The following will be done to balance the energy balance [27, 28]:

$$m_f^{\cdot} C_f \frac{dT_f}{dX} + U_b(T_f - T_a)bdx = h_T(T_{bs} - T_f)bdx, \quad (6)$$

$$\begin{bmatrix}\text{rate of heat transfer}\\ \text{from solar cell to}\\ \text{flowing fluid, i.e.,air}\end{bmatrix} = \begin{bmatrix}\text{rate of heat transfer}\\ \text{flowing fluid}\end{bmatrix} + \begin{bmatrix}\text{an overal heat transfer}\\ \text{from flowing fluid}\\ \text{to ambient}\end{bmatrix}.$$

The outlet air temperature of the N module, which is connected in series, is calculated from the following equation:

$$T_{foN} = \left[\frac{\alpha_{\text{eff}} h_p}{u_l} + T_a\right]\left[1 - e^{\left(-blu_l/m^{\cdot}c_f\right)}\right] + T_{fi}e^{\left(-\left(blu_l/m^{\cdot}c_f\right)\right)}. \quad (7)$$

If the size of the modules is the same, the useful heat obtained from the N modules that are connected in series

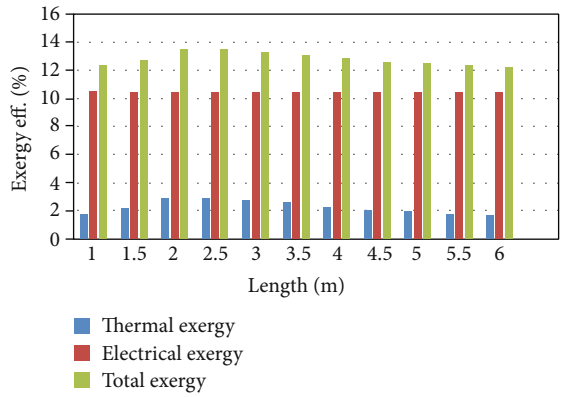

Figure 5: The effect of length change on exergy efficiency.

is calculated from the following equation [27, 28]:

$$Q_U.N = n_{pv} \times \dot{m_f} c_f \left[1 - e^{\left(Nblu_l/\dot{m} \cdot c_f\right)}\right] \left[\frac{h_p.\alpha_{\text{eff}}}{u_l} I(t) + T_{fi}\right],$$
$$K_k = \frac{b.l.u_l.F_R}{m_f \cdot c_f} \tag{8}$$

Finally, the electrical energy obtained from the panel is calculated from the following equation:

$$Ex_{\text{electrical}} = \eta.N.I(t).A. \tag{9}$$

3. Results

The parameters affecting the exergy analysis are the intensity of solar radiation in the environment, wind speed, ambient temperature, inlet and outlet air temperature, the surface temperature of the photovoltaic module, open-circuit voltage, short circuit current, voltage, and current at the maximum power point, panel length photovoltaics (the number of modules that are connected in series to form a module), input flow, etc. are many other parameters. Among these, we have selected four mechanical performance parameters, namely, modulus length and radiation intensity, inlet temperature, and flow rate, and simulated the effect of changing each of the parameters on total exergy, thermal efficiency, and electrical efficiency. This research is based on Saveh weather conditions. Information about the weather conditions of Saveh has been extracted from valid research on the intensity of radiation in Saveh and data of the Meteorological Organization. One of the disadvantages of the work of the past was the lack of sufficient attention to the influence of climate on the efficiency of exergy and mere parametric research. Except for a few specific cases, the research is based on the performance of the collector on a few specific days. In this research, it has been tried to do this based on meteorological and weather information of Saveh for a long time, and the results of the research are as practical as possible. Figure 3 shows the changes in exergy over temperature. It is observed that the exergy efficiency decreases with increasing the inlet temperature to the collector. This is due to the limited heat capacity of the air. In fact, by increasing the inlet temperature to the inlet air panel, it has less capacity to carry heat. Therefore, less heat is dissipated from the panel, resulting in a hot collector and reduced efficiency.

Figure 3 examines the performance of the panel in the temperature range of 270 to 330 degrees Kelvin. It is observed that for each degree of temperature increase, 0.6% exergy efficiency and 0.5% electrical efficiency decrease and 0.01% exergy efficiency due to exhaust air decreases. Note that if cool air was not used, the exergy efficiency would be reduced by 0.5% for each degree of temperature increase, and this diagram clearly shows the superior performance of PVTs compared to solar cells. In Figure 4, the behavior of the solar cell can be seen about the different flow rates of the cooling fluid.

As can be seen in Figure 4, the effect of air inlet flow rate from 0.01 to 0.1 (kg/s) on cell efficiencies has been evaluated. As an observation at first, we see an increase in efficiency with a steep slope. After reaching a peak, the efficiency decreases with a gentle slope and the reason for this behavior is the heat capacity of the air. As the flow rate increases, so does the heat transfer inlet speed. After reaching the peak, due to the reduced exchange of air molecules with the module, due to the high speed of the fluid entering the panel, the heat capacity decreases. As a result, the temperature of the air leaving the panel decreases and as a result, the efficiency of the exergy decreases. As it is known, the specifications of the maximum point are as follows: the optimal air inlet flow is 0.0035, for which the exergy efficiency is equal to 15.2%. Exergy efficiency due to air heat is 4.49%. Electrical efficiency is not dependent on flow; its value will be constant and equal to 10.7%. Figure 5 shows the effect of cool fluid channel length on electrical and thermal exergy efficiencies. The length of each module is 0.4 (m), and the length increase from 1 to 6 modules has been examined.

According to Figure 5, it can be seen that the length of the system does not affect electrical efficiency and the length of the system affects the thermal efficiency, so that the highest thermal exergy efficiency is related to the length of the system which is 2.5 (m) with a value of 3%. Then, with increasing length, a decrease in efficiency will be seen. The reason for this is the saturation of the air due to the absorption of heat by the collector. In this case, the end modules will always be hotter than the initial modules. At the maximum point, exergy efficiency is 13.81%. Thermal efficiency is equal to 3.1050%. The electrical efficiency will be constant and equal to 10.7.

4. Conclusion

In this research, a thermal photovoltaic system with air cooling has been performed to achieve high efficiency by exergy analysis. Observations showed that the photovoltaic/thermal collector performs better when water is injected and its performance in large areas will be very impressive. But for various reasons, such as simplicity of design, cheap, transfer speed, easy transportation, and no need for ancillary

facilities in critical situations such as floods and earthquakes or conditions that only mean electricity generation, a collector with cooling air is recommended. Other results are increased temperature or velocity, reduced contact surface, and reduced air heat capacity.

Nomenclature

C: Specific heat (J/kg·C)
F_R: Flow rate factor (dimensionless)
h_T: Penalty factor due to Tedlar through glass, solar cell
L: Length (m)
$I(t)$: Incident solar intensity (W/m^2)
$\dot{m}$: Mass flow rate (m^3/s)
T: Temperature (C)
U_L: Overall heat transfer coefficient from solar cell to ambient through top and back surface of insulation ($W/m^2 \cdot C$)
T_{cell}: Solar cell temperature
α_c: Solar cell absorption coefficient
η_{el}: Electrical efficiency
τ_G: Glass transfer coefficient
m: Fluid flow rate
U_L: Overall heat loss coefficient.

Data Availability

The data used to support the findings of this study are available from the corresponding author upon request.

Conflicts of Interest

The authors declare that they have no conflicts of interest.

References

[1] T. S. Adebayo and H. Rjoub, "A new perspective into the impact of renewable and nonrenewable energy consumption on environmental degradation in Argentina: a time–frequency analysis," *Environmental Science and Pollution Research*, vol. 29, no. 11, pp. 16028–16044, 2021.

[2] T. S. Adebayo, M. F. Coelho, D. Ç. Onbaşıoğlu et al., "Modeling the dynamic linkage between renewable energy consumption, globalization, and environmental degradation in South Korea: does technological innovation matter?," *Energies*, vol. 14, no. 14, article 4265, 2021.

[3] M. A. Sina and M. A. Adeel, "Assessment of stand-alone photovoltaic system and mini-grid solar system as solutions to electrification of remote villages in Afghanistan," *International Journal of Innovative Research and Scientific Studies*, vol. 4, no. 2, pp. 92–99, 2021.

[4] T. S. Adebayo and H. Rjoub, "Assessment of the role of trade and renewable energy consumption on consumption-based carbon emissions: evidence from the MINT economies," *Environmental Science and Pollution Research*, vol. 28, no. 41, pp. 58271–58283, 2021.

[5] Z. Ahmed, M. Ahmad, H. Rjoub, O. A. Kalugina, and N. Hussain, "Economic growth, renewable energy consumption, and ecological footprint: exploring the role of environmental regulations and democracy in sustainable development," *Sustainable Development.*, 2021.

[6] R. Alayi, N. Khalilpoor, S. Heshmati, A. Najafi, and A. Issakhov, "Thermal and environmental analysis solar water heater system for residential buildings," *International Journal of Photoenergy*, vol. 2021, 9 pages, 2021.

[7] T. S. Adebayo, S. D. Oladipupo, I. Adeshola, and H. Rjoub, "Wavelet analysis of impact of renewable energy consumption and technological innovation on CO_2 emissions: evidence from Portugal," *Environmental Science and Pollution Research*, vol. 29, no. 16, pp. 23887–23904, 2021.

[8] T. S. Adebayo and D. Kirikkaleli, "Impact of renewable energy consumption, globalization, and technological innovation on environmental degradation in Japan: application of wavelet tools," *Environment, Development and Sustainability*, vol. 23, no. 11, pp. 16057–16082, 2021.

[9] M. Jahangiri, O. Nematollahi, A. Haghani, H. A. Raiesi, and A. Alidadi Shamsabadi, "An optimization of energy cost of clean hybrid solar-wind power plants in Iran," *International Journal of Green Energy*, vol. 16, no. 15, pp. 1422–1435, 2019.

[10] B. Z. Adewole, B. O. Malomo, O. P. Olatunji, and A. O. Ikobayo, "Simulation and experimental verification of electrical power output of a microcontroller based solar tracking photovoltaic module," *International Journal of Sustainable Energy and Environmental Research*, vol. 9, no. 1, pp. 34–45, 2020.

[11] R. Alayi, M. Jahangiri, J. W. G. Guerrero, R. Akhmadeev, R. A. Shichiyakh, and S. A. Zanghaneh, "Modelling and reviewing the reliability and multi-objective optimization of wind-turbine system and photovoltaic panel with intelligent algorithms," *Clean Energy*, vol. 5, no. 4, pp. 713–730, 2021.

[12] R. Alayi, M. Jahangiri, and A. Najafi, "Energy analysis of vacuum tube collector system to supply the required heat gas pressure reduction station," *International Journal of Low-Carbon Technologies*, vol. 16, no. 4, pp. 1391–1396, 2021.

[13] M. Wolf, "Performance analyses of combined heating and photovoltaic power systems for residences," *Energy Conversion*, vol. 16, no. 1-2, pp. 79–90, 1976.

[14] J. Zhang, Z. Zhou, J. Quan et al., "A flexible film to block solar radiation for daytime radiative cooling," *Solar Energy Materials and Solar Cells*, vol. 225, article 111029, 2021.

[15] S. Agrebi, R. Chargui, B. Tashtoush, and A. Guizani, "Analyse comparative des performances d'une pompe a chaleur assistee par l'anergie solaire pour le chauffage de serres en Tunisie," *International Journal of Refrigeration*, vol. 131, pp. 547–558, 2021.

[16] M. Sultan S, C. P. Tso, and E. E. Mn, "A case study on effect of inclination angle on performance of photovoltaic solar thermal collector in forced fluid mode," *Renewable Energy Research and Application*, vol. 1, no. 2, pp. 187–196, 2020.

[17] H. Ashofteh and A. Behzadi Forough, "Renewable energy's potential scrutiny by PVSYST and RETSCREEN softwares case study: Khoy Province," *Renewable Energy Research and Applications*, 2022.

[18] A. Taheri, M. Kazemi, M. Amini, M. Sardarabadi, and A. Kianifar, "The performance assessment of nanofluid-based PVTs with and without transparent glass cover: outdoor experimental study with thermodynamics analysis," *Journal of Thermal Analysis and Calorimetry*, vol. 143, no. 6, pp. 4025–4037, 2021.

[19] Z. Fu, X. Liang, Y. Li, L. Li, and Q. Zhu, "Performance improvement of a PVT system using a multilayer structural heat exchanger with PCMs," *Renewable Energy*, vol. 169, pp. 308–317, 2021.

[20] M. Tahmasbi, M. Siavashi, A. M. Norouzi, and M. H. Doranehgard, "Thermal and electrical efficiencies enhancement of a solar photovoltaic- thermal/air system (PVT/air) using metal foams," *Journal of the Taiwan Institute of Chemical Engineers.*, vol. 124, pp. 276–289, 2021.

[21] P. Jagadale, A. Choudhari, and S. Jadhav, "Design and simulation of grid connected solar Si-poly photovoltaic plant using PVsyst for Pune, India location," *Renewable Energy Research and Applications*, vol. 3, no. 1, pp. 41–49, 2022.

[22] O. A. Al-Shahri, F. B. Ismail, M. A. Hannan et al., "Solar photovoltaic energy optimization methods, challenges and issues: a comprehensive review," *Journal of Cleaner Production*, vol. 284, article 125465, 2021.

[23] Z. Molamohamadi and M. Talaei, "Analysis of a proper strategy for solar energy deployment in Iran using SWOT matrix," *Renewable Energy Research and Applications*, vol. 3, no. 1, pp. 71–78, 2022.

[24] A. Shahsavar, "Experimental evaluation of energy and exergy performance of a nanofluid-based photovoltaic/thermal system equipped with a sheet-and-sinusoidal serpentine tube collector," *Journal of Cleaner Production*, vol. 287, article 125064, 2021.

[25] A. Sohani, M. H. Shahverdian, H. Sayyaadi et al., "Selecting the best nanofluid type for a photovoltaic thermal (PV/T) system based on reliability, efficiency, energy, economic, and environmental criteria," *Journal of the Taiwan Institute of Chemical Engineers.*, vol. 124, pp. 351–358, 2021.

[26] B. Kurşun, "Theoretical energy and exergy analysis of a combined cooling, heating and power system assisted by a low concentrated photovoltaic recuperator," *Energy Conversion and Management*, vol. 228, article 113659, 2021.

[27] X. Zhang, X. Zhao, S. Smith, J. Xu, and X. Yu, "Review of R&D progress and practical application of the solar photovoltaic/thermal (PV/T) technologies," *Renewable and Sustainable Energy Reviews*, vol. 16, no. 1, pp. 599–617, 2012.

[28] D. Das, P. Kalita, and O. Roy, "Flat plate hybrid photovoltaic-thermal (PV/T) system: a review on design and development," *Renewable and Sustainable Energy Reviews*, vol. 84, pp. 111–130, 2018.

[29] .

Hindawi
International Journal of Photoenergy
Volume 2022, Article ID 3625541, 9 pages
https://doi.org/10.1155/2022/3625541

Research Article

Gray-Related Support Vector Machine Optimization Strategy and Its Implementation in Forecasting Photovoltaic Output Power

Bo Xiao,[1] **Hai Zhu**,[1] **Sujun Zhang**,[2] **Zi OuYang**,[2] **Tandong Wang**,[3] **and Saeed Sarvazizi**[4,5]

[1]*School of Electronic and Electrical Engineering, Shanghai University of Engineering Science, Shanghai 201620, China*
[2]*Meteocontrol (Shanghai) Data Tech Co., Ltd, Shanghai 200233, China*
[3]*School of Electronics and Information, Northwestern Polytechnical University, Xi'an, Shaanxi 710072, China*
[4]*Department of Petroleum Engineering, Ahwaz Faculty of Petroleum Engineering, Petroleum University of Technology (PUT), Ahwaz, Iran*
[5]*Department of Petroleum Engineering, Amirkabir University of Technology (Tehran Polytechnic), Tehran, Iran*

Correspondence should be addressed to Bo Xiao; 02180013@sues.edu.cn and Saeed Sarvazizi; sarvazizi.saeed@aut.ac.ir

Received 26 November 2021; Revised 2 February 2022; Accepted 11 February 2022; Published 25 February 2022

Academic Editor: Hafiz Muhammad Ali

Reliable and accurate photovoltaic (PV) output power projection is critical for power grid security, stability, and economic operation. However, because of the indirectness, unpredictability, and solar energy volatility, predicting precise and reliable photovoltaic output power is a complicated subject. The photovoltaic output power variable is evaluated in this study using a powerful machine learning approach called the support vector machine model based on gray-wolf optimization. A vast dataset of previously published papers was compiled for this purpose. Several studies were carried out to assess the suggested model. The statistical evaluation revealed that this model predicts absolute values with reasonable accuracy, including R^2 and RMSE values of 0.908 and 74.6584, respectively. The practical input data were also subjected to sensitivity analysis. The results of this analysis showed that the air temperature parameter has a greater effect on the target parameter than the solar irradiance intensity parameter (relevancy factor equal to 0.75 compared to 0.49, respectively). The leverage approach was also used to test the accuracy of actual data, and the findings revealed that the vast majority of data is accurate. This basic but accurate model may be quite effective in predicting target values and could be a viable substitute for laboratory data.

1. Introduction

Given the challenges such as climate change and the fossil energy crisis, renewable energy production has become much more vital [1–3]. Photovoltaic power production has gained more attention and increased each year because of the benefits of plentiful resources and minimal pollution [4–6]. Improving the reliability and accuracy of photovoltaic output power prediction is an excellent approach [7, 8]. Accurate and consistent prediction results may assist the power grid in improving power quality and reducing system reserve capacities [9]. However, due to climate change, severe weather events have become more common in recent years, making it challenging to construct an accurate and reliable prediction model [10–12].

Several photovoltaic output power predictive models, including the time series model [13, 14], physical model [15], and artificial intelligence model [16, 17], have lately been proposed. The precision of the physical model prediction is heavily reliant on the accuracy of the numerical weather forecast. However, improving NWP accuracy is challenging at the moment [18]. The nonlinear properties of photovoltaic output power cannot be represented using a time series model. As a result, the prediction accuracy is low. The artificial intelligence model is capable of nonlinear fitting [19].

There are essentially three types of hybrid models for predicting photovoltaic output power. The first type predicts photovoltaic output power using an AI model paired with an

optimization technique [20–23]. Photovoltaic output power was effectively estimated using an upper lower limit approximation and ELMs, as proved by Ni et al. [20]. According to work done by Liu and his colleagues, few investigations have assessed the uncertainty of predicting photovoltaic power outputs [24]. As a result, several neural networks paired with genetic algorithms were created [25]. The combined model has greater prediction accuracy and reliability, according to empirical data. Using a backpropagation neural platform with the evolving mental technique, Wang and Shen proposed a mixed framework that may be used in many situations [26]. The modeling revealed that the hybrid model outperformed the other methods in terms of predicting photovoltaic output power. While the first type produced acceptable predictive performance, it is challenging to enhance the accuracy further. The reason for this is that the first type did not extract various characteristics of photovoltaic output power. The second type is proposed to overcome this issue. First, the photovoltaic output power is decomposed into its constituent parts using a signal disintegration method. As a result, many characteristics may be retrieved. After that, an artificial intelligence model was created for the prediction of these elements. Wavelet deconstruction and minimal squares support vector systems were used by Giorgi and his colleagues to forecast photovoltaic production potential [27]. In addition, a thorough error assessment was performed to compare the model's efficiency to that of competing models. To forecast photovoltaic output strength, Wang and his colleagues used a wavelet transformation paired with a definitive method [28]. A significant ability to enhance prediction reliability was shown numerically by the recommended technique. WT was utilized by Malvoni and his colleagues to deconstruct the historical data [29]. LSSVM and the group technique were then used to predict photovoltaic output power. Majumder and his colleagues proposed a more reliable photovoltaic output power predictive model for different weathers and times [30]. The prediction model was used in conjunction with altering mode decomposition as well as an extreme learning machine. Even though the signal decomposition model was effectively employed for extracting features, the single artificial intelligence model has its disadvantages. Variables are assigned haphazardly and are prone to falling into local optimum. It is difficult for the 2nd type to enhance the projection any further. The third type has been proposed to address the issues mentioned above. To begin, the signal decomposition model is utilized on the original photovoltaic output power. Subsequently, for prediction, an artificial intelligence model mixed with an optimization method is constructed. Lin and Pai used seasonal decomposition to manage the initial photovoltaic output power [31]. Subsequently, evolutionary algorithm-optimized minimal squares support vector regression was introduced for forecasting purposes. The suggested model outperformed the competition in terms of predicting accuracy, according to empirical data. Prediction is challenging due to the significant volatility of photovoltaic production power. A new approach based on enhanced experimental deconstruction modeling as well as support vector regression utilizing an improvement approach was developed to solve this problem by Shang and Wei [32]. WT was utilized by Eseye and his colleagues to divide the original photovoltaic output power into finer elements [33]. Next, the regression of the support vector was used. Particle swarm optimization was used to enhance the variables of regression of support vector to increase predicting accuracy. The findings revealed that the hybrid model was more accurate. An ELM improved via the sine cosine approach was utilized by Behera and Nayak to disassemble and anticipate the initial photovoltaic output power employing experimental pattern disintegration [34]. The findings revealed that the suggested model worked well in terms of predicting photovoltaic output power. Even though the third type produces superior predicting results, it nevertheless has the following disadvantages. Since photovoltaic output power has high fluctuation and changeability, no constant-variable simulation can provide a reliable estimation. The versatility of existing prediction models is sometimes overlooked. Secondly, the present decomposition models have not efficiently recovered distinct information from photovoltaic output power. The purpose of writing this article is to propose a model for estimating photovoltaic (PV) output power with higher accuracy compared to previous works. Therefore, the GWO-SVM model was studied, and the performance of this model was estimated by examining the related statistical analyses.

2. Support Vector Machine

When it comes to identifying patterns and analyzing data, SVM is one of the monitored training approaches established employing numerical modeling principles [35, 36]. Additionally, statistical analysis and categorization are performed using this parameter [37]. The purpose of our study is to use this technique as a regression approach by employing a nonlinear component of $\Phi(x)$ to move information from a high-dimensional environment to a first-dimensional one [38–40]. The aforementioned nonlinear mapping is accomplished by the creation of the appropriate kernel component of $K(x_i, y_i)$ [41]. Additionally, it is considered that certain points are not categorized adequately by a hyperplane; hence, the slack variable is used for this problem [42]. Using m data points in the data space as well as a training dataset of $D = \{(x_i, y_i) \mid i = 1, 2, 3, \cdots, m\}$, a regression function may be presented with $y = w^T\Phi(x) + b$, where $\Phi(x)$ represents nonlinear topography function and b and w indicate offsets as well as weight vectors, respectively [43, 44]. As a result, the optimal formula for the support vector regression model is as follows [45, 46]:

$$\min \frac{1}{2}\|w\|^2 + c\sum_{i=1}^{m}\left(\xi_i + \xi_i^*\right)$$
$$\text{s.t.}\begin{Bmatrix} y_i - w^T.\Phi(x_i) - b \le \varepsilon + \xi_i \\ w^T\cdot\Phi(x_i) + b - y_i \le \varepsilon + \xi_i^* \\ \xi_i \ge 0, \xi_i^* \ge 0 \end{Bmatrix}, \tag{1}$$

where C is the penalty parameter, ε displays the loss function variable, and ξ_i^* and ξ_i are the slack parameters [47]. The model loss is calculated once the decisive fault between anticipated and actual scores is more extensive [48, 49]. This problem foundation relates to convex quadratic programming. The Lagrangian function is utilized to integrate the constraint into the cost function, and the dual question may be dissolved in the following manner [50]:

$$\max \left[-\frac{1}{2}\sum_{i=1}^{m}\sum_{j=1}^{m}(\alpha_i - \alpha_i^*)\left(\alpha_j - \alpha_j^*\right)\Phi(x_i)\cdot\Phi\left(x_j\right) + \sum_{i=1}^{m}(\alpha_i - \alpha_i^*)y_i - \sum_{i=1}^{m}(\alpha_i - \alpha_i^*)y_i\varepsilon \right]$$
$$\text{s.t.} \sum_{i=1}^{m}(\alpha_i - \alpha_i^*) = 0, 0 \le \alpha_i \le C, 0 \le \alpha_i^* \le C. \tag{2}$$

Here, α indicates the Lagrangian multiplier, and the kernel function computes the movement relation of the used data collection [51]. The function of kernel radial foundation is utilized in this study as [52]

$$K\left(x_i, x_j\right) = \exp\left(-\gamma\left\|x_i - x_j\right\|^2\right), \tag{3}$$

where γ denotes the RBF variable. Based on the above explanations, there are two deciding factors in this learning, notably forfeit variable C and the RBF variable, which refers to generalization capacity and estimation performance, respectively. Lastly, the SVM hyperparameters must be optimized [53, 54].

3. Gray-Wolf Optimization

The GWO algorithm is among the optimization algorithms generated from simulations of gray wolf social hierarchy and predation behavior [55, 56]. The gray wolf pack has a solid social structure, shown in a pyramidal hierarchy [57]. The gray wolf pack is divided into four categories depending on rank. The low-level wolf follows the high-level wolf in such grades. The gray wolf pack is responsible for hunting actions such as aggressiveness, encirclement, and prey capture. The wolf pack explored for their predation once GWO had found the optimum option [58]. After that, it rummages for the optimum choice based on the gray wolf performance score as well as the relationship among the different levels [59, 60].

In the training phase, 70 percent of the records have been employed, with the remainder 30 percent being used to assess the generalizability of the algorithm. All data were normalized between -1 and 1 and put into the SVM model [61].

4. Sensitivity Analysis

To examine the effects of the input parameters on the outputs, a mathematical approach known as sensitivity analysis was used [62]. There are many different uses for SA, including determining research priorities, detecting technological flaws, and identifying essential regions [39, 63]. There are two types of SA analyses: global and local [64]. Assuming other factors stay unchanged, local sensitivity examines the impact of one factor on the objective. On the other hand, global sensitivity is a common approach that investigates the influence of inputs on the target once all parameters are changed. Figure 1 shows the efficacy of the input parameters in GWO-SVM for predicting photovoltaic output power. As can be seen, the air temperature has the most significant influence on the photovoltaic output power. The results show that all defined inputs have a considerable impact on the photovoltaic output power values.

5. Designing a GWO-SVM Model

Based on previous discussions, C, ε, and γ control the performance of the SVM algorithm. As a result, GWO was employed to improve these variables in the current investigation. The GWO is divided into four sections: tracking, social hierarchy, encircling, and attacking prey. For modeling wolf hierarchy, four types of gray wolves, namely, alpha (α), beta (β), delta (δ), and omega (ω), are employed with α, β, δ, and ω as solutions. The a, b, and d scores are computed according to the associated fitness values so that the top three strategies may predict the prey's location. The literature has detailed information detailing all elements of this method. The GWO is terminated once the last condition is met.

6. Outlier Analysis

Outlier diagnosis is a critical statistical method utilized to distinguish sets of data from a larger data collection [65]. Outliers are detected using an efficient technique, termed leverage statistics [66]. The crucial leverage extent H^* Hat indicators (H) and standard (R) were all taken into account in the current technique. The Hat index is written as follows [65, 67]:

$$H = X\left(X^tX\right)^{-1}X^t, \tag{4}$$

where X and t represent the two-dimensional $n \times k$ matrix and the transpose matrix symbol, respectively. The primary oblique of H is where the most likely Hat decision lies in this issue [68]. The presentation of the Williams plot identifies the outliers. The correlation between normalized residue and the Hat indicator is shown in this chart [69, 70]. The valid range of data is specified as a squared area with a range of ± 3 standard

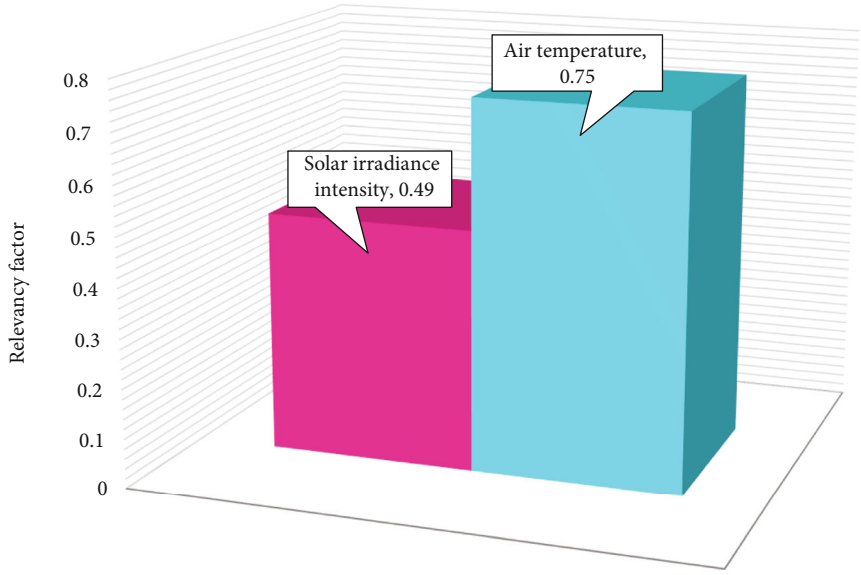

Figure 1: Sensitivity analysis on parameters affecting output.

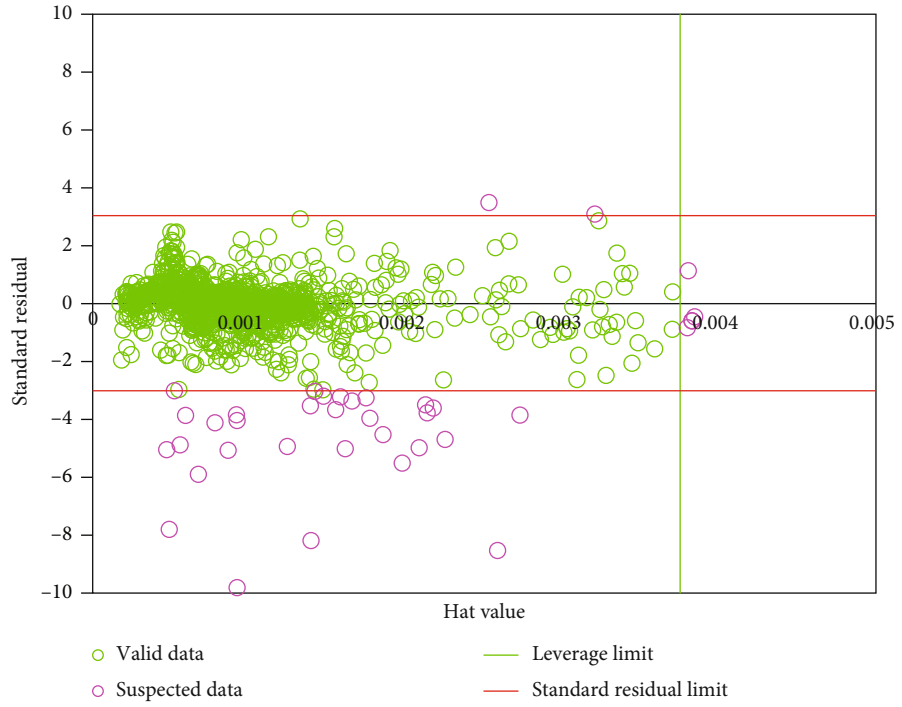

Figure 2: Williams plot and analysis of data to determine suspicious points.

deviations and a strength domain of $3n/(p+1)$ (p and n indicate the number of inputs of the model and the learning nodes). The significant frequency of data put in the spectra of $-3 \le R \le 3$ and $0 \le H \le H^*$ reveals that GWO-SVM may be used in a wide range of domains. Outliers are described as data (R and H) that exceed the ranges $[-3, 3]$ and $[0, H^*]$. The Williams plot of GWO-SVM outputs is depicted in Figure 2. Except for one node in the spectrum of $R < -3$, most photovoltaic output power values investigated in this research fell within the domain of $[0, H^*]$ and $[-3, 3]$, demonstrating that the GWO-SVM algorithm is impressive in statistical analysis and may also enhance the capacity to portray the internal relations among the photovoltaic output power score and inputs.

7. Model Evaluation

Figure 3 shows the photovoltaic output power value calculated using the GWO-SVM method. The acquired photovoltaic output power values are presented vs. the data index, showing the training and testing results. As can be observed, the suggested model has a high prediction capacity.

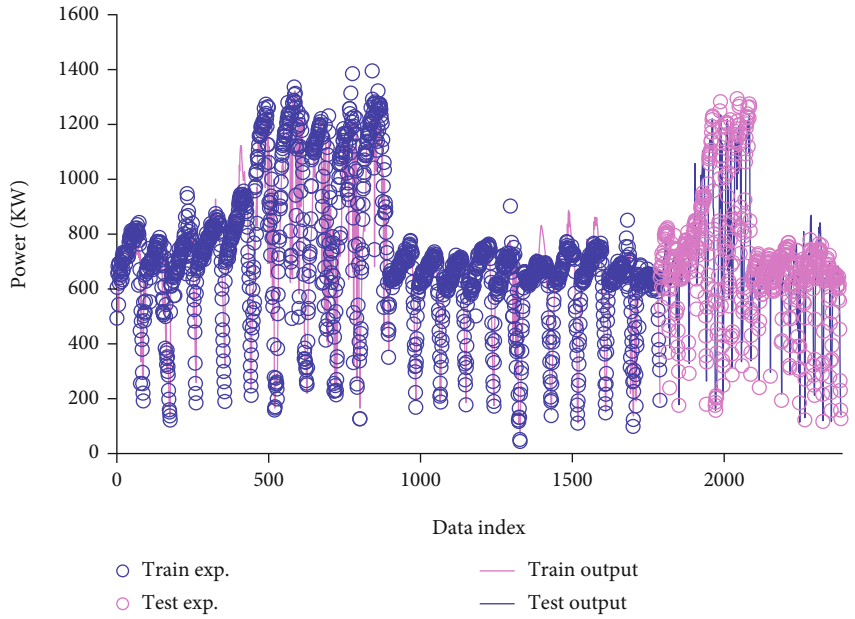

Figure 3: Simultaneous observation of predicted and actual values of the target parameter.

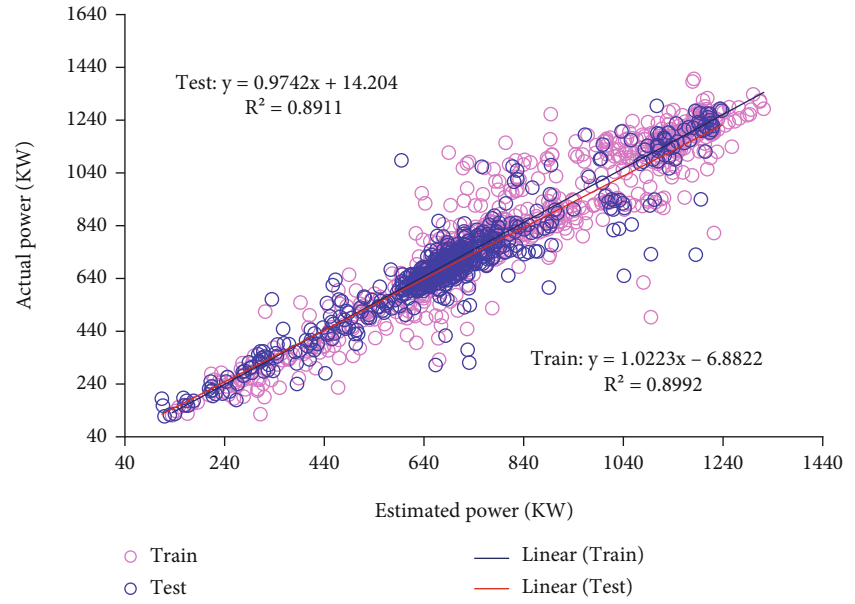

Figure 4: Regression analysis performed on the proposed model.

The determination coefficient (R^2) indicates how close determined values are to actual values [44]. R^2 is a number that ranges between 0 and 1.0. The model predicts more correctly as this parameter approaches unity. The created model's near-unity R^2 reflects its ability to estimate the photovoltaic output power value. The R^2 coefficients for the learning and evaluation components of the GWO-SVM algorithms are 0.913 and 0.891, correspondingly, as shown in the intersecting graph of modeled and actual scores in Figure 4. There are numerous scores around the bisector path in learning and validation data collection, showing that the GWO-SVM has been correctly computed. The prediction capabilities and precision of the GWO-SVM model are shown in Figure 4.

The relative deviation percentages for the GWO-SVM simulation are also demonstrated in Figure 5. It is shown that the GWO-SVM model has high accuracy, with the determined variation not exceeding the 50% band.

Table 1 shows the values of different statistical parameters in order to evaluate this model in estimating the target parameter.

In order to compare the accuracy of the model proposed in this paper, with the most accurate models ever suggested to predict this parameter by Zhang et al. in 2020, statistical parameters were used [71]. According to Table 2, it is clear that the model proposed in this paper shows higher accuracy in estimating the target parameter.

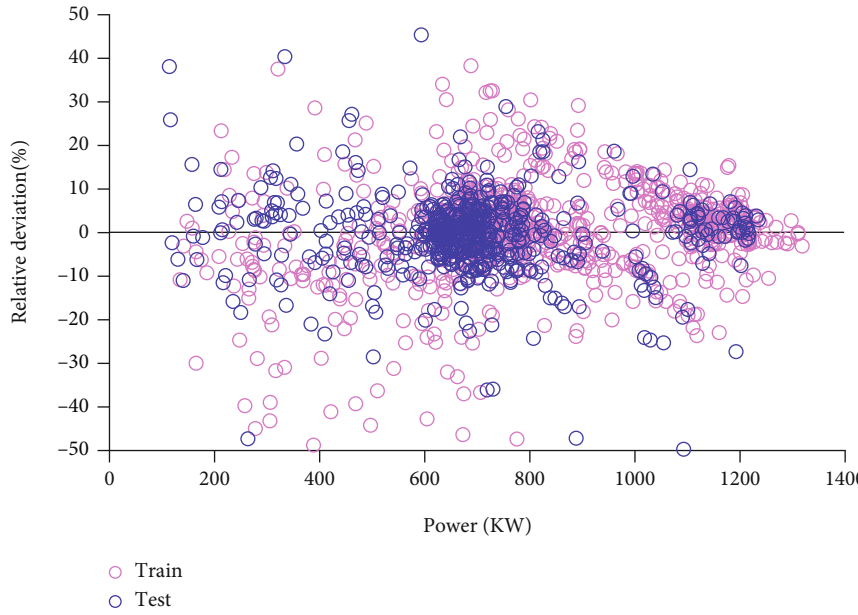

Figure 5: Relative deviation values calculated on the model to evaluate its accuracy in predicting target data.

Table 1: Values of statistical parameters obtained for the proposed model.

Group	R^2	MRE (%)	MSE	RMSE	STD
Train	0.913	7.103	5029.275084	70.9174	53.8453
Test	0.891	7.088	5573.878233	74.6584	59.9669
Total	0.908	7.099	5165.425871	74.6584	55.4307

Table 2: Comparing the accuracy of different models in predicting the target parameter.

Model	RMSE
ARIMA	193.29
LSSVM	272.51
WNN	188.30
This work	74.6584

8. Conclusions

This study is aimed at evaluating how effectively a statistical learning-based model may predict the output. For that purpose, the GWO was included in the SVM model. The GWO method performed well when it came to determining tuning parameters. When compared to actual data points, estimations were proved to be highly accurate. The efficiency of the suggested methodologies was established by a definitive agreement between model outputs and absolute values while evaluating the model throughout the training and testing phases, as evidenced by statistical analysis. Comparing the suggested models' results with another reported correlation validated the models' accuracy as expected. In contrast to the robust mathematical methodologies used for this output prediction, the suggested strategy for predicting photovoltaic output power is user-friendly, making it a helpful tool for academics, especially in related domains.

Data Availability

Data references are described in the text of the article.

Conflicts of Interest

The authors declare that they have no conflicts of interest.

Acknowledgments

This work was supported by the National key research and development program (2018YFB1500800), Sailing Program of Young Science and Technology Talents supported by Shanghai Science and Technology Commission (Grant No. 19YF1418200), and Young Scientists Fund of the National Natural Science Foundation of China (Grant No. 61902237).

References

[1] S. R. Sharvini, Z. Z. Noor, C. S. Chong, L. C. Stringer, and R. O. Yusuf, "Energy consumption trends and their linkages with renewable energy policies in east and southeast Asian countries: challenges and opportunities," *Sustainable Environment Research*, vol. 28, no. 6, pp. 257–266, 2018.

[2] C. Viviescas, L. Lima, F. A. Diuana et al., "Contribution of variable renewable energy to increase energy security in Latin America: complementarity and climate change impacts on wind and solar resources," *Renewable and Sustainable Energy Reviews*, vol. 113, article 109232, 2019.

[3] U. Bulut and G. Muratoglu, "Renewable energy in Turkey: great potential, low but increasing utilization, and an empirical analysis on renewable energy-growth nexus," *Energy Policy*, vol. 123, pp. 240–250, 2018.

[4] B. Lin and J. Zhu, "The role of renewable energy technological innovation on climate change: empirical evidence from China," *Science of the Total Environment*, vol. 659, pp. 1505–1512, 2019.

[5] Y. Song, Q. Ji, Y. J. du, and J. B. Geng, "The dynamic dependence of fossil energy, investor sentiment and renewable energy stock markets," *Energy Economics*, vol. 84, article 104564, 2019.

[6] T. Xia, Q. Ji, D. Zhang, and J. Han, "Asymmetric and extreme influence of energy price changes on renewable energy stock performance," *Journal of Cleaner Production*, vol. 241, article 118338, 2019.

[7] K. Solaun and E. Cerdá, "Climate change impacts on renewable energy generation. A review of quantitative projections," *Renewable and Sustainable Energy Reviews*, vol. 116, article 109415, 2019.

[8] N. Vidadili, E. Suleymanov, C. Bulut, and C. Mahmudlu, "Transition to renewable energy and sustainable energy development in Azerbaijan," *Renewable and Sustainable Energy Reviews*, vol. 80, pp. 1153–1161, 2017.

[9] B. Liu, J. Chen, H. Wang, and Q. Wang, "Renewable energy and material supply risks: a predictive analysis based on an LSTM model," *Frontiers in Energy Research*, vol. 8, p. 163, 2020.

[10] K. Nam, S. Hwangbo, and C. Yoo, "A deep learning-based forecasting model for renewable energy scenarios to guide sustainable energy policy: a case study of Korea," *Renewable and Sustainable Energy Reviews*, vol. 122, article 109725, 2020.

[11] M. I. al Irsyad, A. Halog, and R. Nepal, "Renewable energy projections for climate change mitigation: an analysis of uncertainty and errors," *Renewable Energy*, vol. 130, pp. 536–546, 2019.

[12] B. Wang, Q. Wang, Y. M. Wei, and Z. P. Li, "Role of renewable energy in China's energy security and climate change mitigation: an index decomposition analysis," *Renewable and Sustainable Energy Reviews*, vol. 90, pp. 187–194, 2018.

[13] L. Martín, L. F. Zarzalejo, J. Polo, A. Navarro, R. Marchante, and M. Cony, "Prediction of global solar irradiance based on time series analysis: application to solar thermal power plants energy production planning," *Solar Energy*, vol. 84, no. 10, pp. 1772–1781, 2010.

[14] Y. Li, Y. Su, and L. Shu, "An ARMAX model for forecasting the power output of a grid connected photovoltaic system," *Renewable Energy*, vol. 66, pp. 78–89, 2014.

[15] M. Pierro, M. de Felice, E. Maggioni et al., "Data-driven upscaling methods for regional photovoltaic power estimation and forecast using satellite and numerical weather prediction data," *Solar Energy*, vol. 158, pp. 1026–1038, 2017.

[16] H. T. Pedro and C. F. Coimbra, "Assessment of forecasting techniques for solar power production with no exogenous inputs," *Solar Energy*, vol. 86, no. 7, pp. 2017–2028, 2012.

[17] M. Hossain, S. Mekhilef, M. Danesh, L. Olatomiwa, and S. Shamshirband, "Application of extreme learning machine for short term output power forecasting of three grid-connected PV systems," *Journal of Cleaner Production*, vol. 167, pp. 395–405, 2017.

[18] K. Wang, X. Qi, and H. Liu, "A comparison of day-ahead photovoltaic power forecasting models based on deep learning neural network," *Applied Energy*, vol. 251, article 113315, 2019.

[19] F. Rodríguez, A. Fleetwood, A. Galarza, and L. Fontán, "Predicting solar energy generation through artificial neural networks using weather forecasts for microgrid control," *Renewable Energy*, vol. 126, pp. 855–864, 2018.

[20] Q. Ni, S. Zhuang, H. Sheng, G. Kang, and J. Xiao, "An ensemble prediction intervals approach for short-term PV power forecasting," *Solar Energy*, vol. 155, pp. 1072–1083, 2017.

[21] W. VanDeventer, E. Jamei, G. S. Thirunavukkarasu et al., "Short-term PV power forecasting using hybrid GASVM technique," *Renewable Energy*, vol. 140, pp. 367–379, 2019.

[22] U. K. Das, K. S. Tey, M. Seyedmahmoudian et al., "Forecasting of photovoltaic power generation and model optimization: a review," *Renewable and Sustainable Energy Reviews*, vol. 81, pp. 912–928, 2018.

[23] M. Seyedmahmoudian, E. Jamei, G. Thirunavukkarasu et al., "Short-term forecasting of the output power of a building-integrated photovoltaic system using a metaheuristic approach," *Energies*, vol. 11, no. 5, p. 1260, 2018.

[24] L. Liu, Y. Zhao, D. Chang et al., "Prediction of short-term PV power output and uncertainty analysis," *Applied Energy*, vol. 228, pp. 700–711, 2018.

[25] L.-L. Li, S. Y. Wen, M. L. Tseng, and C. S. Wang, "Renewable energy prediction: a novel short-term prediction model of photovoltaic output power," *Journal of Cleaner Production*, vol. 228, pp. 359–375, 2019.

[26] H. Wang and J. Shen, "An improved model combining evolutionary algorithm and neural networks for PV maximum power point tracking," *IEEE Access*, vol. 7, pp. 2823–2827, 2019.

[27] M. G. De Giorgi, P. M. Congedo, M. Malvoni, and D. Laforgia, "Error analysis of hybrid photovoltaic power forecasting models: a case study of Mediterranean climate," *Energy Conversion and Management*, vol. 100, pp. 117–130, 2015.

[28] H. Wang, H. Yi, J. Peng et al., "Deterministic and probabilistic forecasting of photovoltaic power based on deep convolutional neural network," *Energy Conversion and Management*, vol. 153, pp. 409–422, 2017.

[29] M. Malvoni, M. G. De Giorgi, and P. M. Congedo, "Forecasting of PV power generation using weather input data-preprocessing techniques," *Energy Procedia*, vol. 126, pp. 651–658, 2017.

[30] I. Majumder, P. Dash, and R. Bisoi, "Variational mode decomposition based low rank robust kernel extreme learning machine for solar irradiation forecasting," *Energy Conversion and Management*, vol. 171, pp. 787–806, 2018.

[31] K.-P. Lin and P.-F. Pai, "Solar power output forecasting using evolutionary seasonal decomposition least-square support vector regression," *Journal of Cleaner Production*, vol. 134, pp. 456–462, 2016.

[32] C. Shang and P. Wei, "Enhanced support vector regression based forecast engine to predict solar power output," *Renewable Energy*, vol. 127, pp. 269–283, 2018.

[33] A. T. Eseye, J. Zhang, and D. Zheng, "Short-term photovoltaic solar power forecasting using a hybrid wavelet-PSO-SVM model based on SCADA and meteorological information," *Renewable Energy*, vol. 118, pp. 357–367, 2018.

[34] M. K. Behera and N. Nayak, "A comparative study on short-term PV power forecasting using decomposition based optimized extreme learning machine algorithm," *Engineering Science and Technology, an International Journal*, vol. 23, no. 1, pp. 156–167, 2020.

[35] D. A. Pisner and D. M. Schnyer, "Support vector machine," in *Machine Learning*, pp. 101–121, Elsevier, 2020.

[36] S. Muthukrishnan et al., "Support vector machine for modelling and simulation of heat exchangers," *Thermal Science*, vol. 24, pp. 499–503, 2020.

[37] V. Vapnik, *The Nature of Statistical Learning Theory Neural Networks*, Springer Science & Business Media, New York, NY, 2013.

[38] A. Baghban, F. Pourfayaz, M. H. Ahmadi, A. Kasaeian, S. M. Pourkiaei, and G. Lorenzini, "Connectionist intelligent model estimates of convective heat transfer coefficient of nanofluids in circular cross-sectional channels," *Journal of Thermal Analysis and Calorimetry*, vol. 132, no. 2, pp. 1213–1239, 2018.

[39] A. Baghban, M. Kahani, M. A. Nazari, M. H. Ahmadi, and W. M. Yan, "Sensitivity analysis and application of machine learning methods to predict the heat transfer performance of CNT/water nanofluid flows through coils," *International Journal of Heat and Mass Transfer*, vol. 128, pp. 825–835, 2019.

[40] M. H. Ahmadi, A. Baghban, M. Sadeghzadeh et al., "Evaluation of electrical efficiency of photovoltaic thermal solar collector," *Engineering Applications of Computational Fluid Mechanics*, vol. 14, no. 1, pp. 545–565, 2020.

[41] S. Abdollahi, H. R. Pourghasemi, G. A. Ghanbarian, and R. Safaeian, "Prioritization of effective factors in the occurrence of land subsidence and its susceptibility mapping using an SVM model and their different kernel functions," *Bulletin of Engineering Geology and the Environment*, vol. 78, no. 6, pp. 4017–4034, 2019.

[42] Y. Zhou, F. J. Chang, L. C. Chang, I. F. Kao, Y. S. Wang, and C. C. Kang, "Multi-output support vector machine for regional multi-step-ahead PM2. 5 forecasting," *Science of the Total Environment*, vol. 651, pp. 230–240, 2019.

[43] A. Zendehboudi, M. A. Baseer, and R. Saidur, "Application of support vector machine models for forecasting solar and wind energy resources: a review," *Journal of Cleaner Production*, vol. 199, pp. 272–285, 2018.

[44] D. Ahangari, R. Daneshfar, M. Zakeri, S. Ashoori, and B. S. Soulgani, "On the prediction of geochemical parameters (TOC, S1 and S2) by considering well log parameters using ANFIS and LSSVM strategies," *Petroleum*, 2021.

[45] S. Huang, N. Cai, P. P. Pacheco, S. Narrandes, Y. Wang, and W. Xu, "Applications of support vector machine (SVM) learning in cancer genomics," *Cancer Genomics & Proteomics*, vol. 15, no. 1, pp. 41–51, 2018.

[46] J. Cervantes, F. Garcia-Lamont, L. Rodríguez-Mazahua, and A. Lopez, "A comprehensive survey on support vector machine classification: applications, challenges and trends," *Neurocomputing*, vol. 408, pp. 189–215, 2020.

[47] N. A. Almansour, H. F. Syed, N. R. Khayat et al., "Neural network and support vector machine for the prediction of chronic kidney disease: a comparative study," *Computers in Biology and Medicine*, vol. 109, pp. 101–111, 2019.

[48] H. Wang, B. Zheng, S. W. Yoon, and H. S. Ko, "A support vector machine-based ensemble algorithm for breast cancer diagnosis," *European Journal of Operational Research*, vol. 267, no. 2, pp. 687–699, 2018.

[49] S. M. Alizadeh, I. Alruyemi, R. Daneshfar, M. Mohammadi-Khanaposhtani, and M. Naseri, "An insight into the estimation of drilling fluid density at HPHT condition using PSO-, ICA-, and GA-LSSVM strategies," *Scientific Reports*, vol. 11, no. 1, pp. 1–14, 2021.

[50] L. Hu and J. Cui, "Digital image recognition based on fractional-order-PCA-SVM coupling algorithm," *Measurement*, vol. 145, pp. 150–159, 2019.

[51] M. Zamen, A. Baghban, S. M. Pourkiaei, and M. H. Ahmadi, "Optimization methods using artificial intelligence algorithms to estimate thermal efficiency ofPV/T system," *Energy Science & Engineering*, vol. 7, no. 3, pp. 821–834, 2019.

[52] Z. Shao, S. L. Yang, F. Gao, K. L. Zhou, and P. Lin, "A new electricity price prediction strategy using mutual information-based SVM-RFE classification," *Renewable and Sustainable Energy Reviews*, vol. 70, pp. 330–341, 2017.

[53] M. U. Ali, H. F. Khan, M. Masud, K. D. Kallu, and A. Zafar, "A machine learning framework to identify the hotspot in photovoltaic module using infrared thermography," *Solar Energy*, vol. 208, pp. 643–651, 2020.

[54] A. Baghban, J. Sasanipour, F. Pourfayaz et al., "Towards experimental and modeling study of heat transfer performance of water- SiO_2nanofluid in quadrangular cross-section channels," *Engineering applications of computational fluid mechanics*, vol. 13, no. 1, pp. 453–469, 2019.

[55] X. Xue, Y. Zheng, and C. Lu, "Optimal allocation of distributed energy supply system under uncertainty based improved gray wolf algorithm," *Distributed Generation & Alternative Energy Journal*, vol. 37, pp. 381–400, 2022.

[56] C. P. Igiri, Y. Singh, and R. C. Poonia, "A review study of modified swarm intelligence: particle swarm optimization, firefly, bat and gray wolf optimizer algorithms," *Recent Advances in Computer Science and Communications*, vol. 13, no. 1, pp. 5–12, 2020.

[57] E. Emary, H. M. Zawbaa, and A. E. Hassanien, "Binary grey wolf optimization approaches for feature selection," *Neurocomputing*, vol. 172, pp. 371–381, 2016.

[58] K. Qian, X. Liu, Y. Wang, X. Yu, and B. Huang, "Modified dual extended Kalman filters for SOC estimation and online parameter identification of lithium-ion battery via modified gray wolf optimizer," *Proceedings of the Institution of Mechanical Engineers Part D: Journal of Automobile Engineering*, no. - article 0954407021104669, 2021.

[59] L. Sun, C. Tang, M. Xu, and Z. Lei, "Sub-pixel displacement measurement based on the combination of a gray wolf optimizer and gradient algorithm," *Applied Optics*, vol. 60, no. 4, pp. 901–911, 2021.

[60] J. Li and F. Yang, "Task assignment strategy for multi-robot based on improved grey wolf optimizer," *Journal of Ambient Intelligence and Humanized Computing*, vol. 11, no. 12, pp. 6319–6335, 2020.

[61] B. S. Yıldız and A. R. Yıldız, "Comparison of grey wolf, whale, water cycle, ant lion and sine-cosine algorithms for the optimization of a vehicle engine connecting rod," *Materials Testing*, vol. 60, no. 3, pp. 311–315, 2018.

[62] N. Kardani, A. Zhou, M. Nazem, and X. Lin, "Modelling of municipal solid waste gasification using an optimised ensemble soft computing model," *Fuel*, vol. 289, article 119903, 2021.

[63] A. Baghban, M. N. Kardani, and A. H. Mohammadi, "Improved estimation of Cetane number of fatty acid methyl esters (FAMEs) based biodiesels using TLBO-NN and PSO-NN models," *Fuel*, vol. 232, pp. 620–631, 2018.

[64] N. Kardani, A. Bardhan, P. Samui, M. Nazem, A. Zhou, and D. J. Armaghani, "A novel technique based on the improved firefly algorithm coupled with extreme learning machine (ELM-IFF) for predicting the thermal conductivity of soil," *Engineering with Computers*, pp. 1–20, 2021.

[65] A. Ghanbari, M. N. Kardani, A. Moazami Goodarzi, M. Janghorban Lariche, and A. Baghban, "Neural computing approach for estimation of natural gas dew point temperature in glycol dehydration plant," *International Journal of Ambient Energy*, vol. 41, no. 7, pp. 775–782, 2020.

[66] A. Baghban and M. Adelizadeh, "On the determination of cetane number of hydrocarbons and oxygenates using adaptive neuro fuzzy inference system optimized with evolutionary algorithms," *Fuel*, vol. 230, pp. 344–354, 2018.

[67] A. Lekomtsev, A. Keykhosravi, M. B. Moghaddam, R. Daneshfar, and O. Rezvanjou, "On the prediction of filtration volume of drilling fluids containing different types of nanoparticles by ELM and PSO-LSSVM based models," *Petroleum*, 2021.

[68] M. N. Kardani, A. Baghban, J. Sasanipour, A. H. Mohammadi, and S. Habibzadeh, "Group contribution methods for estimating CO_2 absorption capacities of imidazolium and ammonium-based polyionic liquids," *Journal of Cleaner Production*, vol. 203, pp. 601–618, 2018.

[69] F. Mousazadeh, M. H. T. Naeem, R. Daneshfar, B. S. Soulgani, and M. Naseri, "Predicting the condensate viscosity near the wellbore by ELM and ANFIS-PSO strategies," *Journal of Petroleum Science and Engineering*, vol. 204, article 108708, 2021.

[70] R. Setiawan, R. Daneshfar, O. Rezvanjou, S. Ashoori, and M. Naseri, "Surface tension of binary mixtures containing environmentally friendly ionic liquids: insights from artificial intelligence," *Environment, Development and Sustainability*, vol. 23, no. 12, pp. 17606–17627, 2021.

[71] J. Zhang, Z. Tan, and Y. Wei, "An adaptive hybrid model for day-ahead photovoltaic output power prediction," *Journal of Cleaner Production*, vol. 244, article 118858, 2020.

Hindawi
International Journal of Photoenergy
Volume 2022, Article ID 2986004, 27 pages
https://doi.org/10.1155/2022/2986004

Review Article

A Review on Factors Influencing the Mismatch Losses in Solar Photovoltaic System

A. D. Dhass,[1] **N. Beemkumar**,[2] **S. Harikrishnan**,[3] **and Hafiz Muhammad Ali**[4]

[1]*Department of Mechanical Engineering, IITE, Indus University, Ahmedabad 382115, India*
[2]*Department of Mechanical Engineering, FET, Jain (Deemed to Be University), Bengaluru 562112, India*
[3]*Department of Mechanical Engineering, Kings Engineering College, Sriperumbudur 602117, India*
[4]*Mechanical Engineering Department, King Fahd University of Petroleum and Minerals, Dhahran 31261, Saudi Arabia*

Correspondence should be addressed to Hafiz Muhammad Ali; hafiz.ali@kfupm.edu.sa

Received 8 October 2021; Revised 9 January 2022; Accepted 1 February 2022; Published 14 February 2022

Academic Editor: Alberto Álvarez-Gallegos

In the last two decades, it is persistently emphasized to develop energy generation systems free from greenhouse gas emissions since these gases cause global warming, and it leads to unpredictable monsoons. Consequently, it might not be a conducive environment for human beings and animals to dwell. To ascertain the green environment for the next generations and reduce the use of fossil fuels, renewable energy sources are highly suggested to generate electrical energy. Solar photovoltaic is reckoned to be one of the promising methods to generate electricity; however, it has a lower conversion value due to various losses resulting from external and internal parameters. Among various losses that occurred in the solar photovoltaic system, mismatch loss is imperative, which causes the system to perform poorly. Solar photovoltaic systems have made topical advances in the use of highly effective solar cell materials to achieve high efficiency. In this analysis, performance parameters are influenced by the internal and external conditions of the solar photovoltaic systems and they lead to an increase in the loss of the system. The present review is focused to fetch fruitful information on the several studies that analyzed the effects on the solar photovoltaic systems of parasitic resistances, dust generated by tresses, clouds, solar radiation, temperature, relative humidity, different connection topologies, circuit implementation for partial shading, and remedies suggested by the potential authors.

1. Introduction

The conversion efficiency of the solar photovoltaic (SPV) devices can also be improved by minimizing mismatch, temperature, and ohmic losses. Based on the availability of incident solar radiation, the mismatch effect can be reduced by adding an appropriate connection configuration. The SPV cell equivalent circuits consisting of parasitic resistance (shunt and series resistance) should be taken into account to obtain the high performance of devices. To reduce the leakage current, the series resistance is as low as possible, and the shunt resistance should be optimal to ensure that the current passes through the external load. The SPV cell's temperature increases the current flow to the uniform solar radiation and decreases the current flow and produces a hot-spot when partial shading and different solar radiation features are associated with an SPV cell. Effects of mismatch and outdoor conditions should be held to a limited standard and correct chosen connection topologies. For high power output in an SPV cell, appropriate circuit equivalent values and appropriate SPV-cell materials are selected based on the use of solar radiation. In general, prominent SPV cell materials like monocrystalline and polycrystalline silicon (m-Si and p-Si), SPV-based materials have a high fill factor and conversion efficiency [1–3].

The increasing number of photovoltaic plants throughout the world in recent decades has exposed deviation in estimated and actual photovoltaic energy generation. This deviation is due to power losses, more often called mismatch losses, which can be defined as the difference between the maximum power of each array module and the power of the complete SPV plant. The module is mainly distorted by

two factors: the dispersion of electrical properties and the partial illumination of the SPV cell. The SPV panels transform directly solar energy into thermal and electricity. Solar energy is a crucial factor in constructing additional SPV systems (electric and thermal) to meet supply demands, dramatically reducing the energy crisis. SPV's performance is based on the power converter and the characteristic specification of an SPV cell by solar energy. For example, a device's conversion efficiency can be improved by reducing the amount of energy lost due to mismatch and temperature variations. Incompatible losses are caused by partial shading and variations in SPV cell parameters [4].

Solar radiation creates a hotspot, in the presence of partial shading, which raises device temperature. The SPV system involves dissymmetric gathering, the decaying module layer and the potential break-up of the cell, the accumulation of dust particles in the modules, and unequal exposure to the solar radiation in the modules [5]. Many researchers have made some new developments to enhance energy efficiency such that power losses and incongruity in SPV systems can be minimized at the same time. Increased losses are calculated using two methods: (1) the comparison between the ideal and maximum SPV value and (2) the application of calculating losses by Bucciarelli equations. Incompatible losses in fresh and old SPV cells are calculated using Bucciarelli equations. In general, low (<0.01%) losses were observed for fresh SPV cells and high (>10%) in aging SPV cells. The integrated bypass diode is added to minimize SPV module errors, parallel connections are selected, and shunt resistance is reduced [6].

An SPV system uses various methods to avoid mismatch losses. The passing clouds were blocking the incident of solar radiation on the surface of SPV, causing partial shading of the SPV module and the proxy maximum power point (MPP) monitoring rather than the actual MPP. The available solar radiation creates a hotspot in the SPV module. To overcome this issue, all the connecting modules, the Total Cross Tied (TCT) connection provided the maximum output and fill factor, with low power losses in the SPV module, as compared with the simple series (SS), series-parallel (SP), honeycomb (HC), and bridge link (BL). Incompatibility caused a 4.8% loss of electrical shading due to partial shading. By implementing correct connections and sorting various modules, this problem can be solved. With reconnection topology, insufficient losses in uniform solar radiation are reduced and the power efficiency of the 3 kW SPV system increases by 22.4% by an interval of 1 minute [7, 8].

Dynamic reconfiguration and Sudoku constructions can help to minimize losses in the SPV system without altering TCT connections. A Sudoku automatic method is also implemented to minimize wire losses in an SPV system that reduces partial shade losses significantly [9]. Mismatch losses are due to electrolightning, infrared imaging, current voltages (I-V), and a wide-range laser-beam scan. Based on these data, the effectiveness of SPV cells is easily assessed [10].

The power output of the SPV module is determined by selecting the correct crystalline material. Equivalent to a single diode circuit, the two- and three-diode SPV cells are also ideally suited to high solar radiation conditions. Likewise, crystalline Si materials are two types of monocrystalline silicon (m-Si) and polycrystalline (p-Si) materials producing a higher production potential than m-Si in the dry environment. A comparative analysis with m-Si and p-Si SPV with an equivalent power rating is performed in dry weather conditions, and the final average annual potential is achieved by 5.24 and 5.38 kWh per day [11].

The p-Si-based modules, with the thin film providing the best performance, and the cadmium telluride- (CdTe-) and copper indium gallium selenide- (CIGS-) based modules provide significant electrical energy generation. Similar SPV materials are suitable for different weather requirements [12]. In nonhomogenous conditions, it has special SPV array MPPs to set the device with a shadow factor. Various connection schemes (SS, SP, BL, HC, and TCT) were implemented, and one important part of the TCT relationship is the resolution of this problem [13]. By using the Lambert-W function in MATLAB and mathematical equations, the simple exponent and nonlinear SPV equations (Bucciarelli equations) were facilitated [14]. The optimum value of SPV is performed, and a voltage regulator is used to reduce SPV losses during sunny and nonsunny days [15].

Figure 1 shows the research studies starting the period from 2001, in which different mismatch loss values were used to explore the behavior and characterization aspects of photovoltaic systems. Over the past decade, the use of SPV systems has increased, but the issues and shortages related to these systems have become more important. Thus, the number of scientific studies utilizing the photovoltaic influence of internal and exterior factors has significantly expanded, particularly after 2013. Photovoltaic system analysis, taking into account mismatch loss parameters, is emphasized throughout the study. Accordingly, thorough reviews are needed to assess the current situation and give a roadmap for future scientific endeavors under these conditions.

Previous studies have shown improvements in the efficiency of the SPV network through enhanced network connections, the addition of bypass diodes, various internal parameters, selection of suitable places, and periodic system support. The Bucciarelli equations on analog SPV cell circuits and simulation methods support these findings in theory. By comparison, it reduces device efficiency by adding additional components to the SPV unit as it absorbs considerable power from various processes. In this review article, the insufficient loss caused by different factors is considered. The key criteria for an investigation into the mismatch loss of solar photovoltaic systems (SPVs), internal and external parameter impact, system losses, and causes of inconsistent losses in solar power systems are established. For the analysis of solar photovoltaic systems, students, researchers, members, and decision-making personnel, this paper is valuable. This will be useful in improving SPV systems, engineers, scientists, generators, and policymakers. The purpose of this review is to present a comprehensive description of the influence of internal and external parameters, mismatch losses, causes of mismatch losses (solar radiation, temperature, dust, and relative humidity), different topological

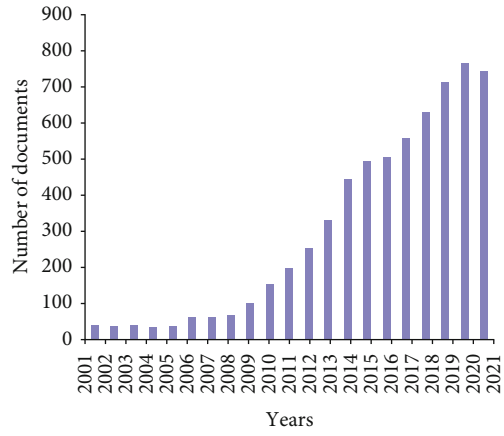

Figure 1: Studies on mismatch losses in the solar photovoltaic systems since 2001.

connections, and the merits and demerits of the solar photovoltaic system.

2. Review on Mismatch Losses

In recent years, the amount of electricity generated from renewable sources has outpaced that generated from conventional sources. In particular in remote areas, this will bridge the gap between energy demand and the end-user supply. Solar conversion is the most efficient way to produce electric and thermal energy. Electric energy is used for domestic and commercial purposes while thermal energy uses industrial applications such as chemical processing. As a result, most scientists have tried to establish effective electricity generation methods. Studies focused primarily on solar energy photovoltaics by either increasing the power generation or reducing photovoltaic energy losses. Highly effective SPV materials can be used for performance enhancement.

Further partial shading losses and changes to SPV cell parameters lead to degradation of the SPV system's performance. Several studies have been performed to increase the processing power, such as comparable circuit parameters, reliable topological relationship regimes, and temperature effects. The system efficiency can be enhanced by maximum parasitic resistance, and the effect of shadow and temperature is under control.

2.1. Classification of Solar Photovoltaic (SPV) Materials. Inorganic or organic materials transform the SPV cell into high-quality electricity incidents caused by solar radiation. Figure 2 outlines the different practical SPV materials [16]. The materials of c-Si are mainly divided into m-Si and p-Si materials by manufacturing technologies. In an arsenide matrix, the photovoltaic material Gallium Arsenide (GaAs) is formed. Depending on the environment, the output of p-Si is ideal for hot climatic conditions, and m-Si and GaAs can work in normal conditions. GaAs provide the best performance in photovoltaic cells among these crystalline materials.

Since material from Si was not available today, SPV thin-film cells were used in the manufacture of thin-film SPV cells, which reduced the cost of production of crystalline SPV cells by up to 50%. The difference between supply and demand has been reduced to the lowest possible level by the use of, for example, [Si-based] and chalcogenide-based SPV cells (cadmium sulfides and cadmium tellurides (CdTe) and copper-indium diselenides) of different SPV cells such as Si (solitary, amorphous Si, and glass) [17].

Thin-film material is having bandgap (1.52 eV) with high open-circuit voltage, and short-circuit current density was evaluated for the performance of bulk heterojoint solar cells based on polymer (naphthobisoxadiazole) [18]. Optical control and systems for high-performance hybrid solar thin-film cells, which use amorphous Si or organic solar cells, achieve 10.5% [19].

This hybrid SPV cell was cheaper and less weighty than other equipment. The basic conduct and values of SPV cell type, namely, color-sensitive SPV cells, are examined to convert solar radiation with photoelectrochemical processes into electric energy [20].

Implementations of SPV systems can be categorized as active and passive, as shown in Figure 3 [16]. In the active systems, electrical or mechanical equipment converts incident solar radiation in the SPV system into a DC source of power or thermal power. The high-quality electrical power is provided by an SPV module, which in comparison to other solar energy sources can be stored in large quantities. SPV panels of various materials, such as crystalline Si, thin film-based materials, and organic materials, can be used for high-performance processing materials. Solar radiation is transferred into heat energy directly in a passive unit, without the use of mechanical or electrical equipment (solar chimney and solar oven).

When solar radiation is lesser than the norms (1000 W/m^2) and the entire cell area is unable to take the same volume, a hot spot inside the system is created that contributes to the failure of the system. The SPV cell current is normally equal to the volume of solar radiation. However, this effect cannot be accomplished in an SPV cell, since only a proportion of the solar radiation incident is transferred into power and the remained heat dissipates; the actual output is measured using a temperature coefficient. Moreover, efficiency decreases as the cell's temperature increases.

The DC energy output causes ohmic loss because of the different resistors of cable and connector connections. To lower shadow loss and block the current flux of the system, the diode is connected to an SPV system. Climate conditions and material degradation have been reported as causing failure in the SPV module. Depending on the construction site, the climatic conditions on the surface of a module include solar radiation, ultraviolet rays, wind, snow, rain, frost, low and high temperatures, salt, sand, and dust [21]. Also essential in improving power loss and reducing the operation time of the SPV module is the material degradation mechanism.

2.2. Current-Voltage Characteristic Curve. Mismatch losses are induced in series and parallel configurations of the combined SPV modules by variations in the current-voltage (I-

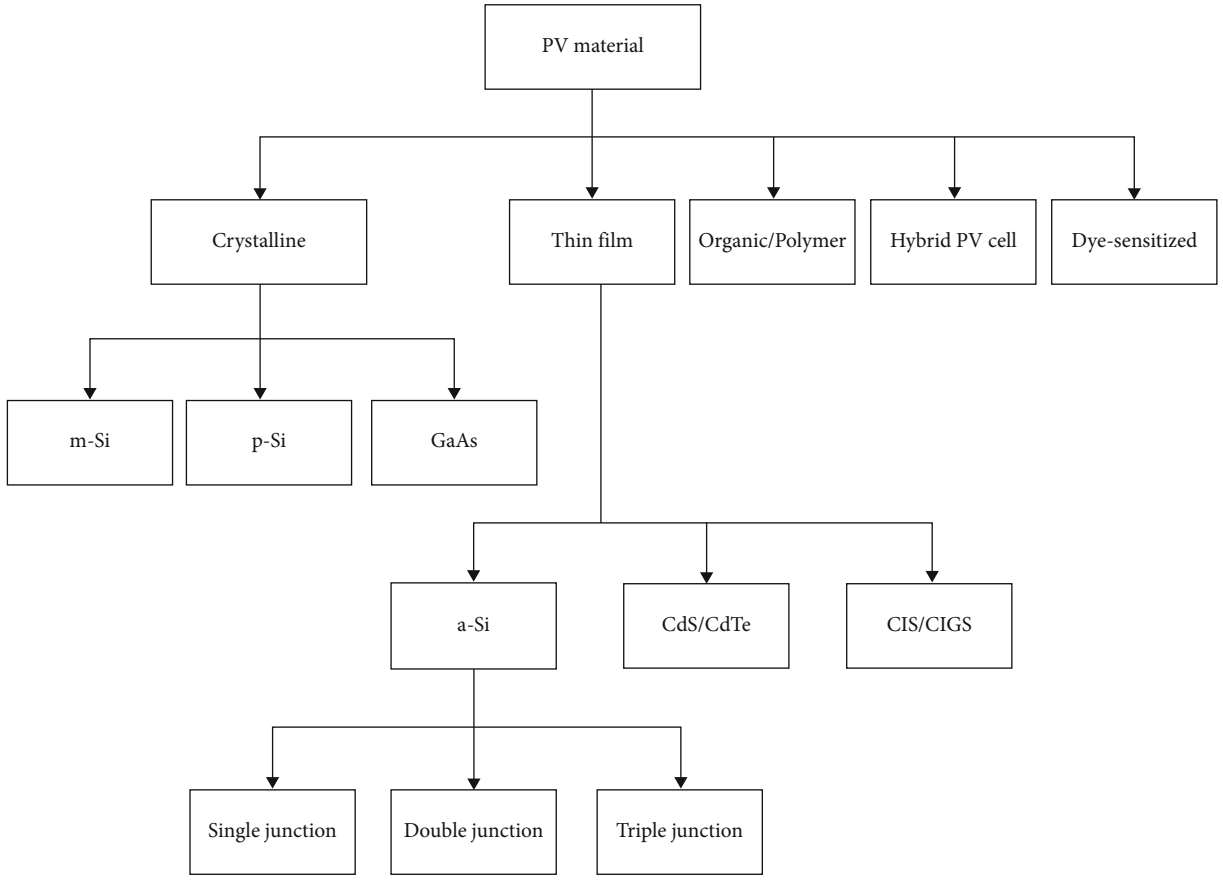

Figure 2: Classification of SPV materials [16].

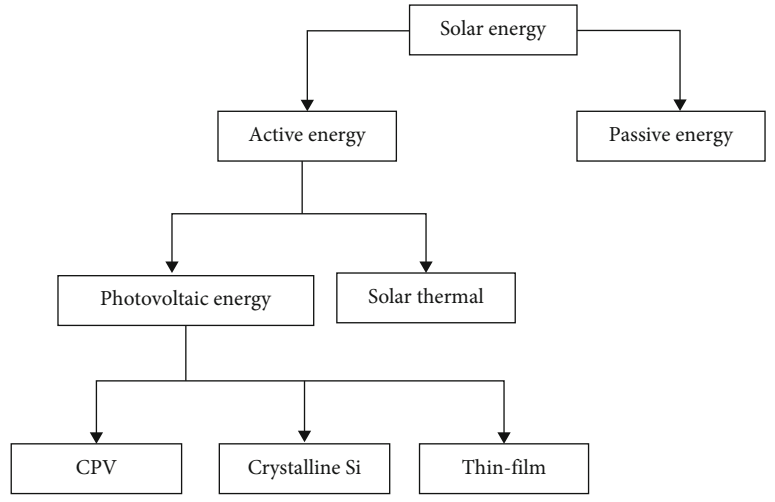

Figure 3: Classification of SPV materials based on SPV applications [16].

V) properties, voltage and current inconsistencies, and lower partial shading. The current output of SPV modules decreased 80% of the actual power output for two decades [22]. The presence of dust, moving nukes, and shadows in solar panels is an obstacle that minimizes incidents of solar radiation. The shadow area in the SPV module decreases current and functions as a terminal load, generating a hot spot on SPV as opposed to the rest of not affected area. Thus, the short-circuit current is adjusted and minor changes in fill factor and efficiency in the SPV module are prominent [23].

The average production decrease of 10.22%, 10.39%, 9.62%, and 8.70% for SPV modules, respectively, was induced when dust particles were deposited per month and per day [24]. The performance and efficiency of the SPV system are affected by overall parameters, such as shading effect, dust removal, operating temperature, and solar angle

tracking systems [25]. We investigate the role of solar radiance, thermal orientation, tilt angle, shadowing, and poisoning by reducing SPV module output parameters. Photovoltaic soiling modules have a degrading effect; cleaner, optimized technology is more energizing than clean technology [26]. In addition, in Kuwait, over 12 months, total land losses of 45% and 42% are reported in clean water technology, respectively, for Azda and Sawda [27]. Without SPV module cleaning, the SPV system production decreases by up to 1% daily. The implementation of a two-axis tracking device on the SPV module also provides solar radiation to boost its output parameters [28]. SPV performance and other factors including nominal plate details, losses in the diode and connection, loss of mismatch, the DC, the AC cable, sun-tracking losses, shading losses, and soil loss were adjusted due to solar radiation incidents and cell temperature [29].

For the precision and degradation factors of the SPV modules, a reliability model is used. The performance of the SPV module reduces the deterioration of packaging materials, cell/module relation, humidity intrusion, semiconductors, and lost encapsulation bonding [30]. The effect of dust is calculated on the surface of SPV monocrystalline and polycrystalline modules, and maximum power losses or losses of current were shown to be between 18% and 78% and between 23% and 80%. The deposition of dust does not affect open-circuit voltage or maximum voltages. The general characteristics of I-V and power-voltage (P-V) are also different from the current curve of the SPV modules [31].

A new theoretical model for the performance parameters of SPV modules/streams/arrays has been developed with MATLAB. This model data is used to check the model precision and viability of the effects of other software simulation models (INSEL and PVsyst) [32]. Measurements of the simulated model are compared to test measurements on a network of grid-connected SPVs. The results of the model matched experimental values because of the effect of the SPV soiling, aging, and deterioration system on the real weather conditions. A new model was developed to estimate the high accuracy and low approximation of SPV cell failure in one diode consisting of series and parallel bypass and blocking diodes [33].

A pattern search technique categorizes problems with SPV cell parameters. This method is used to evaluate a two-diode model's output which gives the actual measured data better results [34]. For a single circuit in a MATLAB Simulink, mathematical models are built that also analyze the effect on three points, namely, open-circuit voltage, high power, and short-circuit current of the external (solar and temperature) parameters and internal (shunt and series resistance) parameters [35].

In different solar radiation and temperature, the dynamical resistance and the MPP values of the SPV modules are measured with the aid of a direct measurement system. The findings of this study closely correlate with the experimental dynamic values of the SPV module [36]. The shunt resistors of each cell are determined without electrical connection estimation. In a-Si, the voltage, fill factor, and efficiency of the individual cell will steadily improve as the shunt resistance increases [37].

2.3. Effects of Internal Parameters. A new partial shade technology, with two different shade ratios consisting of a qualifying test, the accelerated lifetime test, and a long-term I-V characteristic test, enumerates the resistance of individual cells to the sequence. The results of the simulation are compared to the tests for improving controlled performance [38]. The effect of shunt resistance on an SPV crystalline panel on the solar radiation incident is analyzed. The reverse I-V curve determines the shunt resistance of dark light illuminations and shows the reverse dependency on the shunt resistance of incident solar radiation [39].

A single circuit equivalent to a single diode of the solar cell consists of five internal and external factors which influence the performance of a solar cell. Solar radiation variables and external conditions affect the photogenic rating current and the reverse saturation current in the diode ideality, sequence, and resistances. Moreover, the internal parameters necessary to achieve the highly accurate performance of the solar cell should be selected and properly managed [40].

The shunt and series resistance values of an explicit model are contrasted with the experimental values obtained from the SPV module [41]. The Newton–Raphson method measures the shunt parameters and series resistance values and simplifies the Lambert W function of the equations. The values are measured in 3 light conditions (800, 900, and 1000 W/m^2) and checked for the root mean square error analysis to be correctly accurate [42, 43]. These two analytical methods have been compared with experimental short-circuit current data, open-circuit voltage and maximum power point current, and maximum power point voltage [44].

For optimal performance, the resistance values in an SPV cell are calculated on the basis that SPV cell materials have size, shape, and properties [45]. A functional SPV circuit equivalent model takes into account the series resistance of a Si-based SPV cell on each connection area and electrode. In the case of leakage, the current flow through an SPV cell can be reduced due to a defect in the SPV cell structure by introducing a parallel shunt resistance across the P-N junction diode. Microstructure analysis of the polycrystalline photovoltaic lead SnAgPb is performed [46].

A photovoltaic system algorithm is used to estimate current and power in appalling conditions. The proposed algorithm discusses the SPV field, diode blocking, and the bypass diode in sequence and parallel resistance. The Lambert W feature simplifies the explicit I-V characteristic equation. The results show that the relative average SPV power mistake has dropped by 50%. It can be used for other SPV cells such as polycrystalline, thin films, and organically dependent cells [47].

The solar cell temperature, the backside temperature, the atmospheric temperature, the open-circuit voltage, the short-circuit current, the maximum point voltage, and the maximum point current are used to evaluate the thermal and electrical outputs of a photovoltaic device [48]. The Lambert W function for the investigation of capability I-V

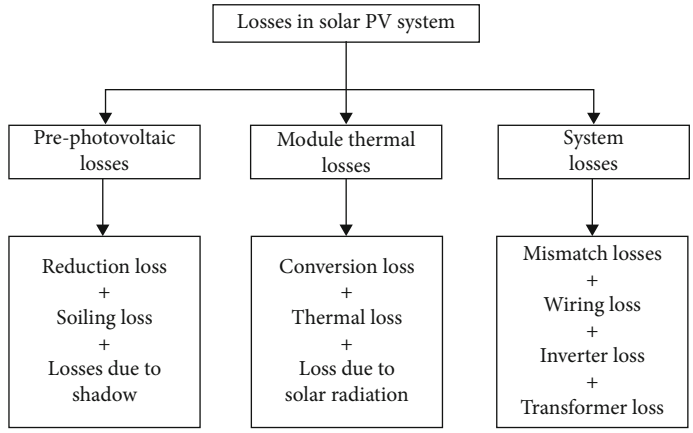

Figure 4: Losses associated in solar photovoltaic system [170].

and P-V effects is applied to compare these results with those of the MATLAB simulation with the simulation outcome both curves become stronger [49].

New technology has been developed for nonlinear output parameters of a single SPV diode cell. The results are calculated using a simulation system with 2 diode model parameters [50]. A single solar cell diode is used to analyze a technology to determine the IV output parameters via the polynomial curvature fitting method and Lambert W function. This method provides good precision and fewer errors, and the typical method of adaptability is an SPV cell product [51]. The thermal activity of SPV cells based on Si and GaAs is investigated. The SPV cell is connected to high and low loads, and the system acts as a source of power and voltage. Effective methods of removal of heat, such as natural or forced flow, reduce the SPV cell temperature [52].

A thin-film cell (amorphous cell) operating in low solar radiation level is efficient material, compared with m-Si and p-Si SPV cells. The solar cell a-Si can only be based at squat lighting rates up to 500 W/m^2 with m-Si and p-Si cells that display better efficiency at a median solar radiation rate up to 900 W/m^2. The conversion efficiency of low bandgap materials was reduced by more than 900 W/m^2 [53]. The parameters for the development of m-Si and p-Si panels are measured in semiarid climatic conditions on selected days and months. The open-circuit voltage, the short-circuit current, and the conversions are related to SPV modules; the m-Si SPV module is higher and slightly lower than the p-Si SPV module [54].

The transparent and infrared areas are amorphous, polycrystalline, and monocrystalline materials, with a maximum exposure of 0.522, 0.922, and 0.704 μm, respectively [55]. In various research laboratories, three SPV module outputs are compared, between Sandia National and the National Norms Institute; the coefficients of temperature were up to 17%, resulting in a decrease in SPV module output of less than 2%. In each three-form SPV module, the relatively short-circuit current differs to 4% [56].

2.4. Effects on Output Parameters. The m-Si p-Si and a-Si solar modules are tested with a single-axis tracking device in Malaysia's hot and moist environments. The higher energy efficiency of the p-Si module was based on the degree of solar incidents. The module with the m-Si solar module has a lower and maximum solar module template [57]. In the same climate with efficiency and energy efficiency, the three SPV modules are compared. The SPV modules are m-Si and amorphous for optimum and lowest efficiency [58].

In total, there will be 5 modules for the tracing and analysis of SPV outputs and efficiency, as well as relative quality losses (m-Si, p-Si, CIGS (copper indium gallium selenide), CIS (Copper Indium Selenide), and CdTe (Copper Telluride), the SPV modules m-Si and CdTe (Copper Indium Telluride)). CIGS showed the complete power output of thin-film SPV modules [12]. In degradation, temperature coefficients, and performance parameters, five SPV modules (Si-1, multicrystallized Si, Si-2, CIGS, and hetero-Si film) are considered to be analyzed. The annual rates for degradation of SPV modules are approximately 0.50-4.95%. The frequency of deterioration in 25 years is around 10-50%. When the photovoltaic modules had an increased annual degradation rate of 5%, the Levelized Cost of Electricity (LCOE) cost doubled [59].

With an SPV device connected to an energy-efficient charge, the full power efficiency of the SPV cannot be achieved. The battery power of the SPV network as well as weather and operating conditions is therefore critically essential for the cable thickness and the temperature and the shading mechanism, the characteristics of I–V, and inverter capacity. The input parameter (solar radiation) of the SPV system depends only on all these variables. The operational efficiency can also easily be modified for the other variables. Therefore, this analysis focuses on the elucidating temperature effect on various SPV parameters.

The effect on the overall performance of a photovoltaic system is examined by solar radiation, temperature, shadow, earth, and snow [60]. SPV cell output decreased gradually as the air temperature increased. However, changes in wind speed led to mixed reactions of the efficiency of the PV system [61].

The generation of electric and thermal energy is favored for green and sustainable methods, such as solar energy systems. These solar energy systems are an appealing choice for

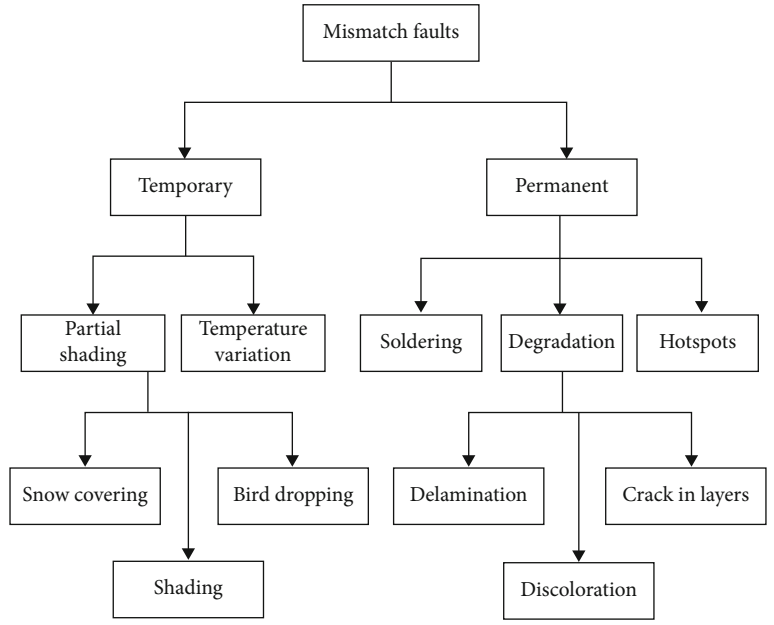

Figure 5: Classification of mismatch losses in solar photovoltaic module [171].

the electricity supply in remote areas and community use in particular. Other types of renewable energy sources (wind and biomass) are unsatisfactory for smaller development due to the high cost of supply and sustaining and operating life and by implementing solar-energy systems; these problems are overcome. However, the SPV systems have an extremely low power conversion performance due to the different types of losses during energy storage and transfer. Mismatch losses are a significant downside of such defeats. Mismatch losses affect the performance of SPV, which results in a hotspot event that decreases the working life of the SPV device and increases the cost of producing electricity.

The SPV method is the most common in space reduction; occurrences of solar radiation at a specific location are less common. Therefore, high energy conversion rates need efficient solar energy use and a suitable transformation process. Furthermore, the optimum power output can be achieved by minimizing power losses and reducing energy costs. Current research focuses on elucidating the inefficiency effect, enhancing performance, and developing SPV systems with optimized technologies.

Each solar power plant string consists of several photovoltaic modules. Each module's I-V characteristics vary because of the difference in internal resistance, short-circuit current, and power modular loss. Strings of SPV power plants are located in parallel. The I-V features of the combined string and length of the outside cable are different [62].

2.5. Impact of Dust on SPV Modules. As the world's energy consumption increases and environmental concerns create, there has been an upsurge in interest in improving renewable power sources, particularly solar energy. Further electrical modeling research will focus on diode-based equivalent circuit models. It was discovered that dereliction of environ-

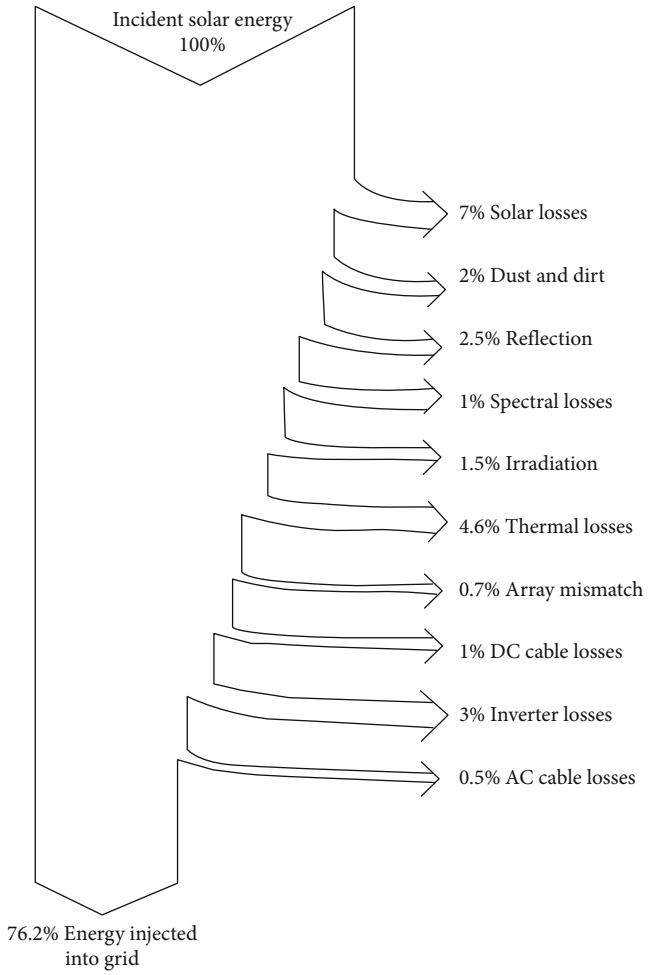

Figure 6: Sankey diagram for photovoltaic system losses [79].

Table 1: Mismatch losses in a solar photovoltaic cell/system.

Connection scheme	Mismatch power loss	Authors
5 × 5 SPV array	Maximum loss at total cross-tied of 1214.93 W and minimum loss at the dominant square of 606.75 W	Dhanalakshmi and Rajasekhar[114]
40 modules	Mismatch loss is about 0.23% of the nominal power	Lorente et al. [115]
2.85 kW power plant	Annual electrical mismatch loss factor from 3.8% to 13.2%	Rodrigo et al. [116]
190 kW power plant	Total loss including solar radiation, temperature, module quality, array mismatch, ohmic wiring, and inverter is found to be 31.7%	Sharma and Chandel [117]
SPV cells connected in a string	Fractional power loss due to mismatch is 2.35%	Bucciarelli Jr. [70]
Series string	15-20%	Wang and Xuan [118]

mental conditions could result in significant errors of up to 17%. The accuracy of the predictions can be improved by up to 35% with simple model modifications like taking dust into account [63].

Red soil, ash, sand, calcium carbonate, and silica are examples of several types of pollution deposits. When SPV panels are exposed to the dust elements for short period (two months) without being cleaned of pollutants in the air, their energy yield can be reduced by as much as 6.5% [64, 65]. Multicrystalline PV modules were tested in both indoor and outdoor environments for the influence of dust on their performance. Under varied contaminants, the PV module's performance has been evaluated. Due to the mass and kind of pollution, dust particles depositing on the PV module cause voltage and output power to decline [66].

There were detrimental effects on output power and short-circuit current when dust was collected on the polycrystalline silicon photovoltaic module. However, the open-circuit voltage was not significantly influenced by this phenomenon. Coal dust was shown to have the greatest impact on module efficiency, with a 64% reduction, followed by 42%, 30%, and 29% for aggregate, gypsum, and organic fertilizer dust, respectively [67]. PV modules can be partially or completely shaded by dust accumulation on them. As a result, shading effects are not the same as those caused by dust or dust soiling. In PV modules with dust-soiled solar cells, the power output of the cells is lowered because less or no current is created [68].

2.6. Mismatch Effects. Depending on the system configuration and string length, the manufacturing assessment found changes between 0.01% and 3%. Besides the module's electrical characteristics, a loss difference includes string length and edge effects [69]. When modules are connected to serial and parallel combination networks known as arrays, varying current-voltage characteristics of the photovoltaic modules result in a form of power loss called an electric mismatch. The "mismatch loss" (MML) effect is that the SPV-array total power output is less than the total module power output as if it was operating independently [3, 70].

A comprehensive performance model at the cell level is used to classify the actual array and P_{Array} efficiency, which includes losses in discrepancy, as shown in Figure 4. This is compared to the ideal performance of ubiquitous $\sum P_{\text{Cells}}$, the amount of individual cell-level power minus losses of

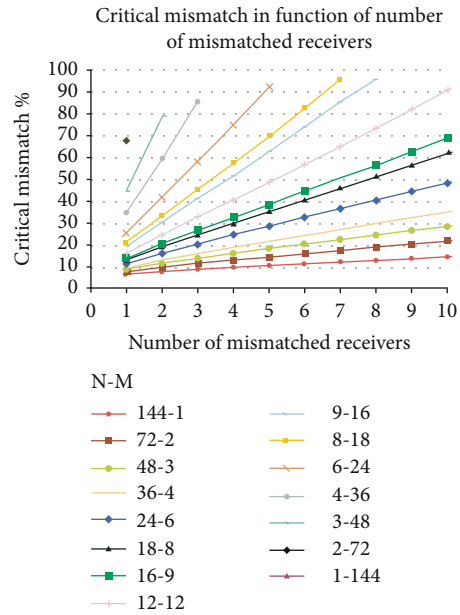

Figure 7: Critical mismatch values in function to the number of mismatched receivers for different electrical module layout configurations [172].

mismatch. Mismatch loss is therefore calculated by [71]

$$\text{Mismatch loss\%} = \text{MML}[\%] = 1 - \frac{P_{\text{Array}}}{\sum P_{\text{Cells}}}. \quad (1)$$

The actual flow through each module must be the same as that when the modules are connected to a string serial and connected to an inverter with a maximum power point for the tracker. The current passing through any module should be the same when the modules are connected to a series string and connected to an inverter with full shadow capacity [72].

The losses in SPV system loss due to the temperature are as follows:

(1) Loss due to the incident solar radiation level

(2) Loss due to the temperature

(3) Loss due to the SPV module quality

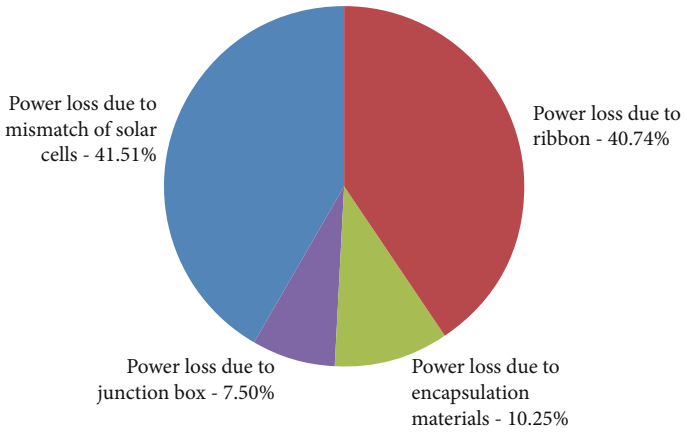

Figure 8: Distribution of power loss in a solar module [173].

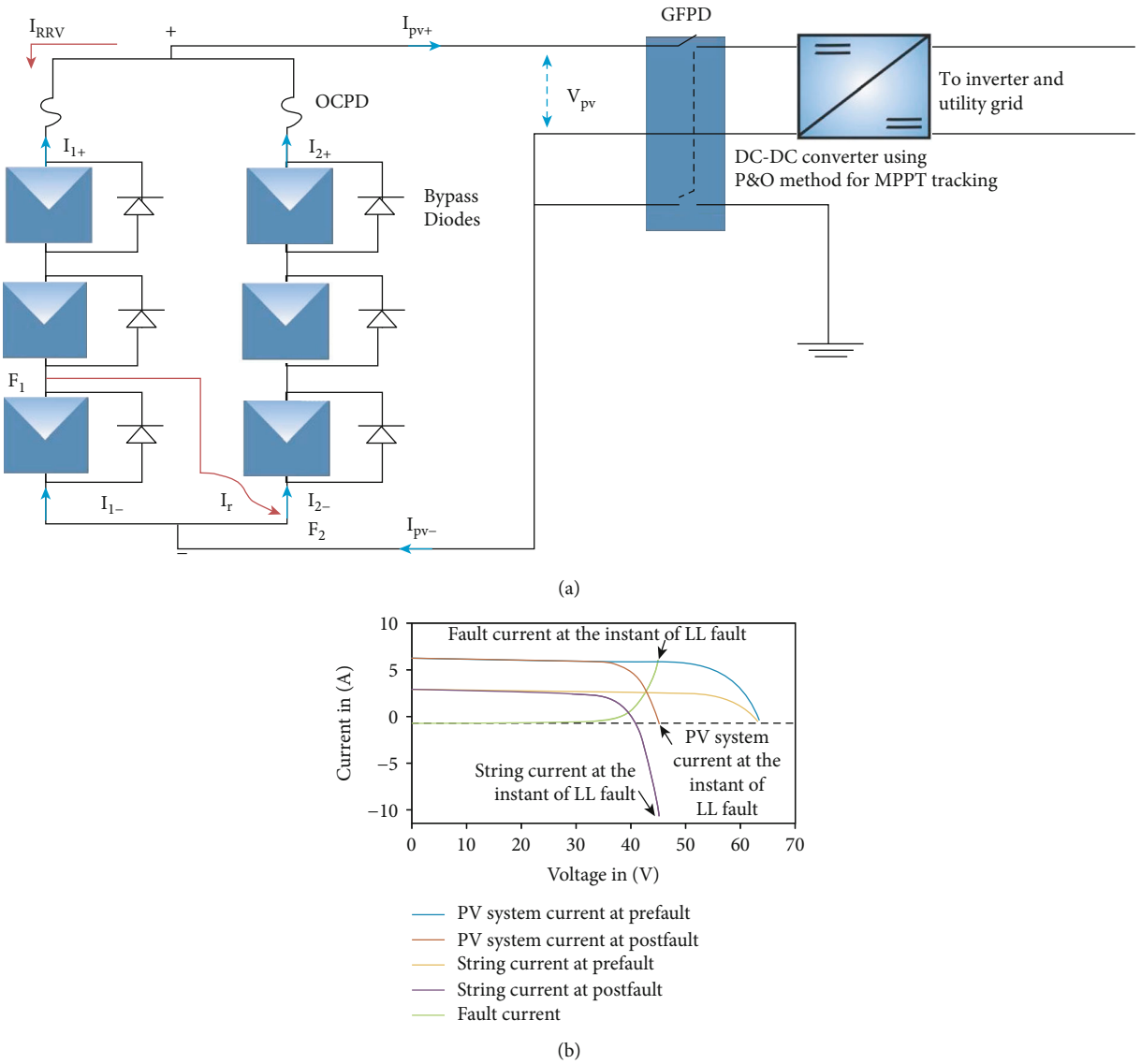

Figure 9: (a) SPV system without blocking diodes in the event of a fault. (b) I-V without blocking diodes [82].

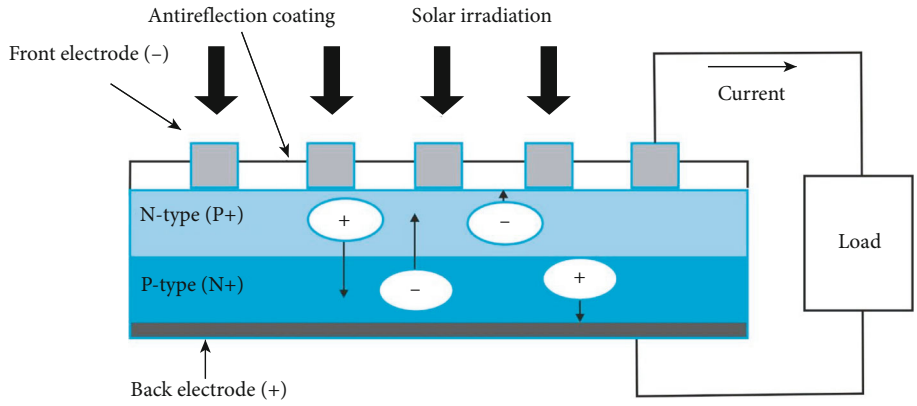

Figure 10: A p-n junction SPV cell structure [83].

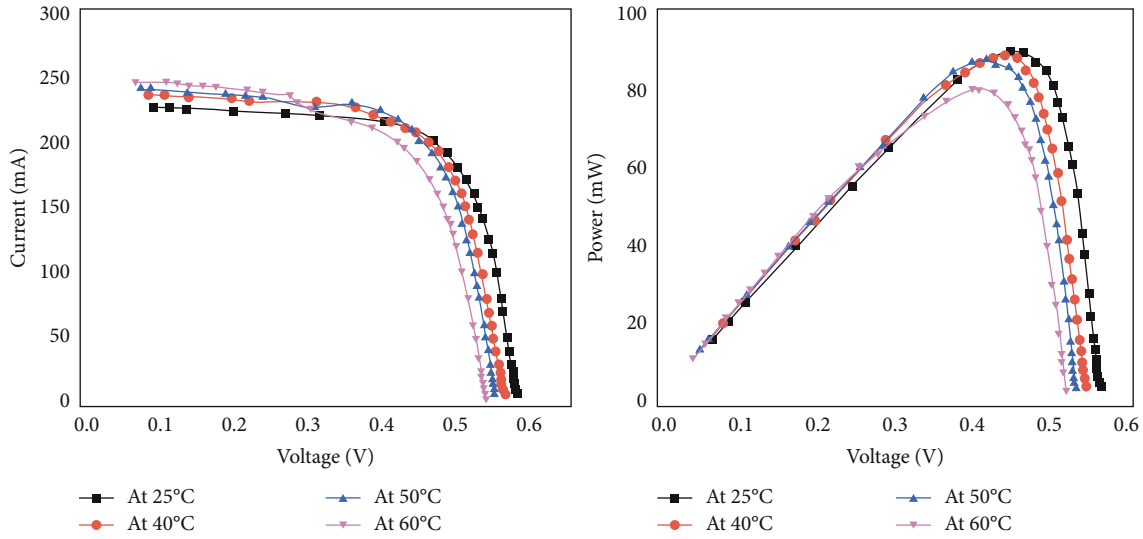

Figure 11: An m-Si SPV cell's current-voltage and power-voltage characteristics are displayed at solar radiation of 515 W/m^2 [84].

(4) Loss due to mismatch phenomenon between strings

(5) Ohmic loss due to wiring

(6) Loss at the inverter level due to its efficiency and its operation

In addition, it is crucial to match the maximum power output of the SPV modules to the accurate DC-AC inverter size to avoid unaccounted losses [73].

2.7. Mismatch Loss in Solar Photovoltaic Modules. Figure 5 demonstrates the description of the SPV module defects. It has briefly and permanently broken up into incompatibility losses. Temporary partial shade loss, temperature variations, covering snow, and falling birds are barriers to maximum solar light absorption by prominent photovoltaic components. The effect of defects in the photovoltaic module is equally soiling defects, corrosion, lightning, delaminating, cracking of the coating, and coloration.

The Sankey diagram indicates some losses in photovoltaic systems shown in Figure 6. Due to the low energy efficiency of SPV systems, the energy produced should be with minimum losses, be moved to consumers as much as possible. Through the elimination of loss factors in the photovoltaic systems, these losses must be minimized.

Factors that may cause SPV system losses include environmental factors such as wind, dust, snow, heat, temperature, and other losses caused by device components such as cables, inverters, and batteries. Given the losses, the SPV system should be installed and used to the greatest extent possible for the energy generated in local regions.

Photovoltaic plates are caused by the deposition of soil and dust. The powder is used in any event to wash rainfall off the module's surface, and even bird waste remains on the panel's surface after heavy precipitation. One of the main parts of the SPV unit is the lower edge of the module. The module is usually mounted on the ground with slight inclines such that the water between the container edges is

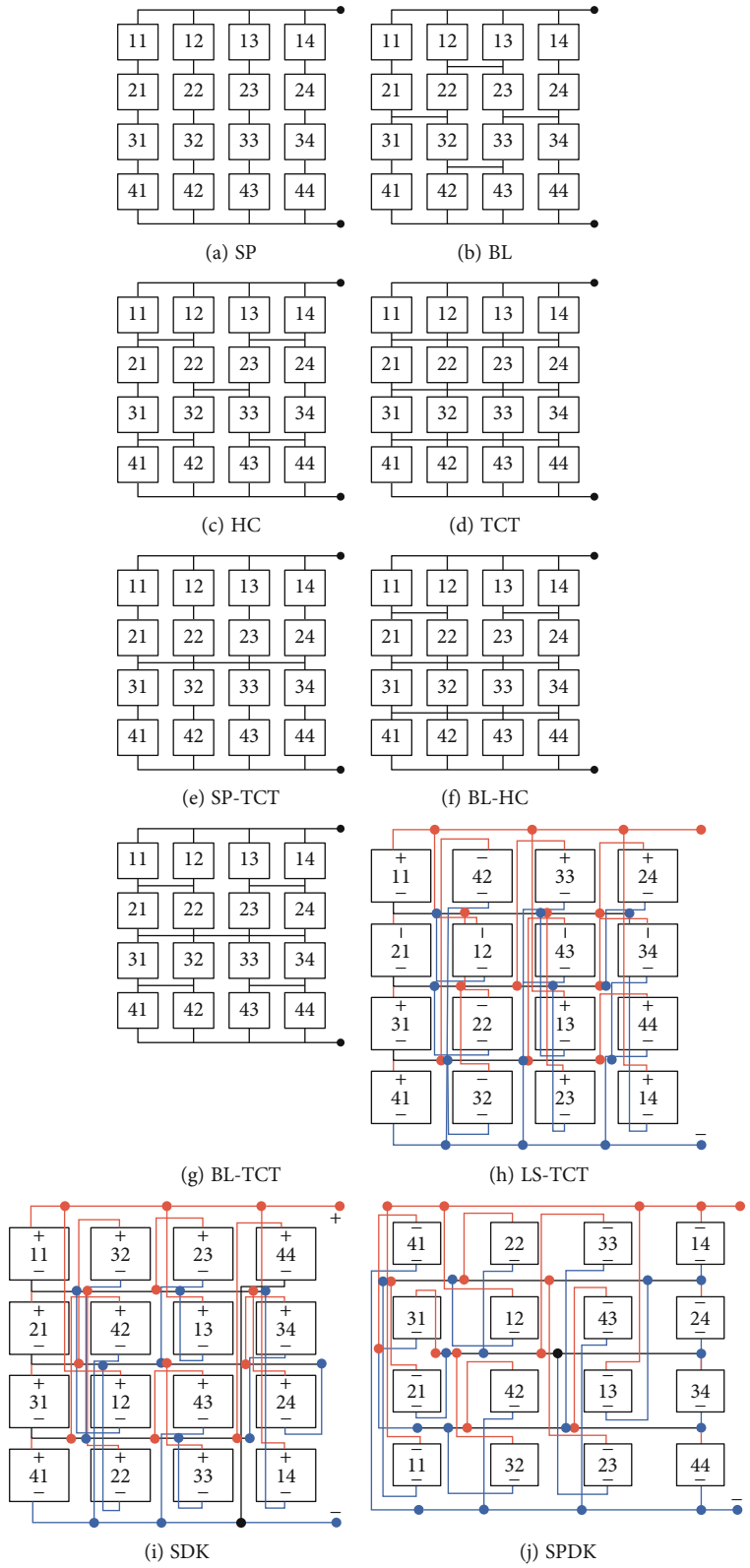

Figure 12: Continued.

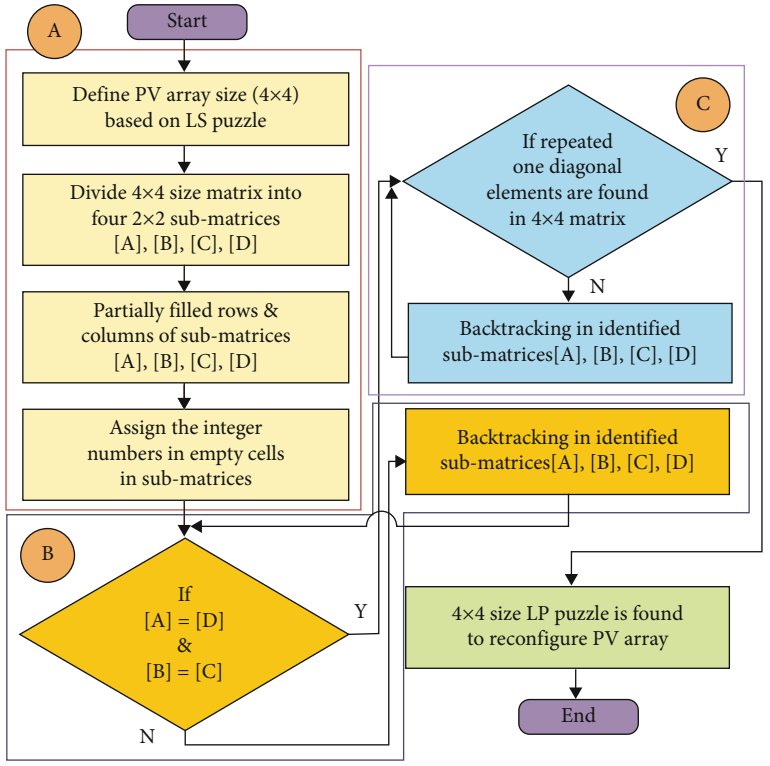

(k) Flow chart for LS methodology to design 4 × 4 size of PV array

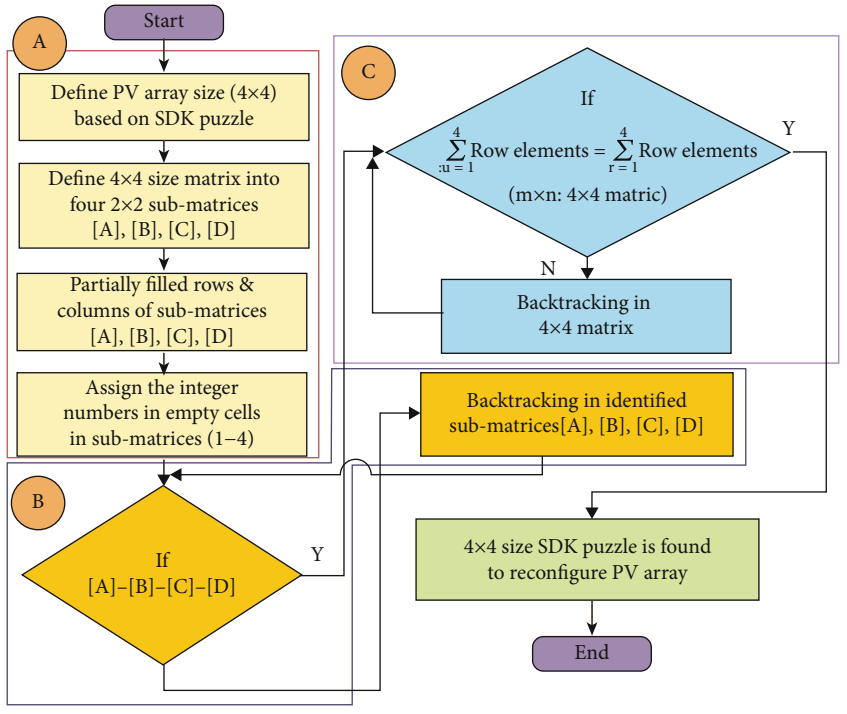

(l) Flow chart for SDK methodology to design 4 × 4 size of PV array

Figure 12: Continued.

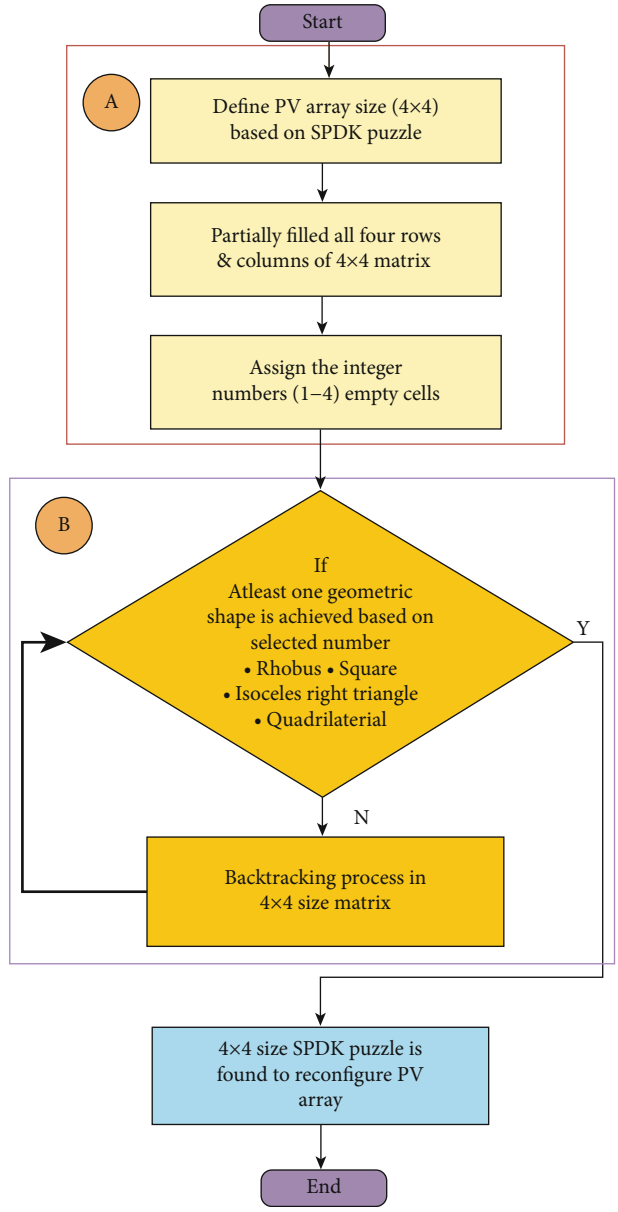

(m) Flow chart for SPDK methodology to design 4 × 4 size of PV array

Figure 12: (a–m) Configurations and flow charts for conventional, hybrid, game puzzle-based SPV arrays [85–89].

constantly not collected at the ends of the kit. The dust reduces a module's maximum power by shielding the cells from the soil. Loss should be less than 1 to 2% to return to power when the modules are periodically cleaned and to eliminate soil losses from the modules only through frequent cleaning cycles [74, 75].

Photovoltaic panel surfaces should be kept clean at ground level for good system performance during service so that solar radiation can be absorbed more effectively. A smart machine can be used in some studies to clean the floor, whether manually or automatically. The design is aimed at reducing productivity losses by dust and dirt on the surface of the panel and at maximizing power production. The energy loss without the purification cycle has been reduced and efficiency increased by 15-20% [76]. Mismatch loss occurs in various capacity ranges of power plants given in Table 1.

A case study with 180 solar panels from Panasonic N285 and multiple SMA inverter topologies has been presented in a 51 kW SPV array on the roof. Listing has been measured for low, medium, and shaded scenarios. Six configurations of SPV strings have been analyzed ((1) system with 10×5 kW, (2) 5×10 kW, (3) 5×10 kW, (4) 3×15 kW, (5) 2×25 kW, and (6) 1×51 kW). The control demonstrated the varying output in all configurations when shading scenarios were considered, resulting in maximum power available in shadow conditions. Shade losses of 21.4%, 22.9%, 26%, 24.2%, and 23% have been observed during testing with the free online simulation PV∗SOL software for all six configurations [77].

Table 2: Studies on the effect of solar radiation.

Objectives	Result	References
Examine the solar photovoltaic panel's surface temperature about solar radiation and ambient temperature.	At an ambient temperature of 36°C, the solar panel reached a temperature of 78.50°C when exposed to 1140 W/m^2 of solar radiation. The performance of SPV panels can be harmed by extended exposure to high panel temperatures, even at typical levels of solar radiation and ambient temperature.	Tripathi et al. [119]
The SPV performance characteristics were calculated using measurements of the panel's output voltage and current, as well as the amount of solar radiation incident on its surface and the panel's surface temperature.	Humidity causes a decrease in solar radiation and panel output, according to the studies. The SPV panel's power output drops by 34.22% when humidity rises by 50.15%. It was also discovered that an 11.40% drop in panel temperature was caused by a rise in humidity from 65.40% to 98.20%.	Tripathi et al. [120]
According to the location and time of day, the amount of solar radiation that falls on SPV panels might vary significantly.	A small increase in SPV panel voltage is observed when panel current rises in direct proportion to solar radiation. Similarly, the power of a solar panel increases as a function of the amount of solar radiation it receives.	Karafil et al. [121]
When the atmosphere is partly cloudy, the differences in solar radiation can produce considerable oscillations in system currents, notably in battery currents.	Cycled battery charge/discharge currents are directly affected by changes in solar radiation. Battery current changes caused by solar radiation cannot be modeled using hourly radiation data.	McCormick and Suehrcke [122]
An investigation into the relationship between solar radiation, current, voltage, and solar panel efficiency is the fundamental objective of this research effort.	The temperature rises as a direct result of increased solar radiation, according to the results obtained from the experiment. The output current rises as a result of the increase in solar radiation until the cell's temperature interferes and causes it to fall.	Buni et al. [123]
Solar radiation transfer may be predicted using a new, more comprehensive physical model that incorporates deposition and particle characteristics.	There must be a consideration for all of these factors when forecasting the transmittance of a solar panel covered with dust, according to their studies.	Xingcai and Kun [124]
The solar photovoltaic panels are most efficient when the solar radiation hits them head-on in a direct line. An SPV panel that is stationary can only face the sun for a limited amount of time.	The efficiency of the SPV system was shown to increase significantly when the SPV system was used with a sun tracking system. Depending on the panel's location, it can gain anywhere from 15% to 45% of its original energy throughout the year.	Thorat et al. [125]
Different solar radiation intensities ranging in the range of 1000-3000 W/m^2 have been examined to determine the power and energy of SPV cells.	Increasing solar radiation from 1000 to 3000 W/m^2 increases total energy by approximately 1797.56%.	Nasrin et al. [126]
Aspects such as the amount of solar radiation reaching the panels, the surrounding temperature and humidity, and the wind speed are all readily apparent. The amount of dust or pollution that accumulates on solar panels depends on the local climate and precipitation, which affects the amount of electricity generated.	The wind helps to keep the SPV panel cool by reducing the amount of electricity lost as a result of increased solar radiation or elevated panel back temperature.	Kazem and Chaichan [127]

The contrast was made with the genetic algorithm performance and other conventional techniques using 400 W, 3400 W, and 9880 W arrays, each consisting of 40 W, 10 W, 85 W, and 247 W SPV modules. The respective array output power and MML are calculated for both the long series string- (LSS-) SP and long parallel branch- (LPB-) SP arrays. For this function, array arrangements 1×40, 2×20, 4×10, and 5×8 (parallel × series) are used as LSS-SP array while array arrangements 40×1, 20×2, 10×4, and 8×5 are known as LPB-SP array configuration [78].

The basic inconsistency of the number of inconsistent recipients is shown in Figure 7, for different configurations. The SPV module design with a greater number of interconnected cell series has a lower critical differential value that allows the system to recover better. The nonuniform malfunction distribution has been checked for an erroneous modulus structure analysis (16×9). This means that each receptor gets the inconsistency value by increasing the number of inconsistent cells until the inconsistency of all receptor cells is reached [79]. The relative malfunctions were between 1.4 and 4.0% during the stated solar radiation transfers according to the electric configuration and layout of the SPV array [80].

Figure 8 demonstrates the energy loss distribution of the crystalline silicon solar cell. The electricity loss caused by discord between solar cells and ribbons is 41.51% and 40.74%. The losses in the power of container materials and the link box are 7.5% and 10.25%. The gross Cells to Module

(CTM) of the solar panel of 72 (25 mm/125 mm) is 3.93% [75]. The effect of the shunt on the power output of the module was tested in terms of relative power and relative open-circuit voltage. The important finding is that in so much as 90% variation between shunt positions in relative energy losses and the difference in relatively open circuit voltage losses can also be achieved, which is crucial that the electrical output of the SPV module shunted into the module depends on the mutual location and proximity of metallization. In comparison with metallization shunts, the relative strength of most shunts not for the lowest shunt resistance values has increased by 80% to 90% [81].

2.8. Circuit Implementation. It is common for SPV systems to have problems at various points, including the SPV arrays and power converters. As shown in Figure 9(a), the SPV array errors, such as line to line (L-L) faults, occur between the system's first and second strings. For the SPV system without blocking diodes, the string current at prefault and postfault conditions as well as the fault current (I_F) is shown in Figure 9(b). The L-L faults reverse the flow of current through faulty strings, as shown in Figures 9(a) and 9(b). F_1 and F_2 are separated by one healthy string, which generates an inward or reverse current (I_{REV}) into the faulty string. For SPV systems, the Overcurrent Protection Devices (OCPDs) used in SPV systems can easily detect a short-circuit current that is almost twice as high as that of the string before the fault, as shown by Figure 9(b) [82].

Different semiconductor materials are used to build the solar cell's two layers, each of which is doped differently. Figure 10 illustrates the basic structure of a silicon solar cell. A p-n junction diode is a better analogy for the solar cell. A layer of silicon with integrated metal components is utilized on the upper side of the electrode to prevent direct solar radiation penetration. As a result of connection resistance, SPV cells can be built in a variety of forms to maximize their effective surface area and minimize their losses due to this resistance [83].

Figure 11 depicts the m-Si SPV cell's current-voltage and power-voltage curves at constant solar radiation. Photovoltaic cell temperatures of 25°C, 40°C, 50°C, and 60°C were observed at solar radiation of 515 W/m^2. A direct correlation between cell temperature and current-voltage characteristics can be shown in Figure 11. It has been found that at lower voltages, the current is the largest and most nearly constant, with constant solar radiation of 515 W/m^2 and 220–240 mA [84].

2.9. Configurations for SPV Arrays

(1) Customized SPV array constructions

There are numerous SPV array configurations depicted in Figures 12(a)–12(h). In addition to the SP and BL-based combinations, there are SP-TCT and BL-HC hybrids, as well as the projected LS-TCT variants. Figures 12(a)–12(c) depict the standard SP, BL, and HC configurations for a 44-panel SPV array. It is shown in Figure 12(d) that an SPV panel array of 44 panels can be generated with high power by employing tied across individual rows of interconnections.

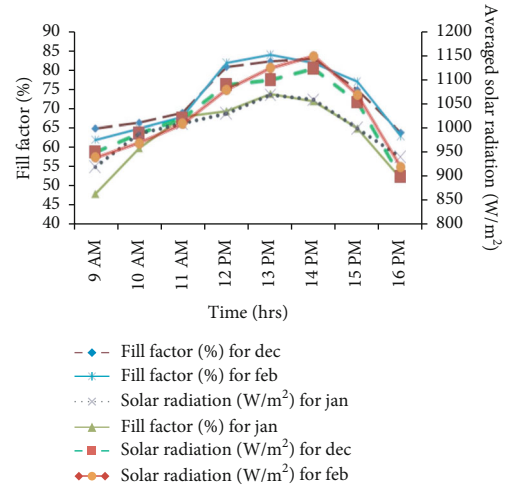

Figure 13: Performance characteristics curve for SPV system with the effect of solar radiation [174].

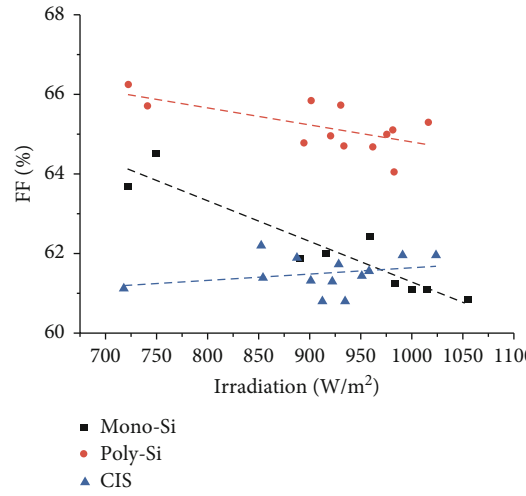

Figure 14: Effect of solar radiation on mono-Si, poly-Si, and CIS materials [132].

Combining the traditional SP, BL, and HC topologies with the TCT topology of an SPV array is shown in Figures 12(e)–12(g) [85].

(2) ls puzzle-based SPV array configuration

Figure 12(h) shows a puzzle pattern-based SPV array topology in which the positions of SPV modules are reallocated according to a modified TCT, but electrical interconnections remain the same. The SPV modules in this array are identified by the first and second numbers of their row and column names, respectively. The purpose of LS is to identify the maximum number of rows and columns that can be employed for an integer. Leonard Euler devised a matrix in which each symbol appears exactly once in every row and column. Perceptible shading dispersion during SPV array reconfiguration is available in the presence of partial shading conditions (PSCs). The shade dispersion property will always change based on the number of integers

Table 3: Studies on the effect of temperature.

Objectives	Result	References
The temperature of SPV panels under realistic settings is being modeled theoretically.	To accurately measure the heating effect, the temperature coefficient of the solar cells is utilized. A decrease in photoelectric efficiency of 2.9–9.0% occurs in solar cells having a temperature coefficient of 2.1–5.0%.	Du et al. [128]
Photovoltaic conversion is mainly influenced by the operating temperature. Temperature affects both the module's electrical efficiency and its output power linearly.	The photovoltaic conversion process is heavily reliant on controlling the operating temperature. An SPV module's electrical efficiency and, by extension, its output power are directly proportional to its operating temperature, which decreases linearly with module temperature.	Dubey et al. [129]
Analyzing the behavior of a monocrystalline SPV panel under various temperatures is done using MATLAB/Simulink software.	Photovoltaic system efficiency is greatly affected by the temperature of the solar cells.	Zaini et al. [130]
Real-time solar radiation and ambient temperature will be used to evaluate the influence of heating on SPV cells' efficiency.	Achieving maximal performance and maximum output from a solar energy harvesting module requires that its temperature be kept within an acceptable range for the SPV module.	Thong et al. [131]
Temperature and solar radiation affect the performance of m-Si silicon, p-Si, and Copper Indium Diselenide (CIS) modules under real-environmental conditions.	Temperature affects the efficiency and fill factor of m-Si and p-Si modules; this is not the case with CIS modules.	Perraki and Kounavis [132]
The temperature coefficients of commercially available solar modules are examined.	CdTe-based modules have an average temperature coefficient of power of -0.446%/°C for m-Si, 0.387%/°C for p-Si, and 0.172%/°C for CdTe-based modules correspondingly.	Dash and Gupta [133]
Filtering certain spectrum solar radiation before entering an SPV panel might result in various temperature profiles and varying output powers.	The temperature profile of an SPV panel is altered when solar energy is filtered before it enters the panel, resulting in lower panel temperatures in all cases (on average 18% reduction).	Schoeman et al. [134]
A p-Si photovoltaic panel is tested for its electrical performance under various temperature conditions.	An increase in temperature reduces panel efficiency by 0.5%/K, in total. In addition, a drop in SPV module efficiency of 1.23% was caused by a rise in temperature of 30°C.	Idzkowski et al. [135]
An investigation into the performance of a specific type of solar panel. Since it has an open design and can therefore benefit from natural ventilation, it is self-cooling and keeps dust from collecting on its surface even during the hottest parts of the day.	With the help of this Computational Fluid Dynamics (CFD) model, it was demonstrated that a lower temperature in this solar system allows for maximum electrical production than a flat SPV system.	Charfi et al. [136]

utilized in the puzzle design. Because of this, it is feasible to place LS puzzles with distinct attributes and multiple placement choices for integer numbers. An SPV array has been reconfigured with the help of the LS puzzle, as shown in Figure 12(k) [86].

(1) Su-do-Ku puzzle-based SPV array configurations

The four-by-four SPV array is rearranged by a series of rules based on integer numbers. Electrical connections and design methods are illustrated in Figure 12(i).

(2) Shape-do-Ku puzzle-based SPV array configuration

It is possible to find the Shape-do-Ku (SPDK) puzzle in a variety of sizes, although it has no technological connection to the Su-do-Ku (SDK) puzzle. This puzzle has only one possible answer, and each number must occur at least once in every row and column. Rearranging the SPV array with a 4

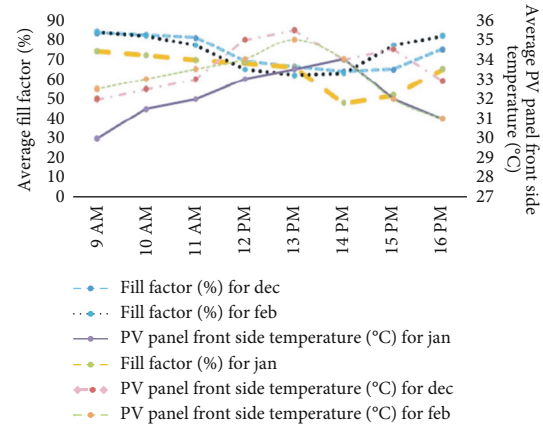

Figure 15: Performance characteristics curve for SPV system with the effect of SPV panel front side temperature [174].

Table 4: Studies on the effect of relative humidity.

Objectives	Result	References
Relative humidity affects the effectiveness of solar panels in Calabar, Nigeria, while converting solar energy to electricity.	It has also been discovered that the voltage is relatively stable between 70 and 74%. Low relative humidity (between 70% and 74%) increases this efficiency even further.	Ettah et al. [137]
Solar modules' primary characteristics, voltage, current, power, and efficiency are all studied parametrically for their effects on each other.	For p-Si modules, generated power and efficiency are more affected by relative humidity variation than the voltage in the range of 10% to 50%.	Sohani et al. [138]
The effects of temperature and relative humidity on the operation of photovoltaics put near the Calabar River were investigated to evaluate their efficiency.	Relative humidity has been found to have a negative correlation with current, efficiency, and photovoltaic system performance.	Njok and Ogbulezie [139]
The deposition of the Hole Extraction Layer (HEL) does not appear to be affected by humidity or oxygen; however, the deposition of the perovskite layer is notoriously affected by humidity and oxygen.	The triple-cation perovskite layer was used to prepare the best-performing device and was deposited under dry air, resulting in an efficiency of 16.7% for power conversion.	Mesquita et al. [140]
Electrical energy production, the efficiency of SPV conversion, and efficiency losses were all examined about weather data. The results show that output is lower during periods of high relative air moisture.	Solar panel designers, installers, and end-users of SPV systems can benefit from the findings for improved system design and more accurate energy production forecasts.	Burduhos et al. [141]
According to research, solar cell performance is affected by weather conditions such as relative humidity and temperature.	There was a significant drop in the efficiency of solar cells when working in conditions like high temperatures and relative humidity of more than 70%.	Hamdi et al. [142]
Under variable humidity and precipitation circumstances, a more generalized mathematical model for dust deposition has been proposed.	As humidity levels rise, the deposition rate of a particle increases, and its rebound rate decreases. With an increase in relative humidity of 40 to 80%, the rebound velocity of a 2.5 μm particle decreases by 73% from 0.073 to 0.019 m/s.	Sengupta et al. [143]
It was found that a two-phase, standing-wave electrodynamic dust shield (EDS) was more successful in removing dust in a single operation mode with constant RH and a cyclic operation mode with alternating RH conditions.	EDS devices can now be designed and operated optimally, including determining the ideal timing of EDS activation and applying appropriate dielectric coverings and hydrophobic coatings to the EDS' top surface.	Javed and Guo [144]
Solar radiation models are adjusted based on the relative humidity and the air quality index (AQI) of a given area.	Relative humidity and AQI were exposed to be the most effective adjustment methods. The accuracy and reliability of solar radiation models that deteriorate layer by layer can be improved using this technique.	Su et al. [145]

×4 SPDK puzzle is done. There is a diagram of electrical connections and design methods in Figures 12(j) and 12(m) [87–90].

3. Causes of Mismatch Losses

Environmental and operational variables have a separate effect on the SPV panel into three groups (solar radiation effect, temperature effect, and relative humidity effect). Input parameters for solar radiation SPV systems are environmental factors that determine the SPV system performance, temperature, and relative humidity.

3.1. Effect of Solar Radiation. Table 2 summarizes research on the impact of solar radiation on solar photovoltaic panels conducted by various researchers. The overall effect of SPV cells has increased the fill factor by increasing solar radiation, as shown in Figure 13. The average fill factor for the SPV module varied between initial and final values of about 22.98%, 54.16%, and 26.19%, with 18.18% and 14.01%, and

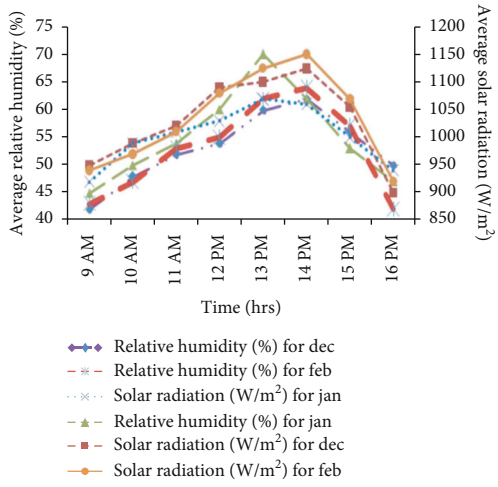

Figure 16: Performance characteristics curve on SPV module with the effect of relative humidity [174].

Table 5: Studies on the effect of internal parameters.

Objectives	Result	References
The model can be built from mathematical equations and an equivalent circuit consisting of a photogenerated current source, a series resistor, a shunt resistor, and a diode.	The I-V and P-V properties of SPV cells are also used in the research of the effect; however, real-time simulations are difficult to apply.	Ahmed et al. [146]
The performance of the Slider Mode Controller (SMC) is substantially affected by the type of sliding surface used.	The generic algorithm (GA) method was used for a more realistic simulation of solar panels.	Chatrenour et al. [147]
The internal properties of a water-based SPV module are examined using single diode models in comparison to land-based SPV modules.	The series resistance of water tank-based modules is higher than that of land-based modules, according to data collected.	Kumar and Kumar [148]
Methodology for detecting photovoltaic system faults based on the various I-V curve effects.	Electrical parameters were examined, inflection spots in the observed curve were tested using a learning technique, and a fault's nature was discovered.	Sarikh et al. [149]
SPV panel's performance parameters that are not generally included in the manufacturer's specifications can be determined via this modified algorithm method.	In a comparison of the two algorithms, it is found that the modified algorithm responds more accurately to sudden increases in solar radiation.	Motahhir et al. [150]
An exhaustive review of the five most common fuzzy logic subsets used in DC-DC boost converters.	With the fewest oscillations and highest system efficiency, the proposed subset can follow the maximum power point in the least amount of time (95.7%).	Hajighorbani et al. [151]
Reducing SPV modeling complexity and implementing a simple fuzzy control system for duty cycle control were the main objectives of this work.	System tracking and dynamic response can be seen in the graphical representation of the system's duty cycle in various environmental conditions.	Mahamudul et al. [152]
An empirical model to predict the effect of temperature on the outdoor performance of p-Si, m-Si, a-Si, and thin-film SPV module technologies will be developed.	The results show that the proposed model estimates can be used to accurately and confidently predict the temperature of SPV modules under similar environmental conditions to those of the study area. SPV systems can be made more efficient and cheaper as a result of this research.	Jatoi et al. [153]
Impedance matching techniques are being used in this study in an attempt to maximize the efficiency of SPV systems.	It was found that SPV panel performance was highest when the 4 Ω electric load was in use for 11 of the month's 12 measurement days, but on the final day, it performed worse than the other two loads (the 6 Ω and 8 Ω electric loads) when they were both in use.	Salilih and Birhane [154]

20% for December, January, and February being the corresponding discrepancy between the total solar radiations.

The number of incidents of solar radiation in an SPV panel can represent various solar-cell fill-factor (FF) outputs as shown in Figure 14. The percentage level for fill factor in mono-Si and poly-Si materials is declining. In other instances, Copper Indium Selenide (CIS) substances will display a percentage increase in fill factor as the solar radiation level increases. It happens with the influence of the material thermal behavior of each solar cell. In this connection, poly-Si can be suitable for high solar radiation incident regions.

3.2. Effect of Temperature. Table 3 summarizes research on the impact of temperature on solar photovoltaic panels conducted by various researchers. In the first and last values, the average fill factor of the SPV module differed by approximately 22.98%, 54.16%, and 26.19%. The equivalent difference between the front and front photovoltaic average temperatures is 10.85%, 11.76%, and 11.42% in December, January, and February (Figure 15). Here in January and then in February and December, a major difference of the fill factor and front side SPV module is achieved. Therefore, depending on climate change, the operating performance parameter degrades.

3.3. Effect of Relative Humidity. Table 4 summarizes research on the impact of relative humidity on solar photovoltaic panels conducted by various researchers. The resulting solar radiation is steadily decreased by increased relative average humidity on the panel's position [73]. The cumulative average relative humidity difference was approximately 35.71%, 32.25%, and 33.5%, respectively, in January, December, and February (Figure 16).

3.4. Effect of Internal Parameters. Table 5 summarizes research by various studies on the impact of internal characteristic parameters on SPV cells. The SPV cell circuit for which the current is exponentially rising during the operating cycle is shown in Figure 17. The SPV cell's efficiency is determined also by the two resistors, namely, series and parallel resistors. A considerable amount of energy loss is normally attributed to manufacturing defections caused by the presence of parallel intensity in the SPV. The majority of the SPV cell has been optimized for a lower shunt resistance than the solar photovoltaic module would cause power loss because the lower resistance value is an alternative way for the circulation of the light current due to the lower power current. Lower load current declines the photovoltaic solar panel's output, which reduced the characteristics of fill

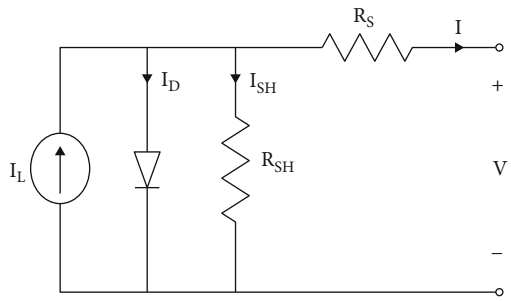

Figure 17: SPV cell equivalent circuit [175].

factor, power supply, and efficiency. The variance in solar radiation, therefore, plays an important part in the parasitic shunt resistance value that can affect performance. The equation for a solar cell when the shunt resistance is present [91] is as follows:

$$I = I_L - I_O \exp\left(e^{q(V_L + I_S R_S)} - 1\right) - \frac{V_L + I_L R_S}{R_{SH}}. \quad (2)$$

A standard solar cell curve with different (constant) shunt resistance values is shown in Figure 18. Shunt resistances are named for Rsh_1 (100 Ω), Rsh_2 (200 Ω), Rsh_3 (300 Ω), Rsh_4 (400 Ω), and Rsh_5 (500 Ω) in this study. The shunt resistance varies drastically, but the voltage is slightly different. Increasing shunt resistance usually increases the point of peak power. Typically, the manufacturer determines the maximum voltage point and current values.

Figure 19 demonstrates the current and shunt resistance function of a typical short-circuit solar cell. The shunt resistors range from 1 Ω to 10 Ω. As a consequence, shunt resistance is very low since the resulting short circuits have a low value. The shunt resistance for the short-circuit current is somewhat different because the effect of the short-circuit current is dependent on an individual material shape's boundary distance. A heavy material short circuit is present on the broadband distance. The maximum value is equal to the higher value in the short-circuit current.

The various losses with the percentage level of the SPV system are mentioned in Figure 19. The output is highly dependent on the module variability which includes the SPV array and solar cell modules. The difference between the highest possible output power from the array and the total output power of every module is called the incongruous losses.

4. Different Topological Connections

Table 6 summarizes research by various academics on the impact of different topological connections on solar photovoltaic modules. Comparisons of I-V properties of different network SPV modules demonstrate incompatible losses on an SPV device. The value of the voltage depends on the usual curve and form method. The temperature difference in the plug is due to incompatible conditions, the variation in the shading level, and the decrease in the connector cable voltage inside the network.

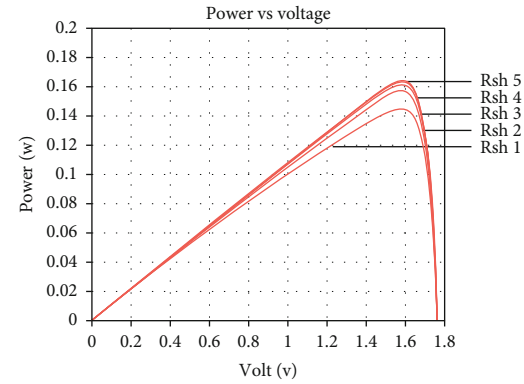

Figure 18: Power vs. voltage characteristic curve [91].

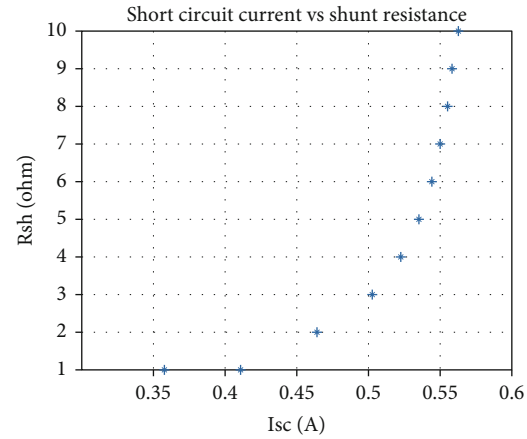

Figure 19: Short-circuit current vs. shunt resistance [91].

A mathematical model for the quantification of energy losses on the SPV system is designed because of the shaded effect. A shadowed portion of the total area and the number of connected blocks in the SPV system required for mathematical model analysis were considered, and the entire I-V curved system area was overlooked [92]. They predicted that power losses in a parallel range and sequence of 2% to 12% and 0.4% to 2.4% could be increased, respectively. The product of the user tolerances, environmental pressures, and cell's shadow effects are such power losses in an SPV cell. A single SPV model with various series and parallel SPV-string link schemes is designed for I-V and P-I [93].

5. Applications

A wide range of experts from academia, industry, and government are working to develop renewable energy sources for use in homes and the industrial sector. The losses must be reduced to obtain more energy from the SPV device; the system should be placed in a location sufficient to obtain high solar incident radiance, and the system should be properly maintained. While the shadow effects for rural electrification are taken into account, a model is developed combining a separate SPV module with an energy collection and control system [94].

Table 6: Studies on the effect of different topological connections.

Objectives	Result	References
Many different types of SPV array problems are discussed in this work, including the more frequent ones such as open circuits, shorts between lines, and ground faults.	It was found that a solar photovoltaic system's performance was affected by various fault conditions on SPV arrays of different topological configurations and fault conditions.	Lipták and Bodnár [155]
New tempered glass-based SPV panels with m-Si and p-Si SPV cells will be tested experimentally to determine their electrical performance.	A solar radiation level of 900 W/m^2 produced results of 67.4 W and 75.67 W from p-Si and m-Si SPV modules, respectively.	Ding et al. [156]
For the SPV system to which it is connected, each converter employs its MPPT algorithm. When subjected to uniform solar radiation, the operational voltage and power output of each panel tend to be equal under this topology.	In both the simulation and the laboratory, the new strategy of comparing the electric properties of nearby SPV panels produced similar results for identifying partial shadow events. System performance was predicted to be in line with the design.	Raeisi and Sadeghzadeh [157]
Maximum power point tracking (MPPT) approaches and SPV system configurations are compared to increase the output of an SPV system in this article.	This study's findings show that intelligent techniques, as opposed to offline and online MPPT techniques, have greater future potential.	Sharma et al. [158]
This paper presents a new architecture based on distinct generation characteristics for the integration of large-scale SPV plants into fragile networks.	Weak grid integration can be better assessed with the proposed framework because it provides accurate voltage and energy estimates that have a high degree of reliability.	Saranchimeg and Nair [159]
This article presents and evaluates the SP, TCT BL, and HC configurations under partially shaded conditions.	The array's generated power was found to be affected by the type and amount of partially shaded modules. TCT configuration outperforms SP design when the shadow is oblique, as proven by the research results and findings.	Kothari [160]
For small-scale photovoltaic solar generation projects, residential complexes are ideal because they have sufficient space and large energy demand.	According to the location where the study is taking place, the process and regulations for connecting a solar photovoltaic system to the energy endorsement firm in charge should be examined.	Muñoz et al. [161]
Direct Power Control (DPC) can be used to improve the quantity of solar power that is fed into the grid from a photovoltaic plant.	This system uses an MPPT (maximum power point tracking) technique-controlled DC-DC converter as its principal renewable source.	Zizoui et al. [162]
In this study, the floating photovoltaic (FPV) system is studied for its possible usage in Egypt's hydropower resources.	The researchers examined both fixed mounting and single-axis tracking FPV, with the latter achieving a 4.96 percent greater energy rate. The combination of FPV technology with a hydrohybrid power system resulted in a 44,270.61-tonne reduction in overall CO_2 emissions.	Ravichandran et al. [163]

Photovoltaic systems in particular are designed to fulfill the demands of industrial energy. However, the extensive reach of the building-integrated photovoltaic (BIPV) system linked to the building is being explored [95]. For every 1°C rise in the temperature of the SPV module, a decrease in power output of about 0.20-0.5% is observed. In a far-reaching country in Nigeria, a hybrid solar photovoltaic/thermal (SPV/T) system offering citizens social and economic opportunities to mitigate the problems that have increased electrical and thermal power generation has been mounted [96]. For different seasons, the plant ensures continuous and economic activity. Because of their high level of diesel price, the hybrid SPV/diesel battery systems are more economic than standalone diesel systems. When considering factors like interest rate and load sizes for a system, the hybrids SPV/diesel are more effective than standalone diesel [97–104].

SPV module measures the effect of the temperatures on electrical parameter output according to Standard Conditions of Testing and outdoor climate (less than 500 W/m^2). For each 1°C rise in the temperature of the SPV module, the loss of power in the outside and STC is 0.48 and 0.52% [105]. For freely installed systems with specific environmental and numerical parameters, the extensive temperature literature of the SPV module has been used. Appropriate correlations should therefore be selected and implemented at various SPV module sites [106]. In superior SPV modules, estimated variations in power and efficiency parameters examined the effect of ambient temperatures between 25°C to 50°C. The ambient temperature of the SPV module was up to 0.50% per °C and 0.05% per °C, respectively, as a considerable decrease in corresponding energy and effectiveness [107, 108].

6. Merits and Demerits of the SPV System

It is more difficult to build, install, and design because of the potential for more backside shade, but its unusual structure produces 5–30 percent more power output and 2-6% cheaper LCOE due to its ability to absorb solar energy from both sides. UV rays from the ground break down typical organic back sheets, and water vapor seeps in through gaps and holes to cause functional failure. A lower cleaning frequency and longer lifetime are achieved with SPV modules

Table 7: Merits and demerits of the photovoltaic system.

Merits	Demerits	References
Because of its lower operating costs, the solar energy industry is growing rapidly around the world. There are two stages to TCT: the modules are connected in parallel and subsequently connected in series. To conserve money, only four modules are cross-tied together in BL, which is a significant reduction. TCT and BL combine to form HC. Depending on how many cross-ties it has (either two, four, or six), it can give the necessary power.	Photovoltaic systems have the major drawback of being completely dependent on changes in solar radiation for their output power. Nevertheless, SPV suffers from partial shading due to a mismatching condition.	Nayak et al. [164]

Table 8: Merits and demerits of various topological connections [165–169].

Configuration	Merits	Demerits
SP	(i) Under the same circumstances, it is effective (ii) Cost-effectiveness (iii) Low level of difficulty	(i) SP is more sensitive to radiation levels than other devices, and the power decreases dramatically when partially shaded (ii) Partially shaded areas will not be covered
BL	(i) With partial shading, this is suitable (ii) In comparison to SP, the maximum power output of BL is 2.5% higher (iii) During periods of partial shading, keep recharging the grid	(i) The level of difficulty is moderate (ii) Inadequate effectiveness
TCT	(i) Possible with some shading (ii) TCT has superior performance, is less susceptible to partial shading, is more dependable, and has higher peak power values and efficiency (iii) During partial shading, keep feeding the grid	TCT has the most connections and is more difficult to implement than other configurations
HC	(i) With partial shade, this is a viable option (ii) MPP improvement on a medium scale (iii) During partial darkening, keep feeding the grid	(i) Moderately difficult (ii) Moderate efficiency

using classic glass organic back sheet architectures compared with those using SPV modules with a lower cell temperature and a more robust resistance to unfavorable environmental conditions. Table 7 summarizes research by various academics on the merits and demerits of solar photovoltaic systems. Table 8 summarizes research by various academics on the merits and demerits of various topological connections on solar photovoltaic modules [109–113].

7. Conclusions

The mismatch loss of the SPV system was analyzed in the influence of performance parameters, including internal and external conditions. The influence of internal parameters like parasitic shunt resistance of different ranges was used in SPV cells, and also, the impact on current-voltage characteristics was studied. The selection of different SPV materials (m-Si and p-Si) and external environmental parameters (solar radiation, temperature, relative humidity, and dust) was considered to evaluate the performance of the system. As far as the present review is concerned, it was aimed at discussing in detail the influences of the parameters mentioned above on the performance of the SPV system. Different topological connections (SS, SP, TCT, BL, and HC) were also considered, and further, TCT configuration was promised to be an improved technique of enhancing performance under influence of partial shading conditions. Similarly, studies on numerous researchers' findings were presented in tables. Recent techniques, circuit implementation for reducing the impact of partial shading, and merits and demerits were discussed. This review covered the indispensable subjects of the causes and effects of mismatch losses and mitigating techniques to the mismatch losses, elaborately. Thus, this review could pave a path for aspiring researchers to attempt numerous analytical and experimental studies, in order to find innovative practices to address the issues existing in external and internal parameters, and thereby, the energy conversion value of the SPV system could be improved remarkably.

Nomenclature

AC: Alternating current
BIPV: Building-integrated photovoltaics
BL: Bridge link
CdTe: Cadmium telluride
CFD: Computational Fluid Dynamics
CIGS: Copper indium gallium selenide
CIS: Copper Indium Selenide
CTM: Cell to Module
DC: Direct current
DPC: Direct Power Control
FF: Fill factor
FPV: Floating photovoltaic

GaAs: Gallium Arsenide
HC: Honeycomb
HEL: Hole Extraction Layer
I: Cell output current (A)
I_L: Light generated current (A)
I_O: Diode darkness current (A)
I_S: Current across series resistance (A)
I-V: Current-voltage
LPB: Long parallel branch
LCOE: Levelized Cost of Electricity
LSS: Long series string
MML: Mismatch loss
MPP: Maximum power point
MPPT: Maximum power point tracking
m-Si: Monocrystalline
p-Si: Polycrystalline
P-V: Power-voltage
P_{Array}: Solar photovoltaic array power
P_{Cell}: Solar photovoltaic cell power
q: Electron charge (1.602×10^{-19}c)
R_{SH}: Cell shunt resistance (Ω)
Rs: Series resistance (Ω)
SDK: So-du-Ku
SP: Series parallel
SPDK: Shape-do-Ku
SPV: Solar photovoltaic
SS: Simple series
SPV/T: Solar photovoltaic/thermal
TCT: Total cross-tied
V_L: Voltage across the cell terminals (V).

Conflicts of Interest

The authors declare that they have no conflicts of interest.

References

[1] D. Picault, B. Raison, S. Bacha et al., "Forecasting photovoltaic array power production subject to mismatch losses," *Solar Energy*, vol. 84, no. 7, pp. 1301–1309, 2010.

[2] J. Guerrero, Y. Munoz, F. C. Ibanez, and A. Ospino, "Analysis of mismatch and shading effects in a photovoltaic array using different technologies," *Materials Science and Engineering*, vol. 59, no. 1, article 012007, 2014.

[3] J. Webber and E. Riley, "Mismatch loss reduction in photovoltaic arrays as a result of sorting photovoltaic modules by max-power parameters," *ISRN Renewable Energy*, vol. 2013, Article ID 327835, 9 pages, 2013.

[4] N. D. Kaushika and A. K. Rai, "An investigation of mismatch losses in solar photovoltaic cell networks," *Energy*, vol. 32, no. 5, p. 755, 2007.

[5] D. Roche, H. Outhred, R. J. Kaye, and R. J. Kaye, "Analysis and control of mismatch power loss in photovoltaic arrays," *Progress in Photovoltaics: Research and Applications*, vol. 3, no. 2, pp. 115–127, 1995.

[6] S. Vijayalekshmy, G. R. Bindu, and S. Rama Iyer, "Estimation of power loss in photovoltaic array configurations under passing cloud condition," in *Proceedings of the World Congress on Engineering*, vol. 1, pp. 1–6, Cochin, India, 2014.

[7] D. Picault, B. Raison, S. Bacha, J. Aguilera, and J. De La Casa, "Changing photovoltaic array interconnections to reduce mismatch losses: a case study," in *2010 9th International Conference on Environment and Electrical Engineering*, pp. 37–40, Prague, Czech Republic, 2010.

[8] H. Obane, K. Okajima, T. Ozeki, and T. Ishii, "PV system with reconnection to improve output under non-uniform illumination," *IEEE Journal of Photovoltaics*, vol. 2, no. 3, pp. 341–347, 2012.

[9] S. R. Potnuru, D. Pattabiraman, S. I. Ganesan, and N. Chilakapati, "Positioning of PV panels for reduction in line losses and mismatch losses in PV array," *Renewable Energy*, vol. 78, pp. 264–275, 2015.

[10] J. L. Crozer, E. E. Van Dyk, and F. J. Vorster, "Characterization of cell mismatch in a multi-crystalline silicon photovoltaic module," *Physica B*, vol. 407, no. 10, pp. 1578–1581, 2012.

[11] S. Edalati, M. Ameri, and M. Iranmanash, "Comparative performance investigation of mono- and poly-crystalline silicon photovoltaic modules for use in grid-connected photovoltaic systems in dry climates," *Applied Energy*, vol. 160, pp. 255–265, 2015.

[12] I. Visa, B. Burduhos, M. Neagoe, M. Moldovan, and A. Duta, "Comparative analysis of the infield response of five types of photovoltaic modules," *Renewable Energy*, vol. 95, pp. 178–190, 2016.

[13] E. Karatepe, M. Boztepe, and M. Colak, "Development of a suitable model for characterizing photovoltaic arrays with shaded solar cells," *Solar Energy*, vol. 81, no. 8, pp. 977–992, 2007.

[14] G. Petrone, G. Spagnuolo, and M. Vitelli, "Analytical model of mismatched photovoltaic fields by means of Lambert W-function," *Solar Energy Materials & Solar Cells*, vol. 91, no. 18, pp. 1652–1657, 2007.

[15] W. R. Anis and M. Abdul-Sadek Nour, "Energy losses in photovoltaic systems," *Energy Conservation and Management*, vol. 36, no. 11, pp. 1107–1113, 1995.

[16] V. Tyagi, N. A. Rahim, N. Rahim, A. Jeyraj, and L. Selvaraj, "Progress in solar PV technology: research and achievement," *Renewable and Sustainable Energy Review*, vol. 20, pp. 443–461, 2013.

[17] M. A. Green, "Thin-film solar cells: review of materials, technologies and commercial status," *Journal of Material Science: Materials in Electronics*, vol. 18, no. S1, pp. 15–19, 2007.

[18] K. Kawashima, Y. Tamai, H. Ohkita, I. Osaka, and K. Takimiya, "High-efficiency polymer solar cells with small photon energy loss," *Nature Communications*, vol. 6, no. 1, 2015.

[19] J. Kim, Z. Hong, G. Li et al., "10.5% efficient polymer and amorphous silicon hybrid tandem photovoltaic cell," *Nature Communications*, vol. 6, no. 1, 2015.

[20] A. N. B. Zulkifili, T. Kento, M. Daiki, and A. Fujiki, "The basic research on the dye-sensitized solar cells (DSSC)," *Journal of Clean Energy Technologies*, vol. 3, no. 5, pp. 382–387, 2015.

[21] C. Ferrara and D. Philipp, "Why do PV modules fail," *Energy Procedia*, vol. 15, pp. 379–387, 2012.

[22] B. Norton, P. C. Eames, T. K. Mallick et al., "Enhancing the performance of building integrated photovoltaics," *Solar Energy*, vol. 85, no. 8, pp. 1629–1664, 2011.

[23] R. B. Sathyanarayana, P. S. Lakshmi Sagar, and G. Kumar, "Effect of shading on the performance of solar PV panel," *Energy and Power*, vol. 5, no. 1A, 2015.

[24] S. Motasem, A. G. Albaali, E. Alasis, and J. K. Kaldellis, "Experimental study on the effect of dust deposition on solar photovoltaic panels in desert environment," *Renewable Energy*, vol. 92, pp. 499–505, 2016.

[25] M. Hosenuzzaman, N. A. Rahim, J. Selvaraj, and M. Hasanuzzaman, "Factors affecting the PV based power generation," in *3rd IET International Conference on Clean Energy and Technology (CEAT) 2014*, pp. 1–6, Kuching, 2014.

[26] S. Kumar and T. Kaur, "Solar PV performance-issues and challenges," *International Journal of Innovative Research in Electrical, Electronics, Instrumentation and Control Engineering*, vol. 2, no. 11, pp. 2168–2172, 2014.

[27] A. Al-Otaibi, A. Al-Qattan, F. Fairouz, and A. Al-Mulla, "Performance evaluation of photovoltaic systems on Kuwaiti schools' rooftop," *Energy Conversion and Management*, vol. 95, pp. 110–119, 2015.

[28] D. Martinez-Plaza, A. Abdallah, B. W. Figgis, and T. Mirza, "Performance improvement techniques for photovoltaic systems in Qatar: results of first year of outdoor exposure," *Energy Procedia*, vol. 77, pp. 386–396, 2015.

[29] M. R. Maghami, H. Hizam, C. Gomes, M. A. Radzi, M. I. Rezadad, and S. Hajighorbani, "Power loss due to soiling on solar panel: a review," *Renewable, and Sustainable Energy Reviews*, vol. 59, pp. 1307–1316, 2016.

[30] M. Vazquez and I. Rey-Stolle, "Photovoltaic module reliability model based on field degradation studies," *Progress in Photovoltaics: Research and Applications*, vol. 16, no. 5, pp. 419–433, 2008.

[31] A. Ndiaye, C. M. F. Kebe, P. A. Ndiaye, A. Charki, A. Kobi, and V. Sambou, "Impact of dust on the photovoltaic (PV) modules characteristics after an exposition year in Sahelian environment: the case of Senegal," *International Journal of Physical Sciences*, vol. 8, no. 21, pp. 1166–1173, 2013.

[32] T. Ma, H. Yang, and L. Lin, "Development of a model to simulate the performance characteristics of crystalline silicon photovoltaic modules/strings/arrays," *Solar Energy*, vol. 100, pp. 31–41, 2014.

[33] J. D. Bastidas, E. Franco, G. Petrone, C. A. Ramos-Paja, and G. Spagnuolo, "A model of photovoltaic fields in mismatching conditions featuring an improved calculation speed," *Electrical Power System Research*, vol. 96, pp. 81–90, 2013.

[34] M. R. Al Rashidi, K. M. El-Naggar, and M. F. Al Hajri, "Parameters estimation of double diode solar cell model," *International Journal of Electrical, Computer, Energetic, Electronic and Communication Engineering*, vol. 7, no. 2, pp. 118–121, 2013.

[35] J. Surya Kumara and S. B. Ch, "Mathematical modeling and simulation of photovoltaic cell using matlab-simulink environment," *International Journal of Electrical and Computer Engineering*, vol. 2, no. 1, pp. 26–34, 2012.

[36] J.-C. Wang, J.-C. Shieh, S. Yu-Li et al., "A novel method for the determination of dynamic resistance for photovoltaic modules," *Energy*, vol. 36, no. 10, pp. 5968–5974, 2011.

[37] A. Al Tarabsheh, I. Etier, and M. Widyan, "Investigation of the shunt effects of parallel-connected a-Si: H solar cells," *International Journal of Sustainable Energy*, vol. 32, no. 2, pp. 71–77, 2011.

[38] Y. S. Kim, S.-M. Kang, B. Johnston, and R. Winston, "A novel method to extract the series resistances of individual cells in a photovoltaic module," *Solar Energy Materials & Solar Cells*, vol. 115, pp. 21–28, 2013.

[39] C. S. Ruschel, F. P. Gasparin, E. R. Costa, and A. Krenzinger, "Assessment of PV modules shunt resistance dependence on solar irradiance," *Solar Energy*, vol. 133, pp. 35–43, 2016.

[40] D. Rusirawan and I. Farkas, "Identification of model parameters of the photovoltaic solar cells," *Energy Procedia*, vol. 57, pp. 39–46, 2014.

[41] M. S. Benghanem and S. N. Alamri, "Modeling of photovoltaic module and experimental determination of serial resistance," *Journal of Taibah University for Science*, vol. 2, no. 1, pp. 94–105, 2009.

[42] F. Ghani, M. Duke, and J. Carson, "Numerical calculation of series and shunt resistance of a photovoltaic cell using the Lambert *W*-function: Experimental evaluation," *Solar Energy*, vol. 87, pp. 246–253, 2013.

[43] F. Ghani and M. Duke, "Numerical determination of parasitic resistances of a solar cell using the Lambert w-function," *Solar Energy*, vol. 85, no. 9, pp. 2386–2394, 2011.

[44] C. Carrero, J. Rodríguez, D. Ramírez, and C. Platero, "Simple estimation of pv modules loss resistances for low error modelling," *Renewable Energy*, vol. 35, no. 5, pp. 1103–1108, 2010.

[45] A. Rezaee Jordehi, "Parameter estimation of solar photovoltaic (PV) cells: a review," *Renewable and Sustainable Energy Reviews*, vol. 61, pp. 354–371, 2016.

[46] H.-H. Hseih, F.-M. Lin, and Y. Shan-Pu, "Performance of low series-resistance interconnections on the polycrystalline solar cells," *Solar Energy Materials & Solar Cells*, vol. 95, no. 1, pp. 39–44, 2011.

[47] J. Bastidas, C. Y. Ramos, and E. Franco, "Modelling and parameter calculation of photovoltaic fields in irregular weather conditions," *En: Ingenieria*, vol. 17, no. 1, pp. 37–48, 2012.

[48] F. Sarhaddi, S. Farahat, H. Ajam, A. Behzadmehr, and M. Mahdavi Adeli, "An improved thermal and electrical model for a solar photovoltaic thermal (PV/T) air collector," *Applied Energy*, vol. 87, no. 7, pp. 2328–2339, 2010.

[49] R. Guliani, A. Jain, S. Sharma, D. Kaur, A. Guliani, and A. Kapoor, "Analysis of electrical characteristics using a Lambert W-function technique and MATLAB simulation for dye sensitised ZnO solar cell," *The Open Renewable Energy Journal*, vol. 6, pp. 23–28, 2010.

[50] R. Dash and S. M. Ali, "Comparative study of one and two diode model of solar photovoltaic cell," *International Journal of Research in Engineering and Technology*, vol. 3, no. 10, pp. 190–194, 2014.

[51] Y. Chen, X. W. Da Li, R. Hong, and H. Shen, "Parameters extraction from commercial solar cells $I - V$ characteristics and shunt analysis," *Applied Energy*, vol. 88, no. 6, pp. 2239–2244, 2011.

[52] E. Radziemska, "Thermal performance of Si and GaAs based solar cells and modules: a review," *Progress in Energy and Combustion Science*, vol. 29, no. 5, pp. 407–424, 2003.

[53] V. K. Sethi, M. Pandey, and P. Shukla, "Thin-film photovoltaic cell compared to mono crystalline photovoltaic cell and multi crystalline photovoltaic cell," *International Journal of Advanced Renewable Energy Research*, vol. 1, no. 2, pp. 117–125, 2012.

[54] M. R. Abdelkader, A. Al-Salaymeh, Z. Al-Hamamre, and F. Sharaf, "A comparative analysis of the performance of monocrystalline and multicrystalline PV cells in semi arid climate conditions: the case of Jordan," *Jordan Journal of*

Mechanical and Industrial Engineering, vol. 4, no. 5, pp. 543–552, 2010.

[55] M. A. Mosalam Shaltout, A. A. El-Hadad, M. A. Fadly, A. F. Hassan, and A. M. Mahrous, "Determination of suitable types of solar cells for optimal outdoor performance in desert climate," *Renewable Energy*, vol. 19, no. 1-2, pp. 71–74, 2000.

[56] A. Hunter Fanney, M. W. Davis, B. P. Dougherty, D. L. King, W. E. Boyson, and J. A. Kratochvil, "Comparison of photovoltaic module performance measurements," *Journal of Solar Energy Engineering*, vol. 128, no. 2, pp. 152–159, 2006.

[57] M. Azhar Ghazali, A. Malek, and A. Rahman, "The performance of three different solar panels for solar electricity applying solar tracking device under the Malaysian climate condition," *Energy and Environment Research*, vol. 2, no. 1, pp. 235–243, 2012.

[58] O.-M. Midtgard, T. O. Saetre, G. Yordanov, A. G. Imenes, and C. L. Nge, "A qualitative examination of performance and energy yield of photovoltaic modules in southern Norway," *Renewable Energy*, vol. 35, no. 6, pp. 1266–1274, 2010.

[59] A. Limmanee, N. Udomdachanut, S. Songtrai et al., "Field performance and degradation rates of different types of photovoltaic modules: a case study in Thailand," *Renewable Energy*, vol. 89, pp. 12–17, 2016.

[60] F. Dincer and M. E. Merat, "Critical factors that affecting efficiency of solar cells," *Smart Grid and Renewable Energy*, vol. 1, no. 1, pp. 47–50, 2010.

[61] R. Siddiqui and U. Bajpai, "Correlation between thicknesses of dust collected on photovoltaic module and difference in efficiencies in composite climate," *International Journal of Renewable Energy Research*, vol. 3, no. 1, pp. 26–490, 2012.

[62] C. Min, "Analysis about modules and strings mismatch loss in the photovoltaic plant," *American Journal of Modern Energy*, vol. 5, no. 3, pp. 63–68, 2019.

[63] A. Gholami, M. Ameri, M. Zandi, and R. G. Ghoachani, "Electrical, thermal and optical modeling of photovoltaic systems: step-by-step guide and comparative review study," *Sustainable Energy Technologies and Assessments*, vol. 49, article 101711, 2022.

[64] A. Hussain, A. Batra, and R. Pachauri, "An experimental study on effect of dust on power loss in solar photovoltaic module," *Renewables: Wind, Water, and Solar*, vol. 4, no. 1, pp. 1–13, 2017.

[65] T. Sarver, A. Al-Qaraghuli, and L. L. Kazmerski, "A comprehensive review of the impact of dust on the use of solar energy: history, investigations, results, literature, and mitigation approaches," *Renewable and Sustainable Energy Reviews*, vol. 22, pp. 698–733, 2013.

[66] T. Khatib, H. Kazem, K. Sopian, F. Buttinger, W. Elmenreich, and A. S. Albusaidi, "Effect of dust deposition on the performance of multi-crystalline photovoltaic modules based on experimental measurements," *International Journal of Renewable Energy Research*, vol. 3, no. 4, pp. 850–853, 2013.

[67] Y. Andrea, T. Pogrebnaya, and B. Kichonge, "Effect of industrial dust deposition on photovoltaic module performance: experimental measurements in the tropical regionInternational Journal of Photoenergy," vol. 2019, Article ID 1892148, 10 pages, 2019.

[68] M. Konyu, N. Ketjoy, and C. Sirisamphanwong, "Effect of dust on the solar spectrum and electricity generation of a photovoltaic module," *IET Renewable Power Generation*, vol. 14, no. 14, pp. 2759–2764, 2020.

[69] https://blog.aurorasolar.com/understanding-pv-system-losses-part-1.

[70] L. L. Bucciarelli Jr., "Power loss in photovoltaic arrays due to mismatch in cell characteristics," *Solar Energy*, vol. 23, no. 4, pp. 277–288, 1979.

[71] C. Deline, S. A. Pelaez, S. MacAlpine, and C. Olalla, *Bifacial PV system mismatch loss estimation and parameterization: preprint*, National Renewable Energy Laboratory. NREL/CP-5K00-73541, Golden, CO, 2019, https://www.nrel.gov/docs/fy20osti/73541.pdf.

[72] M. B. MacAlpine and R. Erickson, "Quantifying mismatch losses in small arrays," in *2013 Sandia PV Performance Modeling Workshop*, Santa Clar, CA, 2013.

[73] T. Selmi and A. Gastli, "Grid-connected photovoltaic system requirement," *Peer Review Journal of Solar & Photoenergy Systems*, vol. 1, 2018.

[74] D. Avithi Desappan, E. Natarajan, and L. Ponnusamy, "Performance evaluation of photovoltaic system in humid atmosphere," in *Applied Mechanics and Materials*, vol. 787, pp. 57–61, Trans Tech Publications Ltd., 2015.

[75] N. HemanthBabu, S. Shivashimpiger, N. Samanvita, and V. M. Parthasarathy, "Performance ratio and loss analysis for 20MW grid connected solar PV system-case study," *International Journal of Engineering and Advanced Technology*, vol. 8, no. 2S2, 2019.

[76] M. Mutluer and A. Erat, "A new intelligent system design for cleaning the photovoltaic solar panel surface," *International Journal of Energy Applications and Technologies*, vol. 6, no. 1, pp. 8–16.

[77] E. Bellini, "Pv magazine," *PV magazine*, vol. 2, 2017.

[78] A. A. Mansur, M. Amin, and K. K. Islam, "Performance comparison of mismatch power loss minimization techniques in series-parallel PV array configurations," *Energies*, vol. 12, no. 5, p. 874, 2019.

[79] S. Ekici and M. A. Kopru, "Investigation of PV system cable losses," *International journal of renewable energy research*, vol. 7, no. 2, pp. 807–815, 2017.

[80] K. Lappalainen and S. Valkealahti, "Photovoltaic mismatch losses caused by moving clouds," *Solar Energy*, vol. 158, pp. 455–461, 2017.

[81] S. Pannientakandi, R. Gupta, and S. Manjoli, "Effect of local shunting on the electrical mismatch losses in industrial silicon photovoltaic modules," *International Journal of Power and Energy Research*, vol. 2, no. 1, pp. 1–15, 2018.

[82] N. Rakesh, S. Banerjee, S. Subramaniam, and N. Babu, "A simplified method for fault detection and identification of mismatch modules and strings in a grid-tied solar photovoltaic system," *International Journal of Emerging Electric Power Systems*, vol. 21, no. 4, 2020.

[83] A. Khatibi, F. Razi Astaraei, and M. H. Ahmadi, "Generation and combination of the solar cells: a current model review," *Energy Science & Engineering*, vol. 7, no. 2, pp. 305–322, 2019.

[84] S. Chander, A. Purohit, A. Sharma, S. P. Nehra, and M. S. Dhaka, "A study on photovoltaic parameters of monocrystalline silicon solar cell with cell temperature," *Energy Reports*, vol. 1, pp. 104–109, 2015.

[85] R. K. Pachauri, I. Kansal, T. S. Babu, and H. H. Alhelou, "Power losses reduction of solar PV systems under partial shading conditions using re-allocation of PV module-fixed electrical connections," *IEEE Access*, vol. 9, pp. 94789–94812, 2021.

[86] G. Madhusudanam, S. Senthilkumar, I. Anand, and P. Sanjeevkumar, "A shade dispersion scheme using Latin square arrangement to enhance power production in solar photovoltaic array under partial shading conditions," *Journal of Renewable and Sustainable Energy*, vol. 10, no. 5, pp. 1–14, 2018.

[87] A. Srinivasan, S. Devakirubakaran, and B. M. Sundaram, "Mitigation of mismatch losses in solar PV system –two-step reconfiguration approach," *Solar Energy*, vol. 206, pp. 640–654, 2020.

[88] G. Rezk, A. Fathy, and M. Aly, "A robust photovoltaic array reconfiguration strategy based on coyote optimization algorithm for enhancing the extracted power under partial shadow condition," *Energy Reports*, vol. 7, pp. 109–124, 2021.

[89] R. Venkateswari and N. Rajasekar, "Power enhancement of PV system via physical array reconfiguration based Lo Shu technique," *Energy Conversion and Management*, vol. 215, article 112885, 2020.

[90] J. J. Wanko and J. V. Nickell, "Reinforcing geometric properties with Shapedoku puzzles," *Mathematics Teacher*, vol. 107, no. 3, pp. 188–194, 2013.

[91] A. D. Dhass, E. Natarajan, and L. Ponnusamy, "Influence of shunt resistance on the performance of the solar photovoltaic cells," in *2012 International Conference on Emerging Trends in Electrical Engineering and Energy Management (ICE-TEEEM)*, pp. 382–386, Chennai, India, 2012.

[92] F. Martinez-Mareno, J. Munoz, and E. Lorenzo, "Experimental model to estimate shading losses on PV arrays," *Solar Energy Materials & Solar Cells*, vol. 94, no. 12, pp. 2298–2303, 2010.

[93] H. Tian, F. Mancilla-David, K. Ellis, E. Muijadi, and P. Jenkins, "A cell-to-module-to-array detailed model for photovoltaic panels," *Solar Energy*, vol. 86, no. 9, pp. 2695–2706, 2012.

[94] W. Grzesiak, P. Mackow, T. Maj et al., "Innovative system for energy collection and management integrated within a photovoltaic module," *Solar Energy*, vol. 132, pp. 442–452, 2016.

[95] W. Zheng, H. Bin, L. Nianping, L. Shan, and Y. Chunni, "Investigation on photovoltaic application in buildings in China," *Energy Procedia*, vol. 70, pp. 673–682, 2015.

[96] A. Makki, S. Omer, and H. Sabir, "Advancements in hybrid photovoltaic systems for enhanced solar cells performance," *Renewable and Sustainable Energy Reviews*, vol. 41, pp. 658–684, 2015.

[97] D. O. Akinyele, R. K. Rayudu, and N. K. C. Nair, "Development of photovoltaic power plant for remote residential applications: the socio-technical and economic perspectives," *Applied Energy*, vol. 155, pp. 131–149, 2015.

[98] K. Y. Lau, C. W. Tan, and A. H. M. Yatim, "Photovoltaic systems for Malaysian islands: effects of interest rates, diesel prices and load sizes," *Energy*, vol. 83, pp. 204–216, 2015.

[99] K. E. Park, G. H. Kang, H. I. Kim, G. J. Yu, and J. T. Kim, "Analysis of thermal and electrical performance of semi-transparent photovoltaic (PV) module," *Energy*, vol. 35, no. 6, pp. 2681–2687, 2010.

[100] E. Skoplaki and J. A. Palyvos, "Operating temperature of photovoltaic modules: a survey of pertinent correlations," *Renewable Energy*, vol. 34, no. 1, pp. 23–29, 2009.

[101] J. P. Kim, J. Ho Lim, H. Song, Y. J. Chnag, and C. H. Jeon, "Numerical analysis on the thermal characteristics of photovoltaic module with ambient temperature variation," *Solar Energy Materials & Solar Cells*, vol. 95, no. 1, pp. 404–407, 2011.

[102] M. M. Fouad, L. A. Shihata, and E. I. Morgan, "An integrated review of factors influencing the perfomance of photovoltaic panels," *Renewable and Sustainable Energy Reviews*, vol. 80, pp. 1499–1511, 2017.

[103] H. Ali and H. A. Khan, "Analysis on inverter selection for domestic rooftop solar photovoltaic system deployment," *International Transactions on Electrical Energy Systems*, vol. 30, no. 5, article e12351, 2020.

[104] K. R. McIntosh, M. D. Abbott, B. A. Sudbury, and J. Meydbray, "Mismatch loss in bifacial modules due to non-uniform illumination in 1-D tracking systems," *IEEE Journal of Photovoltaics*, vol. 9, no. 6, pp. 1504–1512, 2019.

[105] S. K. Cherukuri, P. K. Balachandran, K. R. Kaniganti et al., "Power enhancement in partial shaded photovoltaic system using spiral pattern array configuration scheme," *IEEE Access*, vol. 9, pp. 123103–123116, 2021.

[106] R. Evans, M. Boreland, and M. A. Green, "A holistic review of mismatch loss: from manufacturing decision making to losses in fielded arrays," *Solar Energy Materials and Solar Cells*, vol. 174, pp. 214–224, 2018.

[107] A. Srinivasan, S. Devakirubakaran, and B. M. Sundaram, "Mitigation of mismatch losses in solar PV system - Two-step reconfiguration approach," *Solar Energy*, vol. 206, pp. 640–654, 2020.

[108] P. R. Satpathy, S. Jena, and R. Sharma, "Power enhancement from partially shaded modules of solar PV arrays through various interconnections among modules," *Energy*, vol. 144, pp. 839–850, 2018.

[109] X. Sun, M. R. Khan, C. Deline, and M. A. Alam, "Optimization and performance of bifacial solar modules: a global perspective," *Applied Energy*, vol. 212, pp. 1601–1610, 2018.

[110] M. T. Patel, M. R. Khan, X. Sun, and M. A. Alam, "A worldwide cost-based design and optimization of tilted bifacial solar farms," *Applied Energy*, vol. 247, pp. 467–479, 2019.

[111] C. D. Rodríguez-Gallegos, M. Bieri, O. Gandhi, J. P. Singh, T. Reindl, and S. K. Panda, "Monofacial vs bifacial Si-based PV modules: which one is more cost-effective?," *Solar Energy*, vol. 176, pp. 412–438, 2018.

[112] B. Yu, D. Song, Z. Sun et al., "A study on electrical performance of N-type bifacial PV modules," *Solar Energy*, vol. 137, pp. 129–133, 2016.

[113] J. S. Stein, D. Riley, M. Lave, C. Hansen, C. Deline, and F. Toor, "Outdoor field performance from bifacial photovoltaic modules and systems," in *2017 IEEE 44th Photovoltaic Specialist Conference (PVSC)*, pp. 3184–3189, Washington, DC, USA, 2017.

[114] B. Dhanalakshmi and N. Rajasekar, "Dominance square based array reconfiguration scheme for power loss reduction in solar PhotoVoltaic (PV) systems," *Energy Conversion and Management*, vol. 156, pp. 84–102, 2018.

[115] D. G. Lorente, S. Pedrazzi, G. Zini, A. Dalla Rosa, and P. Tartarini, "Mismatch losses in PV power plants," *Solar Energy*, vol. 100, pp. 42–49, 2014.

[116] P. Rodrigo, R. Velázquez, E. F. Fernández, F. Almonacid, and P. J. Pérez-Higueras, "Analysis of electrical mismatches in high-concentrator photovoltaic power plants with distributed inverter configurations," *Energy*, vol. 107, pp. 374–387, 2016.

[117] V. Sharma and S. S. Chandel, "Performance analysis of a 190 kWp grid interactive solar photovoltaic power plant in India," *Energy*, vol. 55, pp. 476–485, 2013.

[118] A. Wang and Y. Xuan, "A detailed study on loss processes in solar cells," *Energy*, vol. 144, pp. 490–500, 2018.

[119] A. K. Tripathi, S. Ray, and M. Aruna, "Analysis on photovoltaic panel temperature under the influence of solar radiation and ambient temperature," in *2021 International Conference on Advances in Electrical, Computing, Communication and Sustainable Technologies (ICAECT)*, pp. 1–5, Bhilai, India, 2021.

[120] A. K. Tripathi, S. Ray, M. Aruna, and S. Prasad, "Evaluation of solar PV panel performance under humid atmosphere," *Materials Today: Proceedings*, vol. 45, pp. 5916–5920, 2021.

[121] A. Karafil, H. Ozbay, and M. Kesler, "Temperature and solar radiation effects on photovoltaic panel power," *Journal of New Results in Science*, vol. 5, pp. 48–58, 2016.

[122] P. G. McCormick and H. Suehrcke, "The effect of intermittent solar radiation on the performance of PV systems," *Solar Energy*, vol. 171, pp. 667–674, 2018.

[123] M. J. Buni, A. A. Al-Walie, and K. A. Al-Asadi, "Effect of solar radiation on photovoltaic cell," *International Research Journal of Advanced Engineering and Science*, vol. 3, no. 3, pp. 47–51, 2018.

[124] L. Xingcai and N. Kun, "Effectively predict the solar radiation transmittance of dusty photovoltaic panels through Lambert-Beer law," *Renewable Energy*, vol. 123, pp. 634–638, 2018.

[125] P. A. Thorat, A. P. Edalabadkar, R. B. Chadge, and A. Ingle, "Effect of sun tracking and cooling system on photovoltaic panel: a review," *Materials Today: Proceedings*, vol. 4, no. 14, pp. 12630–12634, 2017.

[126] R. Nasrin, M. Hasanuzzaman, and N. A. Rahim, "Effect of high irradiation on photovoltaic power and energy," *International Journal of Energy Research*, vol. 42, no. 3, pp. 1115–1131, 2018.

[127] H. A. Kazem and M. T. Chaichan, "Effect of environmental variables on photovoltaic performance-based on experimental studies," *International Journal of Civil, Mechanical and Energy Science (IJCMES)*, vol. 2, no. 4, pp. 1–8, 2016.

[128] Y. Du, C. J. Fell, B. Duck, D. Chen, K. Liffman, and Y. Zhang, "Evaluation of photovoltaic panel temperature in realistic scenarios," *Energy Conversion and Management*, vol. 108, pp. 60–67, 2016.

[129] S. Dubey, J. N. Sarvaiya, and B. Seshadri, "Temperature Dependent Photovoltaic (PV) Efficiency and Its Effect on PV Production in the World - A Review," *Energy Procedia*, vol. 33, pp. 311–321, 2013.

[130] N. H. Zaini, M. Z. Ab Kadir, M. Izadi, N. I. Ahmad, M. A. M. Radzi, and N. Azis, "The effect of temperature on a monocrystalline solar PV panel," in *2015 IEEE Conference on Energy Conversion (CENCON)*, pp. 249–253, Johor Bahru, Malaysia, 2015.

[131] L. W. Thong, S. Murugan, P. K. Ng, and C. C. Sun, "Analysis of photovoltaic panel temperature effects on its efficiency," *System*, vol. 18, no. 19, 2016.

[132] V. Perraki and P. Kounavis, "Effect of temperature and radiation on the parameters of photovoltaic modules," *Journal of Renewable and Sustainable Energy*, vol. 8, no. 1, article 013102, 2016.

[133] P. K. Dash and N. C. Gupta, "Effect of temperature on power output from different commercially available photovoltaic modules," *International Journal of Engineering Research and Applications*, vol. 5, no. 1, pp. 148–151, 2015.

[134] R. M. Schoeman, A. J. Swart, and C. Pienaar, "Negating temperature on photovoltaic panels," in *2013 Africon*, pp. 1–5, Pointe aux Piments, Mauritius, 2013.

[135] A. Idzkowski, W. Walendziuk, and W. Borawski, "Analysis of the temperature impact on the performance of photovoltaic panel," in *Photonics Applications in Astronomy, Communications, Industry, and High-Energy Physics Experiments*, vol. 9662, Wilga, Poland, 2015.

[136] W. Charfi, M. Chaabane, H. Mhiri, and P. Bournot, "Performance evaluation of a solar photovoltaic system," *Energy Reports*, vol. 4, pp. 400–406, 2018.

[137] E. B. Ettah, A. B. Udoimuk, J. N. Obiefuna, and F. E. Opara, "The effect of relative humidity on the efficiency of solar panels in Calabar, Nigeria," *Universal Journal of Management and Social Sciences*, vol. 2, no. 3, pp. 8–11, 2012.

[138] A. Sohani, M. H. Shahverdian, H. Sayyaadi, and D. A. Garcia, "Impact of absolute and relative humidity on the performance of mono and poly crystalline silicon photovoltaics; applying artificial neural network," *Journal of Cleaner Production*, vol. 276, article 123016, 2020.

[139] A. O. Njok and J. C. Ogbulezie, "The effect of relative humidity and temperature on polycrystalline solar panels installed close to a river," *Physical Science International Journal*, vol. 20, no. 4, pp. 1–11, 2018.

[140] I. Mesquita, L. Andrade, and A. Mendes, "Effect of relative humidity during the preparation of perovskite solar cells: performance and stability," *Solar Energy*, vol. 199, pp. 474–483, 2020.

[141] B. G. Burduhos, I. Vişa, A. Duță, and M. Neagoe, "Analysis of the conversion efficiency of five types of photovoltaic modules during high relative humidity time periods," *IEEE Journal of Photovoltaics*, vol. 8, no. 6, pp. 1716–1724, 2018.

[142] R. T. Hamdi, S. A. Hafad, H. A. Kazem, and M. T. Chaichan, "Humidity impact on photovoltaic cells performance: a review," *International Journal of Recent Engineering Research and Development (IJRERD)*, vol. 3, no. 11, pp. 27–37, 2018.

[143] S. Sengupta, S. Sengupta, C. K. Chanda, and H. Saha, "Modeling the effect of relative humidity and precipitation on photovoltaic dust accumulation processes," *IEEE Journal of Photovoltaics*, vol. 11, no. 4, pp. 1069–1077, 2021.

[144] W. Javed and B. Guo, "Effect of relative humidity on dust removal performance of electrodynamic dust shield," *Journal of Electrostatics*, vol. 105, article 103434, 2020.

[145] G. Su, S. Zhang, M. Hu, W. Yao, Z. Li, and Y. Xi, "The modified layer-by-layer weakening solar radiation models based on relative humidity and air quality index," *Energy*, vol. 239, article 122488, 2022.

[146] M. T. Ahmed, T. Gonçalves, and M. Tlemcani, "Single diode model parameters analysis of photovoltaic cell," in *2016 IEEE International Conference on Renewable Energy Research and Applications (ICRERA)*, pp. 396–400, Birmingham, UK, 2016.

[147] N. Chatrenour, H. Razmi, and H. Doagou-Mojarrad, "Improved double integral sliding mode MPPT controller-based parameter estimation for a stand-alone photovoltaic system," *Energy Conversion and Management*, vol. 139, pp. 97–109, 2017.

[148] M. Kumar and A. Kumar, "Experimental validation of performance and degradation study of canal-top photovoltaic system," *Applied Energy*, vol. 243, pp. 102–118, 2019.

[149] S. Sarikh, M. Raoufi, A. Bennouna, A. Benlarabi, and B. Ikken, "Photovoltaic system fault identification

methodology based on IV characteristics analysis," *AIP Conference Proceedings*, vol. 2123, no. 1, article 020037, 2019.

[150] S. Motahhir, A. El Ghzizal, S. Sebti, and A. Derouich, "Modeling of a photovoltaic system with modified incremental conductance algorithm for fast changes of irradiance," *International Journal of Photoenergy*, vol. 2018, Article ID 3286479, 13 pages, 2018.

[151] S. Hajighorbani, M. M. Radzi, M. Z. A. Ab Kadir, S. Shafie, R. Khanaki, and M. R. Maghami, "Evaluation of fuzzy logic subsets effects on maximum power point tracking for photovoltaic system," *International Journal of Photoenergy*, vol. 2014, Article ID 719126, 13 pages, 2014.

[152] H. Mahamudul, M. Saad, and M. Ibrahim Henk, "Photovoltaic system modeling with fuzzy logic-based maximum power point tracking algorithm," *International Journal of Photoenergy*, vol. 2013, Article ID 762946, 10 pages, 2013.

[153] A. R. Jatoi, S. R. Samo, and A. Q. Jakhrani, "An improved empirical model for estimation of temperature effect on the performance of photovoltaic modules," *International Journal of Photoenergy*, vol. 2019, Article ID 1681353, 16 pages, 2019.

[154] E. M. Salilih and Y. T. Birhane, "Modeling and analysis of photovoltaic solar panels under constant electric load," *Journal of Renewable Energy*, vol. 2019, Article ID 9639480, 10 pages, 2019.

[155] R. Lipták and I. Bodnár, "Simulation of fault detection in photovoltaic arrays," *Analecta Technica Szegedinensia*, vol. 15, no. 2, pp. 31–40, 2021.

[156] K. Ding, J. Zhang, H. Ding, Y. Liu, F. Chen, and Y. Li, "Fault detection of photovoltaic array based on Grubbs criterion and local outlier factor," *IET Renewable Power Generation*, vol. 14, no. 4, pp. 551–559, 2020.

[157] H. A. Raeisi and S. M. Sadeghzadeh, "A novel experimental and approach of diagnosis, partial shading, and fault detection for domestic purposes photovoltaic system using data exchange of adjacent panels," *International Journal of Photoenergy*, vol. 2021, Article ID 9956433, 19 pages, 2021.

[158] S. Sharma, M. Pattnaik, M. Sarswat, and L. Varshney, "Comprehension of different techniques used in increasing output of photovoltaic system," in *Innovations in Electrical and Electronic Engineering*, Lecture Notes in Electrical Engineering, M. N. Favorskaya, S. Mekhilef, R. K. Pandey, and N. Singh, Eds., pp. 203–218, Springer, Singapore, 2021.

[159] S. Saranchimeg and N. K. Nair, "A novel framework for integration analysis of large-scale photovoltaic plants into weak grids," *Applied Energy*, vol. 282, article 116141, 2021.

[160] D. P. Kothari, A. Pathak, and U. Pandey, "Comparative study of different solar photovoltaic arrays configuration to mitigate the negative impact of partial shading conditions," *Journal of Mechanics of Continua and Mathematical Sciences*, vol. 16, no. 2, pp. 102–111, 2021.

[161] Y. Muñoz, L. H. Carvajal, J. P. Méndez et al., "Technical and financial assessment of photovoltaic solar systems for residential complexes considering three different commercial technologies and Colombia's energy policy," *International Journal of Energy Economics and Policy*, vol. 11, no. 2, pp. 272–280, 2021.

[162] M. Z. Zizoui, B. Tabbache, and M. Benbouzid, "Direct power control approach for a grid-connected photovoltaic power system," in *Advances in Green Energies and Materials Technology*, pp. 295–302, Springer, Singapore, 2021.

[163] N. Ravichandran, H. H. Fayek, and E. Rusu, "Emerging floating photovoltaic system-case studies high dam and Aswan reservoir in Egypt," *Processes*, vol. 9, no. 6, p. 1005, 2021.

[164] B. Nayak, A. Mohapatra, and P. Das, "Optimal hybrid array configuration scheme to reduce mismatch losses of photovoltaic system," in *2017 Second International Conference on Electrical, Computer and Communication Technologies (ICECCT)*, pp. 1–7, Coimbatore, India, 2017.

[165] H. M. Farh and A. M. Eltamaly, "Maximum power extraction from the photovoltaic system under partial shading conditions," in *Modern Maximum Power Point Tracking Techniques for Photovoltaic Energy Systems*, pp. 107–129, Springer, Cham, 2020.

[166] A. Bidram, A. Davoudi, and R. S. Balog, "Control and circuit techniques to mitigate partial shading effects in photovoltaic arrays," *IEEE Journal of Photovoltaics*, vol. 2, no. 4, pp. 532–546, 2012.

[167] R. Ramaprabha and B. Mathur, "A comprehensive review and analysis of solar photovoltaic array configurations under partial shaded conditions," *International Journal of Photoenergy*, vol. 2012, 16 pages, 2012.

[168] Y.-J. Wang and P.-C. Hsu, "Analysis of partially shaded PV modules using piecewise linear parallel branches model," *World Academy of Science, Engineering and Technology*, vol. 60, no. 2, pp. 783–789, 2009.

[169] Y.-J. Wang and P.-C. Hsu, "An investigation on partial shading of PV modules with different connection configurations of PV cells," *Energy*, vol. 36, no. 5, pp. 3069–3078, 2011.

[170] https://www.slideshare.net/premunknown/solar-design-premkumar1.

[171] K. A. K. Niazi, Y. Yang, and D. Sera, "Review of mismatch mitigation techniques for PV modules," *IET Renewable Power Generation*, vol. 13, no. 12, pp. 2035–2050, 2019.

[172] A. Minuto, G. Timò, P. Groppelli, and M. Sturm, "Concentrating photovoltaic multijunction (CPVM) module electrical layout optimisation by a new theoretical and experimental "mismatch" analysis including series resistance effects," in *2010 35th IEEE Photovoltaic Specialists Conference*, pp. 003081–003086, Honolulu, HI, USA, 2010.

[173] H. Yang, H. Wang, D. Cao, D. Sun, and X. Ju, "Analysis of power loss for crystalline silicon solar module during the course of encapsulation," *International Journal of Photoenergy*, vol. 2015, Article ID 251615, 5 pages, 2015.

[174] A. D. Dhass, P. Lakshmi, and E. Natarajan, "Analysis of performance degradation parameters of the photovoltaic system in Chennai," *International Journal of Pure and Applied Mathematics*, vol. 118, no. 20, pp. 439–447, 2018.

[175] L. Ponnusamy and D. Desappan, "An investigation of temperature effects on solar photovoltaic cells and modules," *International Journal of Engineering*, vol. 27, no. 11(B), pp. 1713–1722, 2014.